Transforming Growth Factor-β signaling in thymic epithelial cells

Its role in development, steady-state and immune reconstitution

Inauguraldissertation

zur Erlangung der Würde eines Doktors der Philosophie
vorgelegt der
Philosophisch-Naturwissenschaftlichen Fakultät
der Universität Basel

von

Mathias Martin Hauri-Hohl

aus Reinach, Aargau

Basel, 2010

creative commons

Namensnennung-Keine kommerzielle Nutzung-Keine Bearbeitung 2.5 Schweiz

---

Sie dürfen:

das Werk vervielfältigen, verbreiten und öffentlich zugänglich machen

Zu den folgenden Bedingungen:

Namensnennung. Sie müssen den Namen des Autors/Rechteinhabers in der von ihm festgelegten Weise nennen (wodurch aber nicht der Eindruck entstehen darf, Sie oder die Nutzung des Werkes durch Sie würden entlohnt).

Keine kommerzielle Nutzung. Dieses Werk darf nicht für kommerzielle Zwecke verwendet werden.

Keine Bearbeitung. Dieses Werk darf nicht bearbeitet oder in anderer Weise verändert werden.

- Im Falle einer Verbreitung müssen Sie anderen die Lizenzbedingungen, unter welche dieses Werk fällt, mitteilen. Am Einfachsten ist es, einen Link auf diese Seite einzubinden.

- Jede der vorgenannten Bedingungen kann aufgehoben werden, sofern Sie die Einwilligung des Rechteinhabers dazu erhalten.

- Diese Lizenz lässt die Urheberpersönlichkeitsrechte unberührt.

Quelle: http://creativecommons.org/licenses/by-nc-nd/2.5/ch/   Datum: 3.4.2009

Abstract

The thymus constitutes the primary lymphoid organ responsible for the generation of naïve T cells. Its stromal compartment is composed of a scaffold of different subsets of epithelial cells that provide soluble and membrane-bound molecules essential for thymocyte maturation and selection. With senescence, a steady decline in the thymic output of T cells has been observed. Numeric and qualitative changes in the stromal compartment of the thymus resulting in reduced thymopoietic capacity have been suggested to account for this physiological process. The precise cellular and molecular mechanisms underlying thymic senescence are, however, only incompletely understood. Here, we demonstrate that TGFβ signaling in thymic epithelial cells exerts a direct influence on the cell's capacity to support thymopoiesis in the aged mouse as the physiological process of thymic senescence is mitigated in mice deficient for the expression of TGFβ receptor type II on thymic epithelial cells. Moreover, TGFβ signaling in these stromal cells transiently hinders the early phase of thymic reconstitution following myeloablative conditioning and hematopoietic stem cell transplantation. Hence, inhibition of TGFβ signaling decelerates the process of age-related thymic involution and may hasten the reconstitution of regular thymopoiesis following hematopoietic stem cell transplantation.

Table of Contents

1. Introduction

1.1 A general introduction to the thymus

The thymus is the primary organ of T-lymphopoiesis. As a mere "transit" organ – allowing differentiation of pro-thymocytes to naïve T cells – the thymus does not house stem cells with self-renewing potential[1], and thus requires continuous 'feeding by seeding' of blood-bourne precursor cells from the bone marrow. The reason for the inability of the thymus to accommodate and keep stem cells in an undifferentiated state remains unknown. However, the issue of out-sourcing T cell development to a specialized tissue (i.e. thymus) is remarkably conserved during evolution, with cartilaginous fish being the most ancient representatives showing spatially clearly definable T cell development[2].

1.1.1 Organogenesis of the thymus

The microenvironment supporting T cell development consists of epithelial cells, fibroblasts and HSC-derived dendritic cells. Thymic epithelium is a derivative from the 3rd pouch endoderm[3], which buds out into the surrounding mesenchyme. Interaction with mesenchymal cells – partly of neural crest origin – and HSC-derived cells, but also cell-autonomous processes are required for the development and maturation of the epithelial compartment. The latter include the expression of genes encoding transcription factors, such as homeotic genes.

1.1.2 Cell-autonomous processes in TEC development

Expression of the transcription factor **Foxn1** (forkhead box n1, previously called winged helix nude (whn) or hepatocyte nuclear factor 3/forkhead homolog11 hfh11; gene localized on chromosome 11) identifies cells with a thymic fate. Yet, commitment of the endodermal lining to thymic epithelial cell lineage is likely to occur before Foxn1 expression can be traced at E11.25 in the ventral aspect of the 3rd pouch. However, earlier markers distinguishing committed thymic epithelial precursors are not yet available.

The requirement of Foxn1 expression does not apply to the formation of the primordium[4] but is important for the differentiation and function of thymic epithelium[5]. Foxn1 deficiency leads to an arrest in thymic epithelial cell (TEC) differentiation at an early stage, which precludes immigration of thymocyte precursors into the rudiment and ultimately results in severe T cell immunodeficiency ([6]), as demonstrated by the naturally occurring nude (nu/nu) mutant, as a result of defective Foxn1 expression. On the other hand, expression of Foxn1 in epithelial cells within the thymic rudiment of nude mice results in the development of thymic lobuli containing specialized compartments, to which T cell progenitors are attracted and T cell development is efficiently supported[7]. The fact that only a relatively small fraction of TEC in the adult mouse expresses Foxn1 is in line with the notion that Foxn1 expression is not continuously required but is essential for TEC differentiation[8]. Thymic epithelium devoid of Foxn1 expression – as seen in nu/nu mice – fails to acquire markers of committed

TE, and is incompetent to attract lymphoid precursors, potentially due to dysregulated chemokine production[9].

Foxn1 is expressed not only in developing TECs [6, 5] but also in keratinocytes and precursor cells of the hair bulge [10]. In mice, its expression marks the first step of terminal differentiation of the dermal epithelium and thus is found in the first suprabasal layer of the epidermis and in the supramatrical region of the hair bulb [11]. Mutations leading to inactivation of Foxn1 affects keratinization of epidermis and hair shaft [12, 13, 10], thus impairing coat and stratum corneum formation. The informations about Foxn1-regulated molecules are scarce but include PKC in keratinocytes and acidic hair keratin 3 in the hair follicle [13, 10].

Hoxa3 is a member of the transcriptional regulator – Hox – gene family, containing a homeobox sequence. Expression of Hoxa3 in the pharyngeal endoderm and neural crest can be detected as early as E8.5 [14]. Inactivation of the gene results in complete athymia, due to a failure of the 3rd pouch endoderm to detach from the foregut and form a thymic primordium. In addition, apoptosis in the 3rd pouch endoderm was increased in Hoxa3$^{-/-}$ embryos [15]. Yet number and migration of neural crest-derived cells was not affected in these mutants [15,16]. Hoxa3 is required for the sustained expression of Pax-1 and Pax-9, which are expressed in 3rd pouch endoderm from E9.5 onwards. These two members of the Pax family of transcription factors are involved in the proper formation of the thymus. Interestingly, the fine-tuned expression of Hoxa3 in the 3rd pouch region is crucial for the development of 3rd pouch derivatives. Increased Hoxa3 expression due to retinoic acid-exposure increases Pax1 expression[17,18]. This correlates with severe thymic hypoplasia as well as ectopia and as a consequence thymocyte development is severely perturbed.

Pax-1 is detected in the 3rd pouch endoderm as early as E10, remains expressed in the developing thymus and postnatally in a subpopulation of cortical stromal cells. Pax1-deficient embryos show a normal thymic development and migration until E13.5. Thereafter, the thymus fails to grow in size and is unable to support regular thymocyte development [19-21]. However, Foxn1-expression is unaffected by the absence of Pax-1.

The expression of *Pax-9*, a paralog of Pax-1 is detected around E9 – i.e. prior to Pax-1 expression – in the pharyngeal endoderm and in neural crest-derived cells. Pax-1 and -9 are the only Pax family members, which are not expressed in the central nervous system but – with the exception of the thymus anlage and the facial skeleton – are detected in structures undergoing chondrogenesis (reviewed in 22). Pax-9 is not required for the formation of the thymic anlage, but in its absence the 3rd pouch endoderm fails to detach from the foregut. The result is a bilateral polyp-like structure in the larynx region, which expresses Foxn1, IL-7 and SCF and is able to attract thymocyte precursors. Yet, thymocyte development is severely perturbed due in part to increased thymocyte apoptosis [23-25]. The specific roles for these two Pax family members in thymic development remain to be addressed but probably include the regulation of genes involved in cell differentiation and apoptosis [26].

Besides these cell-autonomous regulators of TEC differentiation and migration, interactions known as cross-talk with other cells in situ, including thymocytes and mesenchymal cells, play a crucial role in the differentiation of TEC precursors into terminally differentiated cortical and medullary epithelial cells with distinct phenotypic and functional characteristics.

1.1.3 Surface molecules expressed by TEC

The identification of thymic epithelial subpopulations was addressed using morphological and ultrastructural characteristics as well as antigenic determinants applying a panel of antibodies [27-29]. Antibody-mediated staining of cytokeratins has proven particularly useful and has – in conjunction with other markers, such as UEA-1 and MTS-10 – led to the classification of distinct thymic epithelial subsets [30].

The major keratins expressed in the thymus include the type II keratins K5 and K8. They assemble with the type I keratins K14 (for K5) and K18 (for K8). The major cortical TEC subset expresses both K8 and K18, whereas the major medullary subset of thymic epithelia co-expresses K5 and K14, and in addition stains for MTS10. Minor subsets include cortical $K8^+K18^+K5^+$ expressing cells and medullary $K5^-K14^-K8^+K18^+UEA1^+$ cells. Although a differential expression of cytokeratins in different TEC subsets may imply a direct or indirect role in their specialized function, this remains to be addressed.

It is easily perceived that for the multitude of tasks performed by stromal cells tight intercellular interactions between TEC themselves or between TEC and thymocytes are required. A number of adhesion molecules facilitate these encounters.

Cadherin family members play a crucial role in the formation of adherens junctions in keratinocytes [31]. The majority of cadherins solely mediate Ca^{2+}-dependent homophilic adhesive interactions. Yet, E-Cadherin forms also a heterophilic interface with the integrin α_E (CD103) β7 heterodimer, which is expressed by several thymocyte subpopulations [32,33]. In the adult thymus E-Cadherin expression is largely confined to the epithelium, however, fetal thymocytes – in particular $CD4^-CD8^-CD25^+$ precursor stages also show a strong surface staining for this molecule [33]. Different studies demonstrated the essential contributions of these homo- and heterophilic interactions for the *in vitro* development of a functional thymic organoid [32-34]. The regulation of E-Cadherin expression in TEC is to date unknown. Cell-cell interaction is however not only required for the structural integrity of the stroma as it was shown that ***B7*** and ***ICAM-1*** (expressed on cortical and medullary TEC) as well as ***VCAM-1*** (expressed on HSC-derived APC) are important for thymocyte selection processes [35,36]. The expression of ***MHC class II*** molecules on the surface of thymic epithelium is required for their essential role in T cell development [37].

1.1.4 Cell-cell interactions in TEC development

The influence of ***maturing thymocytes*** on the developing epithelium during embryogenesis has long been appreciated [30,38-41]. Mice with a block in thymocyte development at different stages have proven

helpful for the study of this interaction. The hCD3ε26 transgenic mouse line shows a developmental arrest of thymocytes at the DN1 stage. TEC differentiation in these mice is restricted to an immature K5$^+$K8$^+$ phenotype. The TEC display a disorganized cortical architecture while a separate medullary region is completely lacking. Whereas Rag1$^{-/-}$ mice with their developmental arrest at the DN3 stage of thymopoiesis also lack a medulla, their cortical epithelial compartment shows proper maturation with a large population of mature K8$^+$K5$^-$ TEC. Maturation of TEC in these mice can be achieved by transferring wildtype hematopoietic stem cells with a normal thymocyte development.

Interestingly, the plasticity of the epithelial compartment is retained only during a relatively short period of time, as hCD3ε26 transgenic mice develop a normally sized and functional thymus only if normal prothymocytes reach the thymus during embryonic development. A recent paper however questions the requirement of lymphocyte precursors for the differentiation of TEC [42]. Using hCD3ε26 transgenic mice, Jenkinson et al. demonstrate, that the presence of normal T cell development during embryogenesis is not required for the initial steps of TEC differentiation (measured by cytokeratin stainings and Aire and Plunc expression). However, this study does not provide an explanation for the phenotypically immature stages of thymic epithelium in the adult hCD3ε26 mouse.

During embryogenesis, neural crest-derived **mesenchymal cells** surround and later invade the epithelial rudiment, forming a network, interacting with epithelial and lymphoid cells. A study, using a neural crest-specific marker has demonstrated the intimate relation between these cells and the endoderm-derived thymic primordium[43]. However, at later time points, i.e. in the newborn mouse, NCC-derivatives are restricted to a small portion in the posterior thymic capsule. Whereas the patterning of pharyngeal arches occurs independently of neural crest cells in the chick embryo[44], the importance of neural crest-derived cells not only for epithelial differentiation but also for thymocyte development is demonstrated by experiments involving neural crest ablation or depletion of surrounding mesenchyme in culture systems [45,46]. Potential mechanisms include the secretion and membrane-bound presentation of growth and differentiation factors. These molecules may act either directly or be deposited in the extracellular matrix, which is itself produced by stromal cells[45,47,48]. Likely candidates for such growth and differentiation factors are fibroblast growth factors (FGF) and TGFβ family members. Indeed, TEC deficient in the expression of FGFR2IIIb – the receptor for FGF7 and FGF10, which are typically detected in the mesenchyme surrounding the thymic primordium – fail to proliferate and demonstrate a partial block in differentiation. Despite these alterations, normal thymocyte development is not affected. Ablation of FGF10 – a ligand for FGFR2-IIIb –results in a similar though somewhat mitigated phenotype[49]. Pax-1 and Pax-9 expression is not disturbed by the absence of FGFR2-IIIb expression. PDGFRa$^+$ mesenchymal cells are transiently important for the expansion of epithelial cells and, as a consequence, for the quantity of intrathymic niches available for thymocyte precursors [50]. In addition to their role in TEC expansion, mesenchymal cells and extracellular matrix molecules provided by them, are required for the differentiation of prothymocytes (in particular at the DN2 stage) but not of DP thymocytes [45,47].

Neural-crest cells – a vertebrate 'invention' – develop at the border between the neural plate and the epidermis, delaminate from the dorsal part of the neural tube after its closure and acquire a high grade of mobility. They differentiate into a multitude of specialized cells such as neurons, glial cells, pigment cells as well as craniofacial cartilage and bone. The induction of the neural crest is tightly regulated by BMP and Wnt signaling in an antagonistic fashion [51,52].

The induction, differentiation, proliferation, maintenance and migration of NCC rely on timed Hoxa3 expression, as its absence results in delayed differentiation and malformation of the third arch[53]. The expression of Hoxa3 therefore influences TEC development both in a cell-autonomous direct fashion via TEC as well as in an indirect way via expression in NCC.

TGFβ-family members instructively influence differential specifications of NC stem cells *in vitro* [54-56], whereby the concentration and combination of signals provided by these molecules determine the fate of NCC[57]. Recent reports highlight the involvement of several TGFβ-signaling components in late specification and survival of NCC [58-64]. The importance of TGFβRII-mediated TGFβ signaling in neural crest-derived cells was demonstrated[65], since the absence of functional TGFβRII in NCC led to the loss of region-specific differentiation (but did not affect cell migration). As a consequence features typically seen in DiGeorge syndrome such as thymic and parathyroid hypoplasia develop in these mice. Furthermore, a recent study has demonstrated the involvement of the common mediator of TGF/BMP-signalling mediator Smad4 in the maintenance of NCCs. A potential role for TGFβ during thymic development might therefore lay in the instruction of NCCs to acquire their requested region-specific phenotype. However, both the nature of the cell types providing this cytokine and the identity of additional signals other than TGFβ remain to be investigated.

1.1.5   Thymocyte development

A continuous supply of T cell precursors is crucial for thymopoiesis, as the thymus lacks hematopoietic stem cells and supposedly also the niches needed for their survival. Substantial effort has gone into the identification of the phenotype of precursors with intrinsic T-lineage potential. This has led to the characterization of separate precursor populations that have individual lineage potentials. The subsequent development of these precursors into mature T cells requires their dramatic expansion. Indeed, each single precursor will give rise in two separate ways to roughly 10^6 descendants. This expansion is effected by a 4000-fold expansion at the DN and by a 250-fold expansion of the early DP stages.

Homing of blood-bourne precursors to the intrathymic microenvironment is considered a rare event with only an estimated 200 cells entering on a single day[66]. Progenitor cells enter the thymus through transmigration of postcapillary venules in the region of the corticomedullary junction [67]. A recent report has shown that PSGL-1 expression on homing cells greatly facilitates this process as it allows the binding of P-selectin, that is typically expressed on thymic endothelial cells. Availability of empty progenitor cell niches by a yet unknown mechanism leads to up-regulation of P-selectin on the endothelium [68]. Several chemokines have been implicated in the attraction of prothymocytes. Whereas

thymic vasculature is involved in the attraction of prothymocytes in the adult, gathering of thymocyte precursors in the fetus occurs prior to vascularisation of the thymus.

Bleul and Boehm[9] demonstrate the constitutive expression of CCL21, CCL25 and CXCL12 in the alymphoid thymic anlage and show that CCL25 and CXCL12 act as strong chemoattractants to fetal thymocyte precursors whereas CCL19 was much less potent. Mice deficient for the functional transcription factor Foxn1, show a normal thymic anlage by E12.5 however lack the immigration of thymocyte precursors. Detailed analysis showed that the presumptive thymus is devoid of CCL25 and CXCL12 message. Surrounding tissue on the other hand expressed normal CXCL12 levels. Interestingly, the adjacent parathyroid in wildtype as well as in *nude* mice shows high expression of CCL21. Mice deficient for the CCL25 receptor CCR9 do not show a defect in thymocyte development under steady-state conditions. However, they reveal a disadvantage in repopulating the thymus under competitive conditions[69], despite the absence of the receptor on wildtype DN cells. Liu et al. extend these findings, analyzing embryos lacking the expression of CCR7 and CCR9, the receptors for CCL19/CCL21 and CCL25 respectively, and find a synergistic effect of signaling via the two receptors in attracting precursors to the thymic anlage. Expression of CCR7, the receptor for CCL19 and CCL21, is restricted to immature $CD25^{int}$ $CD44^+$ thymocytes (i.e. cells at the DN1→DN2 transition), and its lack prevents the migration of DN2 to the outer cortex, which results in the disturbance of early T cell development (e.g. the accumulation of DN1) and a reduced number of thymocytes[70]. Chemokines are mainly produced by thymic epithelia in the different anatomical compartments, though other stromal cells also contribute to their production [71, 9, 72]. The consecutive steps during thymopoiesis, i.e. proliferation and further maturation are regulated by additional members of the chemokine family. CXCL12 (a.k.a. stroma-derived factor-1 (SDF-1), pre-B cell growth stimulating facor (PBSF)), originally isolated from bone marrow stromal cell[73], and its corresponding receptor CXCR4 are involved in the development and function of multiple organ systems[73-76]. CXCL12 is ubiquitously expressed in the E14 thymus[77]. Attraction of prothymocytes is however not influenced by the absence of CXCR4[77], but a dramatic increase in the number of post-DN2 thymocytes ensues and is observed in thymi of CXCR4-/- mice at different embryonic stages. This is due to an expansion deficit at the DN3 and DN4 stages, is noted as early as E13.5 and appears to be independent of the pro-survival factor bcl-2. The same study demonstrates a synergistic effect of CXCL12 on SCF-mediated survival of DN2 cells. Plotkin et al. demonstrate[78] the expression of CXCR4 on all DN thymocytes and CXCL12 expression on a subpopulation of cortical TEC in adult mice. Conditional inactivation of CXCR4 in DN leads to their retention at the corticomedullary junction and arrests their development at the DN1 stage.

The earliest intrathymic progenitors (DN1) will remain in a state of asymmetrical division in the zone of entry at the corticomedullary junction for an extended period of about 10 days[79, 80]. Here, survival, proliferation and differentiation signals are provided by IL-7, whereas SCF enhances their proliferation and inhibits their differentiation. In addition, Flt3 affects in a largely positive manner their expansion[81]. The transition to DN2 is recognized by the up-regulation of CD25 and expression of RAG. Restriction to the T cell-lineage is mediated through Notch signaling at the DN3 stage, which is phenotypically characterized by the down-regulation of the CD44 expression, and genotypically by the V-DJ

rearrangement of the TCRβ locus. In-frame rearrangement of one TCRβ allele is a prerequisite for further survival and maturation to the DN4 (CD44- CD25-) stage. Here, cells express on their surface the pre-TCR, a yet immature form of the TCR, allowing them to receive survival signals, a process referred to as β-selection. DN4 cells then undergo further rounds of proliferation, start to recombine the TCRα locus and up-regulate the expression of CD4 and CD8, characteristics of the DP stage of thymopoiesis.

During the development of DN1 thymocytes to DN4 cells Notch signaling plays a key role for specification and survival. Conditional inactivation of Notch1 in BM cells not only leads to a complete developmental block at the DN1 stage but also re-directs the intrathymic cells towards a B cell fate [82,83]. Notch-dependent signals are also implicated in the TCRβ gene rearrangement as well as in the elimination of thymocytes that did not receive a survival signal through the pre-TCR[84,85]. The contribution of Notch signaling to the decision regarding CD4 versus CD8 lineage commitment is still debated, yet survival of DP cells no longer depends on Notch signaling [85].

$CD4^+CD8^+$ thymocytes mark the next key step in development. Their average live span is estimated to be 3-4 days. Interaction of TCRαβ expressed by DP and MHC molecules on radio-resistant stromal cells during this period determines the fate of DP. Failure to successfully recognize MHC molecules commits the individual DP cell to down-regulate anti-apoptotic molecules. The provision of pro-survival signaling via RORγ and Wnt molecules allow limited survival of DP cells, wich further increases the chance of rearranging the TCRα locus to attain TCRαβ that can be positively selected. It is currently believed that low-abundance, low-affinity peptides presented by MHC molecules on cortical epithelium, but not on other types of epithelial cells[89] promote positive selection [90]. The erratic movement of pre-selection DP, termed 'random walk migration`, is swiftly transformed into a rapid, directed movement towards the medulla upon positive selection [93].

Negative selection of the generated TCR repertoire assures non-self reactivity among mature T cells. Depending on the experimental model used, this process may occur at different stages of thymocyte development. This observation has been related to a differential localization of specific accessory cells (i.e. macrophages, dendritic cells, possibly B cells and fibroblasts), and expression levels of TCR. Intrathymic dendritic cells were shown in different experimental models to play a dominant role in tolerance-induction by negative selection[91].

Single-positive (i.e. $CD4^+CD8^-$ or $CD4^-CD8^+$) thymocytes, that have successfully completed thymic selection reside in the medulla for a period of up to 14 days [94]. Initially functionally incompetent [95] and susceptible to various apoptotic stimuli, single-positive (SP) T cells undergo a series of maturational steps prior to their release into the periphery as mature T cells [96, 97, 98, 39]. Phenotypically the SP thymocytes in this phase display changes in the cell surface expression of markers including CD24 (HSA), CD69, CD62L, 3G11 and 6C10 [99]. In addition, CD3 expression is upregulated [100].

Despite the thymocytes long residence in the medulla corresponding to roughly half of their lifespan [86], cellular and molecular mechanisms responsible for the post-selection maturation of SP during their sejourn in the medulla are still largely undefined. Nonetheless this residence constitutes a crucial phase in thymocyte development. The functional immaturity assigned to post-selection DP is characterized by an increased susceptibility for corticosteroid exposure or TCR ligation by antibodies [101, 102, 103]. In

addition, proliferation of Qa2[negative] (i.e. HSA^{high}) SP cells in response TCR ligation is diminished in comparison to mature T cells [95].

The process of negative selection is among the maturational events that occur at the SP stage. This event is dictated by the TCR specificity and the MHC expression in the thymic medulla[104]. Different experimental approaches (e.g. injection of anti-TCR mAb or superantigens in mice; stimulation of isolated thymocyte subpopulations *in vitro* with anti-TCR in the presence or absence of co-stimulation; etc) have been used in an attempt to study this important process that will eliminate potentially auto-reactive thymocytes. A series of studies by Kishimoto et al.[103,105,106] have demonstrated the differential receptiveness of SP subpopulations (in particular CD4+ SP) to TCR engagement, measured as a function of apoptosis and proliferation. Whereas DP thymocytes rapidly undergo apoptosis upon TCR stimulation in the presence of co-stimulation, HSA[high] SP are more resistant to such stimuli (despite their higher TCR expression levels when compared to DP). Moreover, the most mature SP (as identified by low HAS expression) respond to TCR stimulation with activation and proliferation. In parallel, the dependency on co-receptor mediated signaling increases from the DP cell stage (characterized by a lack of apoptosis, and the consequential up-regulation of CD69 and CD25) to the stage of immature and finally mature SP cells, the latter also encompassing cells in the periphery. Furthermore, a requirement for Fas-FasL signaling depends on the maturational stage at which it occurs during thymopoiesis, as apoptosis of DP and immature SP with low TCR expression is fully independent of Fas. However, Programmed cell death of immature SP with high levels of TCR expression is completely dependent on Fas-FasL interaction. Alterations in the receptiveness of thymocytes to TCR-associated signals occur with differentiation thus leading to different interpretations of the same signal [107]. This plasticity prepares T cells for optimal effector functions once they exit to the periphery. TCR-MHC interaction during the transition through the medulla is instrumental in adjusting peripheral T cell reactivity to a higher antigen threshold [108].

Few molecules have been identified as surrogate markers for TCR-MHC affinity. Ror Example, CD4 expression increases proportionally to the strength of the contact between TCR and MHC molecule. In this context, CD5 is thought to be a negative regulator of TCR signal transduction initially after positive selection[109]. However, CD5 is not required for the 'dampening' effect of the medullary education phase [108].

A significant proportion of mature TCRhigh SP thymocytes undergo some level of stroma-dependent, IL-7 driven proliferation immediately before egress into the periphery. This proliferation requires and correlates with a TCR-MHC interaction, but does not change the activation status of the cell (i.e. fails to up-regulate as a result neither CD44 nor CD69). This post-selection expansion is induced by thymic epithelium and potentially other stromal components [110-113].

1.1.6   Thymocyte migration

The ability to enter the thymus, to migrate within the different thymic compartments, and to exit at the appropriate location and developmental stage requires precise regulation. A key role in these processes is attributed to chemokines.

CCR9 – the receptor for CCL25 (TECK) – is highly expressed on DP thymocytes and down-regulated during maturation to SP cells. Following positive selection, DP thymocytes migrate towards the ligand in vitro [114]. Nevertheless, the targeted deletion of CCR9 does not result in obvious alterations of thymocyte development. Yet, a thorough analysis of the localization of the thymocyte subpopulations, which might reveal alterations in aberrant compartimentalisation of DP, has not been published. In contrast, CCR7 is upregulated during the transition from DP to SP [116] and CCR7- or CCR7L-deficient SP thymocytes fail to migrate to the medulla and accumulate in the cortex[115]. The relevance of these findings is of particular importance, as negative selection of SP thymocytes to AIRE-dependent, 'promiscuously expressed' antigens requires their presence in the medulla and the lack of migration leads to autoimmunity towards these antigens. Interestingly, phenotypic maturation and export are not impaired in the absence of CCR7-CCR7L interaction, indicating that for these processes the thymic medulla and its structures are dispensable.

Following negative selection, mature SP thymocytes are reach systemic circulation via medullary blood vessels [117,118]. It was appreciated more than 25 years ago, that egress of mature thymocytes is an active, G protein signaling-dependent process [119]. However, several mechanisms are involved: Attraction by circulating factor(s), loss of responsiveness to thymic retention factors and repulsion by thymic mediators. To date, key players key players include the following ligand/receptor pairs: sphingosine-1-phosphate(S1P)/S1P, CXCL12 (SDF-1)/CXCR4, CCL19/CCR7, CCL25/CCR9 and CCL22/CCR4.

Under steady-state conditions, S1P is constitutively detected at relatively high levels in the plasma. S1P receptor 1 (S1P1) is expressed by the most mature thymocytes [116, 115]. Chemotaxis towards S1P is exclusively displayed by mature thymocytes and resting peripheral T cells [116]. Inactivation of S1P1 in HSC blocks export of mature T cells and leads to their accumulation in the thymus. CXCL12 (SDF-1) is highly expressed in thymic tissue, BM and peripheral lymphoid organs [120] and demonstrates a fugetactic effect on activated T cells at high concentration [121]. Its sole ligand is CXCR4, and deletion of either component results in an almost identical phenotype with multiple developmental defects and increased fetal lethality [73,122]. As these mice do not survive the perinatal period, the effect of the lack of either molecule on thymocyte emigration could not be studied *in vivo* [121], yet CXCL12-deficient mice show essentially normal T cell development. Human mature thymocytes and peripheral T cells demonstrate active movement away from the chemokine[121], which hints towards a role for these partner molecules in thymocyte export. Fetal thymic organ cultures using thymi derived from CXCR4-deficient or wildtype mice confirmed these finding as CXCR4$^{-/-}$ mature SP accumulated intrathymically [123]. In addition, specific pharmacological inhibition of CXCR4 leads to the accumulation of intrathymic mature SP thymocytes. Another chemokine-receptor pairing implicated in thymocyte egress consists of CCL19 and CCR7. In vitro and in vivo assays demonstrate, that CCL19 but not CCL21 (which also binds to CCR7) is a potent chemoattractant for mature SP in the neonatal condition [124].

Potential retention factors, preventing untimely exit of not yet fully educated thymocytes, include CCL25/CCR9 and CCL22/CCR4. Accordingly, CCR9 is highly expressed on DP thymocytes, but down-regulated in SP thymocytes [125, 114]. In addition, DP but not SP thymocytes are attracted by

CCL22 (MDC) [126]. Through a yet unknown mechanism not attributable to increased negative selection, exogenous TCR engagement of mature SP thymocytes impedes their egress [127].

Once mature thymocytes leave the confines of the thymus as so called recent thymic emigrants (RTE), they become relatively difficult to detect in the peripheral T cell pool due to their phenotypic resemblance to naïve T cells [132,133]. RTEs are of particular significance to the organism, as they maintain the diversity of the peripheral T cell pool [134,135]. A multitude of studies address the identification and quantification of RTE, in order to measure thymic export. The frequency of RTE in the periphery directly correlates with the amount of functional thymic tissue. In mice it rapidly increases after birth and gradually declines after a peak at 6 weeks of age [136, 137]. The export rate is independent of the pool size of peripheral T cells, into which RTEs become rapidly integrated [136,138].

Besides tight regulation of thymic export, immigration of mature peripheral T cells into the thymic confinements is largely impeded. Peripheral naïve T cells cannot be detected within the thymocyte pool, even after intravenous injection of vast numbers of naïve syngeneic T cells. These findings however do not apply to newborn mice [140] nor to aged mice [137], indicating leakiness of the blood-thymus barrier in these circumstances. In addition, activated T cells could easily be detected as early as 24 hrs post-injection [139].

1.2   Thymic involution

Thymic function is measured by its ability to provide the organism with newly generated, appropriately selected T cells, thus ensuring a sufficient number of peripheral T cells with a broad repertoire of T cell receptor specificities tolerant to self. Even though the thymus retains the ability to produce T cells even in aged individuals [141], this capacity declines with age-associated involution. Thymic involution shows a biphasic course with a rapid loss of thymic tissue during puberty followed by a slow but constant rate of involution (reviewed in 142, 143, 144). The decrease in thymic output does lead to a decreased number of peripheral T cell, as they regulate their number in response to homeostatic signals. This is reflected by the increase in memory T cells and decrease of naïve T cells in the blood of the elderly. However, this process slowly lessens the variability of the TCR repertoire and eventually leads to an accumulation of 'senescent' T cells with reduced capacity to appropriately respond to antigens and IL-2 [145, 146]. A characteristic feature of age-associated changes in the peripheral T cell pool includes the decrease in the CD4/CD8 ratio from roughly 1.8 in young individuals to about 1.0 in older subjects. Furthermore, the higher rate of proliferation is associated with reduced telomere length and higher susceptibility to apoptotic stimuli. Several functional changes, such as the reduced expression of effector molecules and cytokines, have been observed in T cells from aged humans (reviewed in 147). These alterations put the ageing organism at a higher risk to succumb to infections that are normally controlled by the 'young' immune system and reduce the efficacy of vaccinations [148]. An increase in tumor incidence was also partially attributed to the reduced immune function in the elderly.

Changes in the lymphoid as well as in the stromal compartment of the thymus contribute to its involution, as outlined in the following chapters.

1.2.1   Quantitative and qualitative changes in the T cell progenitor pool

The potential of common lymphoid progenitors to commit towards the T cell lineage decreases with age. In mice, this decline depends on strain-specific genetic modifiers, which remain to be identified [149]. In addition, the potential of hematopoietic precursors to home to the thymus is diminished in old mice [150], demonstrated by comparative transfer of precursors derived from young and aged mice into non-irradiated hosts [151, 152-154, 155].

1.2.2 Trafficking

The egress of lymphoid progenitors from BM underlies active regulation, although the exact mechanisms involved remain unknown. There is evidence that this export is synchronized to concomitant receptivity of the thymus [156, 157]. A potential thymus-bone marrow feedback loop might be established through either soluble or cellular components (or a combination of the two). Candidates regulating prothymocyte mobilization include CD44, β_2m, SDF, TECK, α4 integrins and NK T cells.

1.2.3   Thymic receptivity

In addition to pre-tymic alterations, intrathymic changes modify the occurrence and rate of thymic involution. Availability and appropriate signaling of empty niches for early thymocyte progenitors (ETP) within the thymus seems important and is closely linked to progenitor export from the bone marrow. Importation of ETP is facilitated by the expression of homing molecules on stromal and lymphoid cells. Expression of P-selectin on endothelium or of Flt3 Ligand on perivascular fibroblasts and expression of the corresponding ligands PSGL-1[68] or Flt3[158] respectively on ETP enhances their homing. As the absolute number of niches for ETP directly correlates with the number of thymic stromal cells [152], a decrease in TEC numbers in the aged mouse consecutively results in decreased numbers of ETP. However, ETP derived from old mice also demonstrate a reduced proliferative potential as well as an increase in apoptosis [159].

1.2.4   Ageing stroma

Besides changes in the lymphoid compartment, the thymic stroma including thymic epithelium is subject to age-related alterations. These have been recognized in early studies with a description of functional consequences on T cell development [160]. Morphologically, the most dramatic changes include shrinkage of cortical regions and disruption of the ordered architecture, which were irreversible upon transfer of BM from young mice [161] and thus imply a stromal cell-intrinsic defect. Multiple molecular changes were described in the stromal compartment derived from aged animals. Farr and Sidman demonstrate a prominent reduction of MHC II expression in particular in cortical TEC using immunohistological and biochemical means [162]. Flowcytometric analysis furthermore reveals a decrease in the MHC II^{high} / MHC II^{low} ratio with ageing [163,164]. In addition, changes in TEC-associated

transcription factors and structural genes were found in relation to age [165]. The most prominent decrease is shown for Foxn1 (which gradually declines after birth, see also reference 8), but reduced levels were also demonstrated for cytokeratin 8, a marker for cortical epithelium. The study by Yajima et al. suggests a role for Fas, expressed by the stromal compartment, in these age-induced changes of the epithelium [166].

In addition to morphological changes, the proliferative potential of TEC declines with age [163], which is in close correlation with absolute TEC numbers. This seems to play a particular role in thymic involution as forced epithelial proliferation by means of transgenic overexpression of cyclin D1 reversed this process [167], yet did not overcome thymocyte-dependent specification requirements of thymic epithelium[168].

However, ageing not only affects quantitative but also qualitative aspects of thymic stroma. Stromal-derived factors such as SDF-1, IL-7, SCF, TSLP and TGFβ, which influence precursor recruitment as well as survival, differentiation and apoptosis of thymocytes display age-dependent changes. Thymocyte development in old mice demonstrates a partial block in the transition from the DN1 to the DN2 stage [169, 170]. This finding is concomitant with decreased level of the anti-apoptotic molecule bcl-2 and increased apoptosis in DN2 and DN3 populations in aged mice. This is reminiscent of the situation observed in IL-7-deficient mice [171,172] and in line with the finding that IL-7 (but not SCF) could decrease the level of apoptosis *in vitro* and *in vivo*. In fact, mRNA levels of IL-7 in aged thymi are decreased in comparison to younger mice [173, 169]. Transgenic overexpression of IL-7 within the thymus [170] reverses the developmental block by increasing the local concentration of IL-7 in the thymus, yet without demonstrating an effect on thymic involution and furthermore uncovering an additional, IL-7-independent proliferation deficiency at the DN4 stage. Nevertheless, in contrast with these studies is the finding of unaltered IL-7 levels in young and aged human thymi or thymi derived from myasthenia gravis patients [174]. This however does not preclude changes in post-transcriptional events or in the efficiency of presentation of IL-7 by stromal cells [48].

Elucidating the contribution of systemic administration of IL-7 to reverse thymic involution is complicated by the fact that IL-7 also affects the peripheral T cell pool [175,176]. Additional cytokines and growth factors were assessed for their ability to influence thymic involution[174, 142] and termed either 'thymostimulatory' (s.a. IL-7, KGF, TSLP, hGH, GH secretagogue, Leptin, Ghrelin [177, 178-181]) [182]. In fact, the level of thymopoiesis in human subjects of different age groups correlated indirectly with the expression levels of LIF, oncostatin, SCF, IL-6 and M-SCF [174]. Administration of each of these factors to young Balb/c mice reduces thymic cellularity. In addition, transgenic over-expression of soluble LIF in T cells leads to a dramatic atrophy of the thymic cortex and severely perturbs the development and function of thymic epithelium [183].

Age-dependent differences in thymic involution between BxD recombinant inbred mouse strains have stimulated the mapping of involution-associated quantitative trait loci [154,184,185], which suggest a contribution of IL-12 to thymic involution [185]. In fact, inactivation of IL-12 enhances thymic involution, likely due to a proliferative deficiency of thymocytes, since IL-12 acts in concert with IL-2 and Il-7 to enhance thymocyte proliferation.

Another molecule associated with increased thymic involution in studies of recombinant inbred strains was TGFβ. As homozygous inactivation of each of the three isoforms or their receptors leads to early (i.e. pre- or soon postnatal) lethality, these mice are not amenable to studies of thymic involution. However, earlier studies have shown an increase of TGFβ1 in the human thymus as a function of age [174]. TGFβ induces the thymosuppressive factors LIF and IL-6 in cultured human TEC[186]. Kumar et al. [154] extend these findings using TGFβ2 heterozygous deficient mice, which show a delayed thymic involution, associated with increased numbers of LSK cells in the bone marrow and ETPs in the thymus of old mice. Despite a possible negative regulatory role of TGFβ2 on the lifespan and cycling potential of thymocyte precursor populations, an effect of TGFβ2 heterozygosity on stromal ageing is not excluded.

1.2.5   The role of gonadal steroids in thymic involution

The coincidence of the first, prominent phase of involution with puberty suggests that the increase in sex steroids in this period is instrumental in initiating and mediating the decline of thymic function. In mice, the reduction of thymic mass becomes visible as early as 6 weeks postnatal, concurrent with pubertal changes.

Indeed, it was perceived a long time ago, even before J. Henderson [187] published his findings about thymic atrophy and its correlation with castration and pregnancy in cattle, that the thymic mass decreases with increasing age and that castration prevents such degeneration. This issue has found considerable interest in later studies in rats [188] and mice [189], showing the reversal of thymic involution as well as restoration of T cell function following removal of the gonads. Gonadal steroids replacement after castration rapidly re-induces thymic involution with a reduction in total thymic cellularity, a relative decrease in DP thymocytes and a corresponding increase in SP thymocytes [189]. The increased levels of androgen receptors (*AR*) in TEC relative to thymocytes propose a mechanism via alteration of TEC function [190]. Indeed, bone marrow chimeric mice using AR-deficient bone marrow transferred into castrated wildtype animals demonstrate a reduction of thymic cellularity upon challenge with dihydrotestosterone (DHT), whereas the opposite bone marrow chimeric combination was protected from these changes[191]. Nevertheless, minor direct effects cannot be ruled out completely [192]. Interestingly, fetal thymi are protected from sex steroid-induced but not corticosteroid-mediated alterations. Indeed, mRNA levels of estrogen- and androgen-receptors are undetectable in fetal and neonatal thymi up to two weeks of age [193].

Whereas the short-term effects of sex steroid ablation on thymic regeneration and T cell output are remarkable and have led to promising results in different settings (see below), long-term studies addressing the effect on the protracted phase of involution are scarce.

A recent study by Min et al [194] re-evaluates the role of growth hormone (GH) and sex steroids in inducing thymic involution. The levels of GH and its major effector molecule IGF-I decline gradually with age. The prediction that the GH/IGF-I axis positively influences thymic cellularity was tested using the *lit* strain of mice (GH and IGF-I levels drastically reduced) and *hpg* mice, bearing a mutation in the GnRH gene, which results in gonadal atrophy and diminished sex steroid production. Neither of

these mice show a pronounced resp. delayed thymic involution, thus making a unique and lasting effect of these hormones on thymic regeneration unlikely. In addition, the effect of castration on thymic recovery is only transient, as 5 months after removal of the gonads thymic cellularity was equal to untreated animals and thymic involution proceeded unhindered.

Nevertheless, ablation of sex steroids has proven to be very efficient in enhancing immune reconstitution after myeloablation and stem cell transplantation [195,196].

1.2.5.1 Androgen-regulated cytokines

Despite the large amount of information on the cellular effects of sex steroids, relatively little is known about the mechanism and the mediators leading to steroid-induced thymic involution. A potential mechanism how androgens inhibit thymopoiesis is via the repression of cytokines or their cellular source, which stimulate T cell development (such as IL-7), or on the other hand via the induction of repressive cytokines such as TGFβ. Interestingly, surgical castration results in a significant decrease of TGFβ mRNA levels produced by thymic stroma, whereas the levels of IL-7, KGF and SCF remained largely unaffected [196]. Olson et al. furthermore demonstrate that castration reduces the levels of TGFβ1 protein in the thymus whereas testosterone replacement leads to an increase in TGFβ1 mRNA levels and protein activity in thymi of castrated animals [197]. The functional consequence of this increase in TGFβ1 activity on any thymic compartment was however not further investigated.

Yet, other organ systems were explored for such effects. For example, bone marrow stromal cell-derived TGFβ is responsible for the androgen-induced inhibitory effect on B cell development in co-cultures of B cell precursors with stromal cells, whereas precursor cells alone show unhindered colony-forming capacity [198]. In addition, androgens positively regulate TGFβ1 transcription via direct activation of its promoter in human hepatoma cells [199].

1.3 Irradiation damage to the thymus

The relevance of the post-adolescent thymus was neglected for a long time, as the thymus was believed to gradually degenerate and loose its function. However, functional thymic tissue can be detected even in elderly individuals, showing essentially normal distribution of thymocyte subsets [200, 141], which indicates that the thymus retains its capacity to generate appropriately selected T cells throughout lifetime [161]. T cell output from the thymus shows a remarkable linearity to the amount of thymic tissue [141, 201, 174]. Nevertheless, whereas in a young organism the thymus readily increases *de novo* production of T cells upon peripheral lympho-depletion, the ability of the aged thymus to increase thymic output in response to a sudden loss of peripheral T cells is greatly impaired. This is of particular importance in the setting of stem cell transplantation (HSCT) following myeloablation, where rapid regeneration of T cells is crucial for host immunity. This is primarily established through peripheral expansion of graft-derived T cells with an oligoclonal TCR repertoire. However, T cells generated *de novo* in the thymus

will provide the host with appropriately selected T cells displaying a broad repertoire of TCR specificities [202-207].

Thymic cellularity is dramatically affected by lethal irradiation, showing a rapid decrease within 24 hours after irradiation in particular due to massive apoptosis of DP thymocytes [208-210], leaving a collapsed cortical region. A direct injurious effect of irradiation on the reconstitution potential of thymocyte-depleted thymic stroma was demonstrated [211]. Non-irradiated thymic grafts transplanted after irradiation of the host demonstrate enhanced growth characteristics and peripheral T cell reconstitution in comparison to thymi implanted immediately prior to irradiation. This is accompanied by striking alterations in the non-lymphoid and in particular in the epithelial compartment, reversible within a week post-irradiation [212]. Following exposure to ionizing radiation, TEC rapidly acquire a $CK5^+CK8^+$ double-positive phenotype, and up-regulate the expression of p63, c-myc and Tcf3, which normalize after reconstitution [213]. Whereas low-level doses of γ-irradiation lead to increased thymic production of IL-7, SDF-1 and TECK [214], lethal doses augments the loss of TEC and thymic IL-7 expression, which is reflected by a reduction in thymic cellularity 4 weeks after irradiation and reconstitution [215]. In addition to direct cytotoxicity mediated by γ-irradiation with regards to TEC survival, ionizing radiation triggers the production or release of 'thymoinhibitory' cytokines. Indeed, apoptotic thymocytes – either treated with dexamethasone or γ-irradiation – release prestored TGFβ, which contributes to an immunosuppressive milieu [216]. However, evidence for a specific role for TGFβ in thymic reconstitution is still lacking, though – as mentioned previously – TGFβ was shown to indirectly influence the proliferation of human [217] and mouse cells of the hematopoietic lineage, through down-modulation of stromal IL-7 production[197,198].

With respect to the focus of this study follows an introduction about the general role of TGFβ and downstream molecules involved in signal transduction, regulation and effector functions, followed by a summary of the current knowledge about the specific function of TGFβ in the thymic environment.

1.4   The TGFβ family [218, 219]

Among the molecules involved in regulating cellular proliferation, differentiation, metabolism and apoptosis, the transforming growth factor-β family is of outstanding importance. Besides TGFβ, its members include activins, bone morphogenic proteins (BMP), myostatin, nodals, growth and differentiation factor (GFD)-8 and anti-Muellerian hormone (AMH). Whereas TGFβ shows a broad expression pattern, some of the other members are highly restricted to specific cell types. Alone or in concerted action they control cell division, differentiation and organization, adhesion and migration as well as homeostatic cell death and therefore play non-redundant functions in many biological processes from embryogenesis to immunity but have also been implicated in a multitude of pathological states including skeletal dysfunction, renal disease, fibrotic disorders, autoimmunity and tumorigenesis (reviewed in 220, 218, 219, 221-224). Potential interference of dysregulated signaling pathways using specific inhibitors reveals an emerging therapeutic field [225].

1.4.1   TGFβ isoforms [226]

In mammals TGFβ comes in 3 different, highly homologous isoform, termed TGFβ1 (19q13), 2 (1q41) and 3 (14q24) with the chromosomal localization in humans in shown brackets. The high homology between the isoforms is in marked contrast with the highly diverse phenotypes of the respective knockout mice. Different transcriptional and post-transcriptional regulation, resulting in non-overlapping expression and specific up-regulation under physiological and pathological conditions account for these differences.

In the embryo, the three isoforms show distinct expression patterns measured by in situ hybridization, whereby only TGFβ1 was clearly detected in the thymus as early as E12 [227,228]. Though the signal is dispersed throughout the thymic organoid at E12, expression seems enhanced within the lymphoid compartment [237]. The role of TGFβ during embryonic development was analysed using knockout mice for all three isoforms. Mice deficient for **TGFβ1** survive the postnatal period and show no overt signs of organ malformation or dysfunction. Yet, after weaning they rapidly succumb to a massive auto-inflammatory pathology with expansion and activation of T cells, production of large amounts of pro-inflammatory cytokines and infiltration of inflammatory cells into multiple organs [229]. Analysis of the contribution of TGFβ1 to organogenesis is however complicated by the pre- and postnatal transfer of significant amounts of TGFβ1 from heterozygous mothers to their TGFβ1-deficient offspring via placenta and milk [230]. This vertical transfer of TGFβ1 limits the analysis of detailed contributions of TGFβ1 to embryo- and organogenesis. Cardiac abnormalities comprising valve malformation, ventricular hypertrophy with disorganized proliferation of cardiomyocytes was detected in TGFβ1$^{-/-}$ pups born to a TGFβ1-deficient mother [230].

In contrast to the mild phenotype of TGFβ1-null pups, deficiency for **TGFβ2** results in early postnatal mortality due to a multitude of skeletal and organ malformations, in particular concerning lung, heart, inner ear and eyes as well as the urogenital tract [231]. Yet, defects in the lymphohematopoietic system have not been described, though a correlation between thymic involution and responsiveness of LSK cells to TGFβ2 was described (see section on '*thymic stroma*'). Besides defects in palate fusion mice lacking functional **TGFβ3** display no overt phenotype [232]. Interestingly, **TGFβ2-/- TGFβ3-/-** double knockout mice die during mid-gestation and show severe midline fusion defects, indicating a certain redundancy between the different isoform, which is consistent with the partial overlap found in expression studies [233].

The bioactivity of TGFβ isoforms is tightly controlled by several mechanisms (reviewed in 226). They are encoded as precursor proteins, proteolytically cleaved into the carboxy-terminal mature TGFβ (112 AA) and the 'latency associated peptide' (LAP, 100kDa), which then associates with the mature form to mask its binding domain. Formation of this complex is required for secretion, which occurs as a complex of LAP with the latent TGFβ binding protein (LTBP, 220kDa). LTB proteins stabilize latent TGFβ and anchor it to the extracellular matrix. Association of TGFβ with either of these proteins specifies the trafficking, localization and rate of release of the cytokine. Harsh physical conditions such as high temperature or extremes of pH denature LAP, whereas TGFβ itself remains intact. Under

physiological situations, proteases such as plasmin, thrombospondin-1, reactive oxygen species, and conformational changes of LAP induced by binding to extracellular matrix or immunoglobulin, initiate the release of active TGFβ. The integrins αvβ6 and αvβ8 interact with the amino acid sequence arginine-glycine-aspartic acid (RGD) near the C terminus of TGFβ-LAP, which releases active TGFβ possibly through conformational change of the LAP. A role for mechanical stress in the integrin-mediated activation of matrix-associated TGFβ by myofibroblasts was recently demonstrated [234]. Mice, in which systemic or conditional inactivation of these integrins or the RGD in the LAP sequence was achieved, recapitulate phenotypic characteristics observed in the absence of TGFβ signaling and demonstrate the importance of this interaction for the local control of TGFβ activity [235-237]. This is of particular relevance in the context of vasculogenesis, immune tolerance as well as for the formation of Langerhans cells [238,239]. External physical stimuli, such as injury or ionizing radiation also contribute to the activation of TGFβ from extracellular deposits [240,241], which has implications with respect to fibrotic processes or scar formation [242,243].

1.4.2 The signaling components

TGFβ utilizes several signaling pathways, whereby the best-studied, termed the canonical pathway, involves Smad molecules for transcriptional activation.

The sensing of TGFβ signals by a specific cell involves multiple steps. Homodimers of TGFβ1 or 3 directly bind to TGFβ receptor type II (TbRII), which is a constitutively active serine/threonine kinase. Cytokine binding allows for bi-dimeric complex formation of the type II receptor with the TGFβR I (TbRI, a.k.a. Alk5), which results in the phosphorylation of serine and threonine residues in the GS region – a regulatory region characteristic of type I receptors, sitting immediately upstream of the kinase domain. This phosphorylation leads to the release of the inhibitory factor FKBP12 from this region, allowing the binding of transcription factors of the Smad family.

In mammals, seven type I receptors, which are referred to as activin receptor-like kinases (ALK1-7), and 5 type II receptors (ActR-IIA, ActR-IIB, BMPR-II, AMHR-II and TbR-II) have been identified. In the case of TGFβ signaling the involvement of at least four different receptors was demonstrated (reviewed in 219) with TbRI (53kDa) and TbRII (70kDa) being presumably the main components for initiating TGFβ signaling. TbRIII (a.k.a. betaglycan) serves as an accessory receptor presenting TGFβ to TbRII, thus positively but also negatively influencing the activation of the cascade in a cell type-specific manner [244]. TbRIV was described in a rat cell line, but its identity and function remain to be further defined [245]. The TbRV is co-expressed with TbRI, II and III and in addition to enhancing TGFβ signaling is mediating IGFBP-3 signaling [246].

1.4.2.1 Smad proteins [247]

Intracellular key molecules of the canonical pathway, integrating and relaying signals of TGFβ are comprised of Smad molecules. Out of the eight Smad proteins encoded in the human and mouse genome, five – termed receptor-regulated (R-Smads) – serve as substrates for the serine/threonine

kinases of the type I receptors. Whereas Smad 1, 5 and 8 are utilized to transmit BMP and AMH signals, Smad2 and 3 mediate activin, TGFβ, and nodal signals.

Regulatory elements within the Smad family include Smad4 – a common partner to all R-Smads and therefore named Co-Smad – and the inhibitory factors Smad6 and 7. R-Smads consist of a N-terminal Mad homology (MH) 1 domain, required for nuclear translocation and DNA-binding activity, which is connected with a flexible linker region to an MH2 domain. The latter interacts with a multitude of other components such as the receptor, nucleoporins, partner Smads and other nuclear regulatory factors and thus controls cytoplasmic retention, activation, nucleocytoplasmic shuttling and gene transcription[248]. The receptor-associated Smad2 and 3 proteins are phosphorylated at the carboxy-terminal Ser-Xxx-Ser motif by the TbRI serine/threonine kinase. The interaction between between the activated receptor complex and R-Smads is greatly facilitated by Smad Anchor for Receptor Activation (SARA), a cytoplasmic protein, localizing non-phosphorylated Smad2 in close proximity to TbRI kinases [249]. Further adaptor molecules such as Axin or disabled 2 (Dab2) stabilize the receptor-Co-Smad complex (reviewed in 248). Subsequent phosphorylation leads to the formation of an active complex with the Co-Smad4, allowing nuclear accumulation of the R-Smads inducing transcription of target genes. In addition, Smad2-phosphorylation and nuclear translocation occurs without direct association with the TbRI and independent of the Ser-Xxx-Ser motif, through interaction with activated MAPK/Erk kinase kinase 1 (MEKK1) [250]. In a complex with other factors (in particular p300 or CBP) R-Smads regulate the level of transcription of TGFβ target genes. This seemingly simple and linear signaling pathway of TGFb gains a high level of complexity by input on several levels. The integration of the binary input signal into a cellular response varies greatly between different cell types, which forces studies of the cellular context. As DNA-binding of the MH1 domain of R-Smads is relatively weak, high specificity of transcription is achieved through a complex array of cell type- and context-specific transcriptional regulators and co-factors, of which further details and additional components are just emerging. An immediate gene response mediated via pre-existing co-factors versus late gene responses due to induced expression of co-factors has to be distinguished. Similar gene responses shared by different TGFβ family members due to usage of the same intracellular signaling molecules are referred to as synexpression groups, characterized by rapid activation and repression of hundreds of genes.

1.4.2.2 Regulation of Smad-mediated signaling

These growth and differentiation factors are subjected to tight regulation at different levels, either directly through expression, compartmentalization, modification and degradation of signaling components of indirectly via modification of the signal through co-factors. Receptor elimination from the cell surface is achieved via endosomal internalization. This compartimentalization of activated receptor-ligand complexes in endosomes furthermore enhances signaling through more efficient R-Smad recruitment, followed by receptor degradation. The expression of R-Smads and Smad4 underly temporo-spatial regulation during embryonic development [251] but are widely and constitutively expressed in the adult organism [252]. Compartmentalization of Smads through their association with cytoskeletal components such as microtubules reduces the proportion of protein available for

phosphorylation. Protein degradation is regulated by Smad-ubiquitination-regulatory factors (Smurf-) 1 and 2 [253]. Nuclear importation requires the conformational changes induced by C-terminal phosphorylation of the MH2-domain. The nuclear environment contains constant phosphatase activity. Dephosphorylated and thus inactivated Smads are rapidly exported from the nucleus. Input from signaling molecules other than TGFβ family members (such as HGF or EGF) can negatively influence the nuclear accumulation of R-Smads through phosphorylation of their linker region[254]. In contrast to R-Smads, inhibitory Smads 6 and 7 show a tightly controlled expression pattern. Smad7, which negatively regulates TGFβ-signaling, is induced by TGFβ itself, down-modulating the signal activity in a negative feedback loop [255]. The same mechanism is found for Smad6 in the BMP signaling pathway [256]. Smad7 associates in a complex with Smurf2, which is as a consequenc exported from the nucleus and associates with the activated TGFβR-complex. This leads to upiquitination and degradation of the activated receptors [257,258]. In addition, Smad7 nuclear export is induced rapidly after TGFβ stimulation and the MH2 domain of Smad7 binds to the type I receptor competitively preventing the association thereof with R-Smads. Interestingly, besides its inhibitory activity on Smad-mediated signaling, Smad7 itself is able to induce transcription of target genes, however cellular effects remains to be clarified [259].

In addition to these regulatory mechanisms, distinct pathways were shown to interact with the TGFβ-signaling cascade. Phosphorylation of Smad3 in response to TGFβ stimulation is negatively influenced by Jak1-STAT1-mediated IFN−γ signaling through the induction of Smad7 [260]. In addition, other pro-inflammatory cytokines, such as IL-1b and TNF-α up-regulate Smad7 via activated NF-κB signaling [261]. A further mechanism of negatively regulating the transcriptional activity of Smads is the phosphorylation of the linker region, containing Ser-Pro and Thr-Pro, by MAPKK, CamKII and CDK, which hinders nuclear accumulation and transcriptional activity or promotes 'enucleation' of Smads.

1.4.2.3 Transcriptional regulation

Depending on the recruited co-factors Smad complexes can both activate and repress transcription. CBP and p300 are of prime importance for DNA-binding in Smad-induced transcription [262], as R-Smads themselves (with the exception of Smad2) show a relatively weak DNA-binding activity, contained in the MH1 domain and restricted to Smad-binding elements (SBE). Despite its weakness, this interaction is nevertheless required for transcriptional activation. Smad4 stabilizes the complex formed by R-Smads, CPB/p300 and DNA. Transcriptional co-repressors include TGIF [263], Ski, SnoN [264]and Snip1. They assemble with the Smad/CBP/p300/DNA complex and with histone deacetylases. The relative protein levels of co-repressors and –activators determines the overall transcriptional response of the cell [263].

Enhancement of SnoN and Ski degradation by TGFβ in a Smad-dependent manner - thus reducing its own co-repressor - leads to immediate de-repression of TGFβ-signaling [265], which was recognized as a general early response of a multitude of cell types in response to TGFβ, whereas a delayed up-regulation of Ski provides feedback inhibition of the pathway.

1.4.2.4 Smad-independent TGFβ-signaling

Besides Co-Smad-independent signaling induced by Smad2/3-TIF1γ complexes, which regulate effector functions complementary to Smad2/3-Smad4 activity[267], it was recently appreciated that TGFβ can induce a cellular response even in the complete absence of Smad-phosphorylation [252]. Yu et al. were able to relate cellular responses to the different signaling pathways [268], demonstrating an absolute requirement for p38 MAPK activation in TGFβ-induced apoptosis and epithelial-to-mesenchymal transition (EMT), whereas R-Smads are required for EMT and independently regulate growth arrest. Other pathways, which are activated by TGFβ, include furthermore PI3 kinases, Rho family members and JNK. Yet, the links between the surface receptor and the activation of the kinases is to date largely unknown.

1.4.3 Cellular effects of TGFβ

1.4.3.1 General principles

Cellular effects regulated by TGFβ isoforms are cell proliferation, apoptosis and differentiation and extracellular matrix (ECM) production. TGFβ was primarily recognized as a growth inhibitory factor of most cell types (in particular epithelia) with the exception of mesenchymal cells [219]. Cell cycle arrest – in particular at the G1 to S phase transition – is achieved through transcriptional repression of c-myc, Id1-3, and cyclin-dependent kinases (CDK) as well as induction of CDK inhibitors such as p15 and p21 [252]. Induction or suppression of programmed cell death by TGFβ shows great variability between different cell types and only few of the key molecules have been identified to date. Epithelia can undergo apoptosis involving the TGFβ-inducible early-response gene (TIEG1) [271]. Smad-dependent upregulation of death-associated proteinkinase (DAPK) and SH2-domain-containing inositol-5-phosphatase (SHIP) in hepatocytes and hematopoietic cells, respectively, sensitizes these cells to apoptotic stimuli. Downstream molecules of the apoptotic pathway include bcl family members and effector caspases, which might themselves be subjected to regulation by TGFβ [272].

The most fascinating aspect of TGFβ family members might be their role in regulating self-renewal, lineage selection and differentiation into specific cell types, which is most prominent during embryonic development [273]. I will focus on the effects of TGFβ on thymocyte development.

1.4.3.2 TGFβ and thymocyte development

Early studies demonstrated an inhibitory role of TGFβ on IL-1-, PHA- or ConA-induced proliferation of thymocyte bulk cultures, in parts reversible by IL-2 [274,275], whereas IL-7-induced thymocyte proliferation was less susceptible to inhibition by TGFβ [276]. TGFβ stimulated the differentiation of CD8+CD3- cells from CD25+ CD4-CD8- cells [277], possibly representing intermediate single positive (ISP) thymocytes [278]. TGFβ is expressed by thymic epithelium in the outer cortex and inhibits cell

cycling of ISP as well as their progression to DP thymocytes [279]. Addition of TGFβ1 and -2 to fetal thymic organ cultures (FTOC) led to a partial block at the TN1 stage, reduced total cell recovery in a dose-dependent manner, affecting all cell populations with the notable exception of CD3+ SP8 [280]. Using human thymocytes in an *in vitro* system, Mossalayi et al. demonstrate a role for CD3+CD8+ thymocytes in the activation of TGFβ produced by TN cells, which in turn led to the inhibition of cytokine-induced TN proliferation [281].

Mice deficient for genes of the ligands or their receptors allowed studies of the *in vivo* role of TGFβ. Whereas the lack of TGFβ2 and -3 did affect proper formation of different organs and palate fusion respectively (see section 1.4.1), a regulatory function of TGFβ1 on peripheral T cell function was suspected, as corresponding knockout animals die due to a severe autoinflammatory disease a few weeks after birth [229,231,232]. These mice demonstrate increased levels of pro-inflammatory cytokines such as IFN-γ, TNF-α, IL-1β and MIP-1α in infiltrated organs [229]. Interestingly, prior to development of disease i.e. prenatally and in the second week of life, these mice show a significant decrease of thymic cellularity with enhanced thymocyte apoptosis, whereby inflammatory cytokines as possible factor could be excluded. A potential explanation was sought in a disturbed mitochondrial structure and membrane potential, as TGFβ1 co-localized with mitochondrial proteins. In addition, peripheral T cells showed increased susceptibility to apoptotic stimuli due to up-regulated pro-apoptotic signaling molecules (Fas-FasL, TRAIL, TNFR), which was however not demonstrated for thymocytes. This inclination for cell death was not reversible through the addition of exogenous TGFβ1 and was not seen in Smad-deficient T cells [282]. On the other hand, reports about development of thymocytes deficient in TGFβ-signaling are conflicting. TGFβRI and II-deficient animals die in midgestation (with no live embryos retrieved by E11) due to severe endothelial dysfunction and defects in vasculogenesis in the yolk sac and the embryo proper, and are therefore not amenable to thymic analysis. Erythroid and myeloid potential was intact in TGFbRI knockout precursors [283], which was confirmed using conditional inactivation in hematopoietic cells [284]. T cell development in the thymus was studied using conditional ablation of TGFβ-signaling by either expression of a dominant-negative TGFβRII (lacking signaling activity) directed to T cells (under the control of the murine CD4 promoter [285] or the human CD2 promoter/enhancer [286]) or by conditional ablation of TGFβRII expression (using Mx-Cre [287] or CD4-Cre mice [288,289]).

Yet, the role of TGFβ on thymic epithelial development in vivo has not been addressed.

2   Aim of the Thesis

The aim of this thesis is to elucidate the role of TGFβ-signaling in thymic epithelial cells in (A) their phenotypic development, (B) their potential to support thymopoiesis under steady-state conditions, (C) their involution and (D) their capability for self-regeneration and reconstitution of the T cell compartment myeloablative conditioning.

To this end, conditional inactivation of the TGFβRII specifically in thymic epithelium was applied. Furthermore, mice with inactived Ski – a negative regulator of TGFβ-signaling were analysed.

3 Results

3.1 TGFβ1-3 and the corresponding receptors are expressed in the area of the prospective thymus

The ventral aspect endodermal lining of the 3rd pharyngeal pouch on embryonic day (E)10.25 contains the precursor cells, that will give rise to the thymic epithelial compartment. In an attempt to uncover factors contributing to early thymic organogenesis, using laser capture microdissection this area was subjected to microarray analysis comparing the expression levels either to the dorsal region or the adjacent pouches. In the resulting screen TGFβ family members and the matching receptors as well as downstream molecules showed significant expression (Table 1 and K. Na, Y. Mathieu, G.A. Holländer, unpublished observations). Table 1 shows a summary of data obtained from microarray analysis of the 3rd pharyngeal pouch, as well as from semi-quantitative RT-PCR analysis of TEC at different stages of development and in the adult. In addition, the expression for TGFbRI and II are shown for the cortical and medullary thymic epithelial cell lines, established from neonatal C57Bl/6 mice as previously described [290,291].

3.2 Expression and protein levels of TGFβ in the adult thymus

Transcript levels for TGFβ isoforms were determined in whole adult thymi derived from C57Bl/6 mice at different ages (2, 5, and 24 months). Whereas only slight and transient increases in TGFβ1 levels over time were observed, TGFβ2 levels showed a steady increase with increasing age. As TGFβ is subject to a multitude of posttranscriptional and –translational changes, protein levels were determined in the very same thymi using an antibody detecting TGFβ1, -2, and -3 (clone 1D11). Figure 1B shows a striking, age-related increase of TGFβ protein in these thymi. In an attempt to identify the cell-type involved in the production of TGFβ, different thymocyte (Figure 1C upper panels) and stromal (Figure 1C, lower panel) subpopulation were subjected to intracellular staining for TGFβ1-3, demonstrating significant fractions of positively staining cells in the DN as well as in stromal fractions.

3.3 Thymic epithelial cell lines respond to human TGFβ1

Canonical TGFβ-signaling leads to rapid phosphorylation of Smad2. To measure the kinetics of Smad2 phosphorylation in the cortical TEC line TEC1.2, the cells were exposed to 10ng/ml TGFb1 and harvested at different time points thereafter. The left panel of Figure 2A shows a rapid phosphorylation of Smad2 within 15 minutes post-exposure which slowly declines over $\geq$ 1 hr. In addition, staining of fixed TEC1.2 cells for total Smad2 using a monoclonal antibody revealed that within 30 minutes post-exposure most of the cellular Smad2 translocates to the nucleus, whereas in unstimulated cells the majority of the protein localized to the cytoplasm (Figure 2A, *right panel*).

To investigate the cellular consequences of TGFβ1 on TECs, $1.5x10^5$ cells of different TEC lines were exposed to 10ng/ml human TGFβ1 for 48 hrs. One out of two similar experiments are presented. All of the analyzed cell lines – cortical as well as medullary – show reduced cell number after 48 hours

(Figure 2B) in the presence of the cytokine, however it only reaches statistical significance in the medullary TEC lines 2.3 and C6. To identify whether the reduced cell recovery is due to reduced cell proliferation or an increase in apoptosis or a combination thereof, the cells were again grown in the presence or absence of 10ng/ml human TGFβ1, and either pulsed with 3H-thymidine for the last 16 hours prior to harvest or prepared for cell cycle analysis. Figure 2C shows the quantification of 3H-thymidine incorporation, which is drastically reduced in the medullary TEC 2.3 and C6 and to a lesser extent in the cortical lines 1.2 and 1.4. This is consistent with a reduction of cells in G2/S phase from 13% (TEC 1.2) up to 56% (TEC C6) (data not shown). To discover whether TGFβ1 did induce apoptosis in these cells, they were stained with fluorochrome-labeled AnnexinV, which binds to phosphatidylserine residues in the outer membrane of apoptotic cells, and analyzed by flow cytometry. Dead cells – measured by their incapacity to exclude propidium iodide – were electronically gated out. The cortical TEC1.4 and the medullary TECC6 did show a significant increase in the apoptotic fraction (Figure 2D).

As TGFβ1 is known to induce several cyclin-dependent kinase inhibitors (CKIs) and to repress c-myc in a Smad3 dependent manner, transcriptional changes of these genes in the thymic epithelial cell line TEC1.2 in the presence or absence of TGFβ were assessed. The cells were cultured for 48hrs in the presence or absence of purified hTGFβ1 (10ng/ml) and subsequently analysed for transcriptional changes in the genes indicated in Figure 2E, demonstrating a down-regulation of c-myc and cell-cycle regulators, whereas p53 is up-regulated.

3.4   Effects of TGFβ1 on primary TEC in d-Guo depleted FTOC

To assess the effect of TGFβ1 on cellularity of primary TEC, independent of thymocyte-mediated effects, E15 fetal thymi were depleted of thymocytes using d-Guo for 7 days, washed in medium and exposed to 20ng/ml hTGFβ1 or culture medium for 40 hours. Thereafter, triplicates of pooled thymic lobes (10 each) were assessed for total cellularity, expression of MHC II (I-Ab), E-cadherin and ICAM-1 as well as Ki-67 antigen. Treatment with TGFβ1 significantly decreased total cellularity, in particular due to a significant reduction in EpCAM$^+$ I-Ab^{high} cells, whereas the remaining CD45$^+$ as well as the CD45$^-$ EpCAM$^+$ I-Ab^{low} cells were not significantly affected (Figure 3A).

Measuring Ki-67+ cells by flow cytometry revealed a significantly decreased proportion and absolute numbers of proliferating epithelial cells in TGFβ1-treated FTOC (Figure 3B). Again, proliferation of non-epithelial stroma was not significantly affected by the presence of TGFβ (data not shown).

3.5   Conditional ablation of TGFβRII specifically in thymic epithelium

Mice with a TEC-specific deletion of Smad4 display a dramatic reduction in thymic size, reduced numbers of ETP and pronounced thymic involution [292]. These results in conjunction with the aforementioned results prompted us to further investigate the involvement of TGFβ in TEC development and differentiation. To address this issue we wished to conditionally ablate a crucial component of the TGFβ signaling pathway within the developing TEC. However, to ensure adequate

specificity for TGFβ this element was required to be as far up-stream as possible in the signaling cascade, at best involved in ligand binding. As the TGFβ receptor type II (TGFβRII) constitutes a non-redundant component of the TGFβ -binding and -signaling complex it seemed an ideal target for our studies. The crucial contribution of the type II receptor to normal development was demonstrated from studies of TGFβRII knockout mice, which do not survive past E10.5 due to severe developmental defects, thus precluding the study of thymus development in these mice. Nevertheless, the availability of mice bearing alleles with a floxed exon of this receptor gave us the opportunity to study the effects of its conditional deletion specifically in thymic epithelial cells. This would also give us the opportunity to investigate FTOC in the presence of TGFβ to study its direct as well as indirect effects on thymocyte development via TEC.

3.5.1 Characterization of recombination using Cre expression driven under the control of the Foxn1 promoter

The transcription factor Foxn1 is specifically expressed in developing TEC during development, in a subpopulation thereof under steady-state conditions [8] as well as in precursor cells of the hair bulge. Mutations leading to inactivation of Foxn1 – first observed in the spontaneously appeared *nude* mice – arrests TEC differentiation at an early stage, which precludes immigration of thymocyte precursors into the rudiment and ultimately results in severe T cell immunodeficiency [6]. Driving Cre expression under the control of the Foxn1 promotor therefore provides an elegant and convenient way of conditionally (i.e. specifically in thymic epithelium) ablating genes, that show otherwise early embryonic lethality in the context of germline deficiency. However, as Cre-mediated recombination is occurring with a certain delay with respect to Foxn1 promoter activation, we wished to get an insight into the kinetics and completeness of recombination. To this end, we bred the Foxn1-Cre mice to different indicator strains, whereby expression of Cre will lead to recombination of the target sequence and lead to expression of either eGFP or β-galactosidase specifically in these cells, allowing the visualization and quantification of recombination as measured by β-galactosidase activity or GFP fluorescence.

Analysis of mice expressing the Cre recombinase and either LacZ under the ubiquitously expressed Rosa26 promoter or GFP driven by the chicken β-actin promoter, revealed Foxn1-Cre-mediated recombination (with subsequent β-galactosidase activity) as early as E12 in the thymic primordium (SZ, unpublished observation). By flowcytometric analysis of E15 embryos, eGFP expression was consistently detected in over 80% of thymic epithelial cells, a feature, which persisted until at least 4 weeks after birth (Fig. 4A, upper panels). Thymocytes on the other hand did not express detectable eGFP levels (Fig. 4A, lower panels), consistent with the fact, that they do not express Foxn1 at any stage of their development.

3.5.2 The *Cre* recombinase protein is barely detectable by flow cytometry in TEC from Foxn1-Cre mice

Foxn1 expression was reported for thymic stroma in the adult mouse [165]. Foxn1-promoter driven Cre expression measured on the protein level could be detected by flow cytometry in the adult animal (Fig. 4B) only as a slight shift in a histogram of the MHC class II^{high} population (Figure 4B, left histogram), though not in MHC class II^{intermediate} cells (Figure 4B, right histogram). Thymic epithelial cells derived from a mouse expressing Cre protein under the promotor of the *Auto*immune *Re*gulator served as positive control for the staining and showed a intermediate expression levels of Cre protein in a subpopulation of MHC class II^{high} cells (Fig. 4B, *right panel* and N. Shikama-Dorn, unpublished observations), which is consistent with previously reported expression of Aire in a subpopulations of MHC class II^{high} cells.

Whether the weak signal observed was due to low amount of protein produced or absent transcription or translation respectively has not been verified, and whether Cre protein is detectable at higher levels during embryonic stages remains to be tested.

3.5.3   Hoxa3-Cre is active prior to Foxn1-Cre

Induction of the thymic primordium is independent of Foxn1, concordant with the finding that expression of Foxn1 is first detected around E11.5 [8]. Cre expression driven under the Foxn1 promoter can therefore be expected around this developmental stage, whereas recombination and consecutively loss of transcription of the target gene will follow with a certain delay. Effect(s) of the loss of the protein would thereafter only be recognizable at a relatively late time point – probably within 24-48 hrs after expression of Foxn1 – depending on the half-life/turnover of the protein. As Foxn1 is itself not required for inductive events during thymic organogenesis [6]. Therefore, the Foxn1-Cre mouse is not suitable to study these early events.

To bypass the potential problem of conditionally ablating our gene of interest only late in development, we chose to make use of a knock-in mouse, expressing Cre under the control of the Hoxa3 locus [14]. As published previously, Hoxa3-Cre expression is by no means restricted to thymic epithelium (Figure 5A, top panel), as the GFP-reporter ::Hoxa3-Cre E10.25 embryo shows strong GFP expression downwards of the neck region, sparing the head. Analysis of crossings to the aforementioned reporter lines showed recombination as early as E10.25 in the pharyngeal region, with β-galactosidase activity detectable caudally from the second pouch (Figure 4A, middle and lower panel). In E14 and E19 embryos as well as adults flowcytometric analysis revealed a strong GFP signal in literally all thymic cells of epithelial kind (Figure 5B, top panels) but only in a small fraction of hematopoietic (Figure 5B, middle panels) or non-epithelial stromal origin (Figure 5B, lower panels), disclosing a relatively high specificity of Hoxa3 expression for thymic epithelium. As conditional deletion of Smad4 in thymic epithelium using the Cre-recombinase driven under the Foxn1 promoter has dramatic effects on thymic cellularity and the phenotype of thymic epithelium we used this mouse as a 'functional reporter' to study whether Hoxa3-Cre-mediated deletion would result in a more severe phenotype. Smad4$^{lox/lox}$::Hoxa3-Cre embryos died at E9.5 and only an unrecognizable mass could be recovered at E11.0 (Figure 5C, *right panel*). Despite the impracticality to retrieve a structure reminiscent of a

thymus, this was nevertheless important evidence for the 'high fidelity' of the Hoxa3-promoter driven Cre expression.

3.5.4   Lefty-Cre is not useful for conditional inactivation of genes in mesenchymal cells

Organogenesis in general involves the interaction of epithelial with mesenchymal cell types. The importance of mesenchyme as a support for the expansion – but not for the differentiation – of thymic epithelium during organ formation has been described [50,293]. The idea of conditionally ablating genes in mesenchymal cells, supporting the developing TEC, was of particular interest, as this would reveal the contribution of identified factors on mesenchymal behaviour *in situ* [i.e. without removing the thymus from the developing organism]. To date no mesenchyme-specific promoter region has been identified, that would allow the specific and extensive (i.e. involving a high fraction of cells) recombination in stromal cells of mesenchymal origin surrounding the thymus. Cre recominase expression under the control of the lefty promoter, a mouse generated in A.Moons laboratory in Salt Lake City, was reported to show mesenchyme-specific expression (A.M., personal communication). To test the specificity of Cre expression this mouse was again crossed to the previously mentioned reporter strains. GFP was detected in the upper part of the embryo at E14 (Figure 6Ai). Yet, whereas a strong expression of β-galactosidase activity was detected e.g. in the mesenchyme of the developing lung or in the heart, no such expression was detected in peri-thymic or thymic mesenchyme (Figure 6Aii-iv) in E14 embryos. In E17 thymi only a fraction of endothelial cells revealed expression of the enzyme (Figure 6B, upper and lower panel), whereas in thymi from newborn mice also cells in subcortical areas indicated expression (Figure 6Ci, ii). Furthermore, flowcytometric analysis of adult thymic tissue demonstrated recombination not only in a small fraction of mesenchymal cells (ERTR7+, CD31+) but also in a minority of HSC-derived cells (thymocytes, CD11b, CD11c, CD11b/c) (Figure 6Ci-iv), making the use of this mouse unsuitable for further studies.

3.6   Conditional ablation of TGFβRII

Mice carrying floxed alleles of the TGFb receptor type II – hereafter described as TGFbRII[lox/lox] were generated in different laboratories. We obtained the mice bearing a LoxP-sites flanked exon 3 of the TGFbRII as a kind gift of Dr. J. Roes, London. Cre-mediated recombination results in direct splicing of exon 2 to exon 4, which creates a frameshift mutation generating a stop codon. Translation therefore terminates before the transmembrane domain with complete loss of functional receptor activity [294].

3.6.1   TGFbRII[lox/lox]-Foxn1::Cre mice are viable, fertile and show no macroscopical changes of epidermal appendages

The offspring of the crossing TGFβRII[lox/lox]::Foxn1-Cre x TGFβRII[lox/lox] showed a mendelian distribution of genotypes, with 191 (50.1%) of animals expressing Cre recombinase of 381 animals analysed (Figure 7A). Cre positive mice showed normal viability (up to 72 weeks observed) and

fertility. Foxn1-Cre activity was tested on resting as well as on branching and differentiating mammary glands during pregnancy using the Rosa26-lacZ reporter strain. Whereas no or very little β-galactosidase activity was detected in mammary glands derived from nulliparous adult Rosa26-lacZ::Foxn1-Cre positive female mice, branching epithelia showed intense substrate deposition (data not shown). It was therefore of interest, whether TGFβRII$^{lox/lox}$::Foxn1-Cre mothers were able to sufficiently lactate in order to sustain normal litter sizes. Indeed, litter sizes until weaning were comparable to Cre negative females.

Foxn1 expression was furthermore reported for the matrix, cortex and outer root sheet of the hair during the anagen phase and the nail forming regions with a role in inducing keratin expression [10]. Superficial layers of the adult skin revealed β-galactosidase activity in Rosa26-lacZ::Foxn1-Cre mice (data not shown). However, no macroscopically obvious defect of hair or nail development was discernible (data not shown).

3.6.2 Hoxa3-Cre-mediated deletion of th floxed TGFβRII allele results in mid-gestational lethality

In contrast to TGFβRII$^{lox/lox}$::Foxn1-Cre mice, Hoxa3-Cre expression in conjunction with two floxed alleles of the TGFβRII is embryonic lethal. A more careful analysis of genotypes at different embryonic stages revealed frequencies in accordance with Mendelian expectations in E12 or E13 TGFβRII$^{lox/lox}$::Hoxa3-Cre embryos. However, E13 TGFβRII$^{lox/lox}$::Hoxa3-Cre embryos were slightly smaller and showed a delayed development (upper extremities, separation of fingers). On embryonic day 14 a smaller than expected ratio of embryos with the genotype of interest could be recovered (Figure 7B). These embryos showed furthermore a pronounced delay in development (smaller in size, delay in developmental milestones), a protrusion of the thinned frontal abdominal wall, and irregularly structured blood vessels, sometimes accompanied by hemorrhage. Intact thymic lobes could be recovered as late as E13.5 and used for further studies (see below). However the isolated lobes were usually smaller than those derived from their Cre- littermates. Thus, for transplantation experiments thymic lobes derived from E12.5 embryos were chosen. It is of interest to note that in the presence of Hoxa3-Cre expression one wildtype TGFβRII allele was sufficient to protect the developing embryo from these adverse effects.

Genotyping adult offspring from TGFβRII$^{lox/wt}$::Hoxa3-Cre x TGFβRII$^{lox/lox}$ breedings revealed that most mice devoid of the Cre knock-in were either homozygous for the floxed allele or heterozygous for the floxed and the wildtype allele. However, in some of the Cre negative offspring a deleted allele besides a wildtype or a floxed allele (see also Figure 9B) could be identified. This indicates that in TGFβRII$^{lox/wt}$::Hoxa3-Cre animals Cre-mediated recombination in germ cells can occur.

3.6.3 TGFβRII$^{lox/lox}$::Foxn1-Cre mice display normal thymic migration and architecture

Conditional deletion of the receptor in thymic epithelium showed no influence on migration of the developing thymus, as final positioning of the thymus, as exemplified in 3-week-old mice (Figure 8A)

was normal. Hematoxylin/Eosin staining of thymic sections of 3-week-old mice showed a clear distinction of cortex and medulla, typical for normal thymic tissue (Figure 8B). Confocal microscopy moreover revealed no evident differences between Cre positive or negative littermates in the frequency or distribution of ERTR7+ fibroblasts or distinct cortical or medullary TEC subpopulations, evaluated for expression of Keratin 5 (K5), Keratin 8 (K8) and UEA-1 [30] (Figure 8C-F') as demonstrated for young (i.e. 5 week old) mice.

3.6.4 The floxed TGFβRII alleles are efficiently and specifically recombined in Foxn1-Cre expressing mice at embryonic day 14

To verify, that Cre recombinase did specifically and efficiently excise the floxed alleles of TGFβRII, sort purified TEC and dendritic cells from individual mice were subjected to PCR analysis of the isolated genomic DNA. Purity of the obtained cell populations usually reached 93-95% for TEC and >95% for DC. Whereas no deletion could be detected in DC, TEC showed a high level of recombination on the DNA level (Figure 9A, left side). Nevertheless, a small band characteristic for the floxed allele was apparent. The same analysis was performed on sort-purified TEC and DC derived from TGFβRII$^{lox/del}$::Foxn1-Cre (i.e. crossed previously to a general deleter in order to obtain one deleted allele), which reduced the signal from the floxed band to barely detectable (Figure 9A, right side). In addition, sorted thymic epithelium (CD45- EpCAM+, purity >99%) from E14 thymic lobes was subjected to PCR of genomic DNA to examine deletion at this early time point. As shown in Figure 9B, roughly 10^3 TEC from TGFβRII$^{lox/lox}$::Foxn1-Cre mice showed a very high level of deletion of the floxed alleles of TGFβRII, indicated by the absence of a 'flox' band (left lane), whereas a 'flox' band in sorted TEC from Cre- littermates but none for the deleted allele could be detected (Figure 9B, right lane).

To test the deletion efficiency in TGFbRII$^{lox/lox}$::Hoxa3-Cre TEC, E13 thymi were cultured for 5 days *in vitro* in the presence of deoxy-guanosine, in order to deplete the lobes from developing thymocytes. Analysis of the collapsed thymic rudiment for excision of the floxed sequence gave a similar result as observed with the Foxn1-Cre driver (Figure 9C). It has to be taken into consideration, that d-Guo depleted fetal lobes contain a significant number of non-epithelial stromal cells (20-30%) that may contribute non-recombined genomic DNA.

3.6.5 Hoxa3-Cre-mediated deletion of the TGFβRII allows normal T cell development in short-term fetal thymic organ cultures

The fact, that intact TGFβRII$^{lox/lox}$::Hoxa3-Cre embryos can be obtained up to 13.5 days post-conception allowed us to investigate the potential of the developing thymic lobes to support T cell development of the first wave of precursors that have reached the organ by that time. As recombination in the HSC-derived cells at this point is minimal (see Figure 5B), the effect of missing TGFβ signaling in developing T cells were assumed to be minimal. Isolated, untreated thymic lobes were cultured for 14 days and thereafter assessed for ongoing thymocyte development. As shown in Figure 10, no

significant differences in thymocyte subpopulations could be detected. As digestion was used to obtain a single-cell suspension, the CD4-CD8 double-negative (DN) stages were excluded from the analysis, since this heterogenous population also includes stromal cells, which cannot be safely gated out by forward scatter and side scatter characteristics.

3.6.6 Deletion of TGFβRII in the thymic epithelial compartment is associated with an increase in thymic cellularity

To test whether Foxn1-specific deletion of the TGFβRII did affect T cell development, cell counts and characterization of thymocyte subpopulation by flow cytometry at different time points was performed. Whereas thymic cellularity in TGFβRII$^{lox/lox}$::Foxn1-Cre mice was comparable to control littermates pre- and postnatally up to 4 weeks of age, a consistent and age-dependent increase in thymocyte numbers was noted in Cre-positive animals, with an onset shortly after weaning (5 week old mice: +10%) reaching an increment of > 40% in 16-month old mice (Figure 11A, B).

A similar effect was seen when transferring lymphocyte-depleted E12.5 or E13 thymic lobes from Hoxa3-Cre crossings under the kidney capsule of C57Bl/6 *nude* mice. In general, these grafts are rapidly vascularized and repopulated by T cell precursors. Peripheral T cells were detected as early as 4 weeks after transplantation (data not shown).

Despite their usually smaller size, implants derived from TGFβRII$^{lox/lox}$::Hoxa3-Cre$^{+/-}$ embryos engrafted with similar efficiency (usually 90-100%) as the controls, which contained either a wildtype allele of the TGFβRII or lacked the Cre insertion into the Hoxa3 locus. Sections of grafts were comparable with respect to cortico-medullary demarcation and TEC subpopulations when subjected to H&E staining and immunofluorescence (Figure 12A). Two to three months after transplantation the heterotopic thymus along with the spleen were analysed for T cell development and reconstitution of the periphery. The cellularity in thymi containing TGFβRII-deficient TEC dramatically exceeded the cell number in the control transplants (containing the genotypes TGFbRII$^{lox/wt}$::Hoxa3-Cre, TGFbRII$^{lox/wt}$ and TGFbRII$^{lox/lox}$) by roughly 2.5 fold (Figure 12B). Similar results were obtained in 3 independent experiments.

3.6.7 TGFβ-unresponsive TEC support normal T cell development

To assess whether the increase in cellularity in TGFβRII$^{lox/lox}$::Foxn1-Cre mice is attributed to a specific subpopulation of thymocytes, cell suspensions of thymi at different post-natal stages were stained for classical markers characterizing T cell development.

In general, none of the steps in thymocyte progression was obviously affected, as all populations examined were present (Figure 13A). In particular, there was no difference in relative numbers of early thymocyte precursors on young and aged mice between the groups (Figure 13B) and absolute amounts of the different DN stages (Figure 13C) did not differ.

3.6.8 The increase in SP thymocytes found in TGFβRII[lox/lox]::Foxn1-Cre mice is due to an accumulation of mature SP

A small but significant relative and absolute increase in CD4+ or CD8+ single-positive thymocytes is observed in TGFβRII[lox/lox]::Foxn1-Cre mice in comparison to wildtype littermates as early as 5 days post-partum and increasing with age, summarized in Table 2. In accordance, this is associated with an augmentation of CD3^{high}/TCRb^{high} thymocytes. SP thymocytes undergo a phase of intrathymic maturation within the medulla. These maturational steps include important processes such as negative selection, up-regulation of homing receptors for periphery (CD62L) and are characterized by down-regulation of CD24 and CD69 [39,88,96,97,110].

The increase in SP thymocytes observed in TGFβRII[lox/lox]::Foxn1-Cre mice is due to an accretion of TCR^{high} CD24^{low} cells (Figure 14A) corresponding to mature T cells, ready for egress. Numbers of CD44^{high} SP T cells, i.e. activated or memory T cells recirculating from the periphery do not differ between the groups (data not shown). Both, CD4 and CD8 SP populations however show an increase in frequency and absolute numbers of SP TCR^{high} CD62L^{high} thymocytes in TGFβRII[lox/lox]::Foxn1-Cre mice compared to their wildtype littermates (Figure 14B). The fluorescence intensity of the CD62L^{high} thymocyte populations is furthermore increased in Cre positive mice (Figure 14C). The relative shift towards a more mature phenotype was also reflected in the characterization according to CD69 and TCRb expression. Thymocytes up-regulate CD69 and TCR expression once they receive a positive selection signal. Cre-expressing mice showed significantly enlarged populations of TCR^{high} CD69[positive] and in particular TCR^{high} CD69[negative] thymocytes (Figure 13D). Analysis of TGFβRII[lox/lox]::Hoxa3-Cre thymic transplants into *nude* mice gave a similar picture with a relative increase in CD3^{high} and SP thymocytes by roughly a factor 2 (Figure 14E).

Possible mechanisms for accumulation of mature thymocytes include (A) an increased passage time due to decreased export frequency, (B) an augmented post-selection expansion with normal passage time or (C) alterations in the medullary stromal compartment with a corresponding increase of medullary thymocyte numbers without changes in the velocity of their passage through the thymus.

3.6.9 Analysis of proliferation of mature SP

Several studies have denoted the occurence of a post-selection expansion of mature, pre-migrant thymocytes. Ernst et al. were the first to identify a SP thymocyte population incorporating BrdU in reaggregation cultures of DP with fetal thymic epithelium and and in the normal neonatal thymus. They also proposed a microenvironmental factor – potentially TEC-derived cytokines – responsible for this marked proliferation [88]. It was later shown by Hare [111] et al. that this expansion was in parts IL-7 dependent. To determine whether the increase in SP was due to the more pronounced proliferation of the most mature subset in Foxn1-Cre+ mice, CD24[neg/low] SP were assayed for DNA content and BrdU-incorporation. Neither CD4 nor CD8 SP CD24[neg/low] cells from TGFβRII[lox/lox]::Foxn1-Cre mice showed more incorporation of BrdU after 2 pulses of BrdU within 6 hrs (Figure 15B, left panel) nor higher

DNA content (Figure 15B, right panel), ruling out the possibility of an increased post-seletion expansion.

3.6.10   Adult TGFβRII$^{lox/lox}$::Foxn1-Cre mice display a reduced thymic export in relation to intrathymic SP, although not in absolute numbers

To test whether thymic export is impaired in the absence of TGFβ-signaling in TEC, mice were injected intrathymically with FITC, which is passively taken up by the thymocytes. 20-22 hours after injection recent thymic emigrants (RTE), i.e. FITC+ CD4+ or CD8+ T cells in spleen and lymph nodes, were quantified by flowcytometry and related to intrathymic FITC+ SP cells. As shown in Figure 16A, the number of SP exported from TGFβRII$^{lox/lox}$::Foxn1-Cre thymi in relation to the total number of SP thymocytes is significantly smaller in comparison to their wildtype counterparts. This is true both for CD4 as well as CD8 SP. However comparison of the absolute number of exported single positive cells shows no significantly different amount of RTE in the periphery (Figure 16B).

3.6.11   Export of mature T cells is delayed in neonatal TGFβRII$^{lox/lox}$::Foxn1-Cre mice

Egress of naïve T cells from the newborn thymus provides a different approach to quantify thymic egress, as in mice T cells are exported from the thymus only after birth. However, it is crucial to find the right time point to measure export: adequately late after birth, to be able to reliably measure peripheral T cells, yet early enough not to miss a potential difference as a result of peripheral expansion of the T cells in response to homeostatic signals provided by an "empty periphery".

Whereas three days post-natal thymic cellularity or intrathymic SP (Figure 17A, left panel) numbers do not differ, absolute numbers of splenic $CD4^+$ and $CD8^+$ T cells are – although statistically not significantly – reduced in mice with conditional ablation of TGFβ signaling in TEC (Figure 17A, right panel), showing one out of three comparable analysis). Whereas differences in absolute numbers of peripheral T cells did not reach statistical significance between the groups, pooling the average of the frequencies of splenic $CD4^+$ and $CD8^+$ T cells showed a significantly increased frequency in $CD8^+$ T cells 3 days after birth using a paired T-test (Figure 17B, *right panel*).

3.6.12   S1P$_1$ expression by SP thymocytes

Egress of mature SP thymocytes was shown to be regulated by the sphingosine-1-phosphate receptor 1 (S1P$_1$), which is rapidly up-regulated upon maturation of SP thymocytes [116]. FACS-sorted immature (CD24^{high}) and mature (CD24$^{low/neg}$) were analysed by quantitative PCR for S1P$_1$ mRNA levels. As expected, there is a dramatic – roughly 9 fold – increase in S1P$_1$ expression in mature vs. immature SP of S1P$_1$ in both groups (Figure 18, *left panel*). However, comparison of S1P1 transcript levels in mature SP of Cre+ mice revealed similar levels compared to wildtype littermates (Figure 18, *right panel*).

3.6.13 RTE and TCR repertoire in one year old TGFβRII$^{lox/lox}$::Foxn1-Cre and TGFβRII$^{lox/lox}$ mice

The immediate consequence of thymic involution is a reduction of thymic output, which can be related to TREC+ T cells in the periphery. This appears later as skewing of the TCR repertoire due to unequal peripheral expansion of different TCRVβ specificities. TREC copies were quantified in splenocytes from TGFβRII$^{lox/lox}$::Foxn1-Cre and control mice. In two experiments performed, Cre+ mice showed an increase of roughly 30% in TREC copies among their splenocytes. Statistical significance was however not reached. One experiment is shown (Figure 19A). In addition Vβ TCR specificities were analysed in one-year old mice, which did not show a skewing of the repertoire (Figure 19B) in either group.

3.6.14 Analysis of peripheral T cells in young and middle-aged mice

The peripheral T cell pool is comparable between TGFβRII$^{lox/lox}$::Foxn1-Cre and control littermates concerning $CD3^+$ $CD4^+$ and $CD3^+$ $CD8^+$ cells in young (10 week old, Figure 20A, left and middle panel) and middle-aged (27-30 week old, Figure 20B, left and middle panel). However, whereas the number of $CD44^{high}$, i.e. activated/memory T cells is similar in the young mice (Figure 20A, right panel), it is significantly reduced in middle-aged Cre+ mice in comparison to control littermates (Figure 20B, right panel). α-CD3/α-CD28-induced proliferation of splenocytes derived from young (data not shown) and middle-aged mice (Figure 20C) did not differ between the groups.
C57Bl/6-*nu/nu* mice grafted with d-Guo-depleted E12.5 thymi derived from TGFβRII$^{lox/lox}$::Hoxa3-Cre and control embryos showed comparable number (Figure 20D) and distribution (data not shown) of peripheral B and T cells.

These results demonstrate the indirect effects of abolition of TGFβ-signalling in TEC on thymocyte development. A second set of experiments was designed to identify alterations of TEC in order to explain these findings.

It is well known, that TGFβ negatively regulates the proliferation and induces the differentiation of epithelial cells. Direct evidence for its involvement in proliferation and differentiation in thymic epithelium is however lacking.
Among the questions to address was whether the increase in thymic cellularity in TGFβRII$^{lox/lox}$::Foxn1-Cre was associated with higher TEC numbers or whether an equal number of qualitatively superior epithelial cells supported higher numbers of thymocytes. In addition, does TGFβ affect the survival and/or sustained proliferation of TEC and could thus the mitigated though not abolished thymic involution be explained? How would thymic epithelium non-responsive to TGFβ behave and regenerate in the context of acute 'stressors'? What changes in the epithelial compartment – if any were to be found – could explain the increased fraction of mature thymocytes?

3.6.15 Thymic epithelium is quantitatively and qualitatively altered in the absence of TGFβRII-mediated signaling

Thymic epithelial cells in control littermates show a gradual decline with increasing age (Figure 21A). In contrast, TEC numbers in 28 week old TGFbRII$^{lox/lox}$::Foxn1-Cre mice are unaltered in comparison to 8 week old animals. At the age of 64 weeks Cre+ animals also display a reduction of thymic epithelial cell numbers. Nevertheless, their numbers are statistically increased in comparison to wildtype littermates (Figure 21A). TEC populations can be distinguished according to different MHC II expression levels, i.e. MHCII^{high} and MHCII^{intermediate}. In young mice, i.e. at the age of 8 weeks, no difference in absolute cell numbers of MHCII^{intermediate} TEC was found between the groups, whereas at all time points tested the MHCII^{high} population was significantly increased in Cre+ mice (Figure 21A,B). Further characterization of TEC includes markers to distinguish medullary from cortical epithelium. Most of the MHCII^{high} TEC population is derived from the medulla and can as such be identified according to reactivity with UEA-1. As expected, the majority of MHCII^{high} TEC bound to UEA-1 (Figure 21B) in both mutant and wildtype mice. However, there was a roughly twofold relative increase of MHCII^{high}UEA-1^{+} TEC in TGFβRII$^{lox/lox}$::Foxn1-Cre mice when compared to control littermates (Figure 21B).

To test, whether the sustained TEC number in 28 week old TGFβRII$^{lox/lox}$::Foxn1-Cre mice was associated with an increased proliferative capacity of TEC, mice at the age of 4 month were supplied with BrdU in their drinking water for a period of two weeks. Thereafter, TEC were assessed for incorporation of BrdU into their DNA as an estimate of their proliferative history. Indeed, TGFβRII-deleted TEC showed a roughly 50% higher frequency of BrdU+ cells (Figure 21C).

In addition, the phenotype of TEC derived from TGFβRII$^{lox/lox}$::Hoxa3-Cre show similar characteristics with respect to MHCII expression and UEA-1 reactivity (Figure 21B).

3.6.16 Thymic architecture in aged mice is comparable between TGFβRII$^{lox/lox}$::Foxn1-Cre and control mice

To assess whether thymic architecture was significantly altered in aged mice, section of thymi derived from 54 week old TGFβRII$^{lox/lox}$::Foxn1-Cre and control mice were subjected to H&E (Figure 22 i-iv) and immunofluorescence staining (Figure 22 v-viii). There is a considerable increase in the area of thymic crossection derived from Cre+ mice in comparison to Cre- animals (Figure 22, i&i). Staining for the basic stromal markers cytokeratin (CK)-5, CK18 and ERTR7 for the different medullary and cortical, as well as mesenchymal cell types do however not show any overt differences (Figure 22, iii-viii).

3.7 Thymic reconstitution following lethal irradiation and BMT

The link between ionizing radiation, activation of TGFβ and subsequent tissue fibrosis was recognized already some time ago. In preclinical tumor models it was demonstrated, that inhibition of TGFβ-

activity following irradiation has beneficial effects in protecting healthy tissues from fibrosis, whereas transformed tissue was rendered more susceptible to irradiation treatment (reviewed in [242]). Recently, an *in vitro* study has reported, that apoptotic thymocytes – induced by irradiation or glucocorticoids – release active TGFβ1, which exerts immunosuppressive effects [216].

Therefore, I wished to test (A) whether – and if yes, by what cell type – TGFβ is produced *in vivo* within the thymic confines after lethal irradiation, (B) whether the action of TGFβ on TEC has consequences on the speed of thymic immune recovery after irradiation.

3.7.1 Thymic TGFβ1 levels are rapidly up-regulated following lethal irradiation

Quantification of TGFβ1 protein by ELISA in whole thymic lysates derived from lethally irradiated mice shows a 20 fold increase within 24 hours compared to non-irradiated controls (Figure 23A). RNA message of TGFβ1, measured two and four days after irradiation demonstrates augmented de novo transcription of the cytokine (Figure 23B). To identify the cell type involved in the production, intracellular staining and consecutive flow cytometric analysis at different time points after irradiation was performed. As shown in Figure 23C, the fraction of TEC staining positive for TGFβ increased from around 20% in non-irradiated mice to over 90% 40 hours after lethal irradiation, whereas non-epithelial stromal cells did not show changes in reactivity to this antibody. In non-irradiated animals immunohistochemical detection revealed the previously described reticular pattern of active TGFβ1 [279], mostly localized to subcapsular and cortical areas (Figure 23D i&ii), a feature which was very similar to the staining for LAP (Figure 23D iii&iv). 24 hours after lethal irradiation immunoreactivity for TGFβ1 localized to specific foci, spread throughout the cortex and to a lesser extent the medulla (Figure 23D v&vi)., whereas LAP was barely detectable by these means (Figure 23D vii&viii). In addition, detection of phosphorylated Smad2, as a measure of active TGFβ-signaling, by Western blotting of whole thymic lysates was much more pronounced in irradiated mice (24 hours post-irradiation) than in non-irradiated thymi (Figure 23E). Lethal irradiation led to a dramatic reduction of TEC numbers 6 days after irradiation, with a roughly 8-fold reduction of the MHCII^{high} and a 5-fold reduction of the MHCII^{intermediate} populations (Figure 23F).

3.7.2 Abrogated TGFβ-signaling in TEC enhances thymic reconstitution after lethal irradiation

Our *in vitro* studies demonstrate an antiproliferative and pro-apoptotic effect of TGFβ on TEC. The observed increase in TGFβ levels early after lethal irradiation potentially affects ongoing thymocyte development from residual T cell precursors at the DN stage, on the other hand there might be negative effects of TGFβ on cell death, proliferation and function of thymic epithelium. To test, whether abrogation of TGFβ-signaling in TEC affects reconstitution, TGFbRII$^{lox/lox}$::Foxn1-Cre and control littermates were lethally irradiated and reconstituted with T-cell-depleted bone marrow (TCD-BM). At early time points after irradiation – namely on day 4, 9 and 14 – an equal to or more than 2-fold increase in thymic cellularity was observed in mice with TGFβ-unresponsive TEC (Figure 24A). Four

weeks after transplantation thymic cellularity was slightly, but not significantly higher in TGFβRII$^{lox/lox}$::Foxn1-Cre mice compared to controls. Analysis of thymocyte subpopulations on day 14 post-irradiation showed an equal relative distribution between the two groups in CD4 versus CD8 FACS blots (Figure 24B). Analysis of DN populations revealed a normal relative distribution (data not shown) with a drastic increase in absolute numbers of the different populations (Figure 24C).

3.7.3 The TEC compartment in TGFβRII$^{lox/lox}$::Foxn1-Cre mice is partially protected from irradiation-induced cell loss

As demonstrated in Figure 23F, irradiation drastically reduces thymic epithelial cellularity. I therefore assessed the absolute numbers of thymic epithelium in TGFβRII$^{lox/lox}$::Foxn1-Cre mice and controls on day 4 and 9 after letal irradiation. Whereas TEC cellularity of non-irradiated mice did not differ between the groups (0.42 x10^6 ± 0.07 x10^6 vs. 0.41x10^6 ± 0.07 x10^6, p>0.05, for TGFβRII$^{lox/lox}$::Foxn1-Cre and TGFβRII$^{lox/lox}$ respectively) epithelial cell numbers were drastically reduced in both groups, although in Cre+ mice to a lesser extend (Figure 25A). The difference was most prominent on day 4, and still significant on day 9 after irradiation.

Two days post-irradiation lysates of whole thymi were assessed for a comparative analysis of transcript levels of pro-survival factors. Whereas neither the expression levels of CXCL-12, CCl25 nor IL-7 did differ between the groups, c-kit ligand showed a 2.5 fold up-regulation in thymi from TGFβRII$^{lox/lox}$::Foxn1-Cre mice in comparison to those from control mice (Figure 25B).

3.7.4 Exogenous inhibition of TGFβ prior to irradiation and TCD-BMT enhances early thymic reconstitution

Inhibition of TGFβ provided by neutralizing antibodies or TGFβRI kinase inhibitors has proven a safe and effective mean in the context of irradiation damage [242]. I therefore used purified antibody, reactive to and previously shown to neutralize the TGFβ1-3 isoforms. Two times 450μg per mouse 3 and 0.5 hours prior to lethal irradiation did not affect total thymic cellularity and TEC numbers on day 4 after irradiation (Figure 26A). On day 14 however, there was a substantial – yet statistically not significant – increase in thymocyte (Figure 26A) and a slight, but statistically significant increase in TEC numbers (Figure 26B).

3.7.5 Enhanced thymic reconstitution following lethal irradiation and TCD-BMT requires functional Smad4 but is independent of c-myc expression in thymic epithelium

The common Smad4 is required for mediating signals along the canonical pathway induced by TGFβ family members [295]. C-myc on the other hand is a well-known target gene of the TGFβ signaling pathway, whereby TGFβ negatively regulates c-myc expression, thus inhibiting cell cycle progression. To assess the consequence of Smad4- or c-myc-deficiency in TEC on the ability of the epithelium to

support thymocyte development, Smad4$^{lox/lox}$::Foxn1-Cre, c-myc$^{lox/lox}$::Foxn1-Cre and control littermates underwent lethal irradiation and TCD-BMT.

Four and fourteen days after irradiation thymi were assessed for thymocyte numbers and development and TEC cellularity in relation to their Cre-negative littermates (Figure 27A). Whereas c-myc-deficient TEC support an equal percentage of the original thymocyte number as the control TEC, deletion of Smad4 in TEC leads to a dramatic reduction of the percentage of the initially sustained thymocyte number (Figure 27A). Flow cytometric analysis revealed an increased proportion of thymocytes with a low forward scatter and increased side scatter (Figure 27B, left and middle panel). In addition, the proportion of DN thymocytes is significantly increased in Smad4$^{lox/lox}$::Foxn1-Cre mice 14 days after irradiation (Figure 27B, right panel), although the distribution of the different DN subpopulations is comparable to irradiated control mice at that time point (data not shown).

3.8 Keratinocyte growth factor (KGF) enhances thymopoiesis synergistically with deficient TGFβ-signaling

In several studies KGF was successfully used to reverse thymic involution and enhance thymopoiesis following irradiation and stem cell transplantation.

Six to eight week old female TGFbRII$^{lox/lox}$::Foxn1-Cre and TGFbRII$^{lox/lox}$ mice were injected i.p. with recombinant human KGF once daily for three consecutive days. Two weeks after the last injection thymocyte cellularity was assessed. As demonstrated in Figure 28, a significant increase of thymocyte cellularity relative to the initial thymic cellularity is seen. The composition of thymocyte populations did however not differ between the groups (data not shown).

3.9 Ski-deficiency is associated with alterations in thymic size, architecture and thymocyte development

Ski-deficient, -heterozygotes and wildtype embryos were dissected for thymic analysis at 14, 16 and 18 days post-conception (p.c.). E14 thymi in Ski-/- embryos were smaller in size but showed regular shape and normal localization in the anterior upper mediastinum close to the heart. Sections of embryonic day 18 thymi stained with H&E revealed a 'loose', uniform texture (Figure 29A ii&iv) in comparison to the densely packed thymic lobes with newly forming medullary structures derived from wildtype littermates (Figure 28A i&iii). Immunofluorescence analysis confirmed the presence of CD45$^-$ and CK5$^+$ cells in both groups (Figure 29A v&vi). Yet, whereas wildtype thymi demonstrated a reticular pattern of CK5$^+$ cells, localized mostly in the medullary region with some extensions into the cortex, Ski-deficient animals demonstrated only few, clumped islets of CK5$^+$ cells.

To test, whether Ski-deficiency was associated with changes in thymocyte development, E14 thymic lobes were cultured for 7 days and thereafter quantified and analysed by flow cytometry for CD4 and CD8 expression. Cellularity was reduced slightly in heterozygotes, whereas homozygote deficiency

resulted in a reduction of cellularity to roughly 60% to the cell number recovered from wildtype lobes (Figure 29B).

The relative composition of thymocyte subpopulations in Ski-deficient lobes was skewed towards a reduction in DP and an increase in SP8 (Figure 29C).

3.9.1 Ski-deficient stroma builds regular thymic structure and exports normal numbers of T cells when transferred into *nu/nu* hosts

E14.5 fetal lobes were depleted of endogenous thymocytes using d-Guo treatment for 5 days in vitro. Thereafter the lobes were transplanted under the kidney capsule of C57Bl/6-*nu/nu* hosts. Peripheral blood T cells were collected at 4-weekly intervals, demonstrating similar frequencies of T cells (data not shown). Four months after grafting kidneys containing the graft were harvested for histological analysis. There was no obvious difference in size between the groups (Figure 30A, left panels) and a clear demarcation of cortex and medulla could be seen (Figure 30A, middle panel). Quantification of splenic T cells showed equal numbers of $TCR\beta^+$ cells in both groups.

3.9.2 Ski-deficient hematopoietic precursors show slight alterations in thymocyte development and peripheral T cell pools

To test whether Ski-deficiency influences T cell development, E14.5 fetal liver was harvested from Ski-/-, +/- and wildtype embryos and transferred into lethally irradiated C57Bl/6-Ly5.1 mice. All mice survived and could be analysed as late as 4-5 months post-transfer. Recipients of Ski-deficient fetal liver cells displayed a slight, but significantly reduced thymic cellularity (Figure 30A, left panel). Analysis of thymocyte subpopulations revealed a relative and absolute increase of CD8 SP thymocytes, whereas the other subpopulations showed no gross differences (Figure 31A, middle and right panel and B). Analysis of the different maturational selection stages according to TCR and CD69 expression demonstrated a small yet significant skewing towards the more mature, i.e. TCR^{high} $CD69^{high}$ and TCR^{high} $CD69^{low}$ stages (data not shown).

In addition, less splenocytes were recovered from recipients of Ski-deficient fetal liver cells in comparison to recipients of heterozygote or wildtype fetal liver cells. This decrease was due to a reduction of CD19+ cells (data not shown). Whereas the CD4+ T cells showed a comparable frequency between the groups, Ski-deficient CD8a+ T cells were highly overrepresented in relative (Figure 31C, right panel) and absolute (data not shown) terms.

Analysis of protein levels in wildtype thymocyte subpopulations revealed a drastic increase of Ski expression in DP thymocytes, whereas DN and SP contain relatively low levels of the protein (Figure 31D, left panel). In concurrence with this finding is the inverse pattern for phosphorylated Smad-2 levels in these subpopulations with barely detectable levels in DP but relatively high levels in DN and especially SP thymocytes (Figure 31D, right panel). Peripheral lymphocytes (assumed from total splenic lysates) express relatively low levels of Ski protein.

4   Discussion

There is virtually an endless wealth of literature the many facets of TGFβ, including expression patterns, production and its regulation, distribution and activation in tissues, signaling components and regulators thereof, and finally its effects, which on the one hand seem to induce stereotypical cellular responses via 'canonical' pathways, but on the other hand – after more than two decades of intense research – never ceased to stimulate and surprise the research community.

Whereas an increasing number of reports has elucidated TGFβ-mediated effects on the development and function of immune cells, its *in vivo* role for TEC development and function remain enigmatic.

4.1   Expression of TGFβ during embryogenesis and in the adult mouse

Early studies have resolved the spatial and temporal resolution of TGFβ expression in the mouse embryo [227,228,296], demonstrating strong expression in the developing thymus as early as E12.5 in the mouse embryo [228,297]. Previous lab members have extended these findings by carefully analyzing the 3rd pharyngeal pouch containing the precursors that will give rise to thymic epithelium around E10.5, i.e. prior to immigration of T cell precursors (Y. Mathieu, K.Y. Na). Table 1 summarizes qualitative data (i.e. obtained by end-point PCR) of TGFβ isoform transcripts and their respective ligands at different time points during embryogenesis and in the adult. TGFβRI and II show a wide tissue distribution and are believed to be constitutively transcribed [295]. This is reflected by the fact that their signal was detected in all samples tested in primary TEC and TEC lines (Table 1). TGFβ-induced transcription is tightly regulated by association of nuclear factors with the transcriptionally active complex[298]. Ski and Sno negatively regulate TGFβ-signaling and transcription. Ski, but not Sno was detected in the 3rd pharyngeal endoderm demonstrating the presence of at least one negative regulatory element in developing TEC. These findings suggest a role for TGFβ during early thymic development, in particular with respect to TEC development, proliferation and differentiation. This issue has not been addressed so far. In the ageing organism on the other hand, increased TGFβ expression in human thymic tissue is suspected to negatively influence involution and possibly enhances tissue fibrosis [174]. We therefore tested, whether TGFβ expression was altered in aged versus young mice. In fact, there was only a slight and transient increase in TGFβ1 expression with age, whereas TGFβ2 expression showed a steady increase. Nevertheless, as these findings might not reflect the actual protein levels of TGFβ, due to extensive post-transcriptional regulation, we performed analysis for total TGFβ protein by Western blot, demonstrating indeed a steady increase of TGFβ on a protein level. However, interpretation of these findings in terms of biological relevance has to be made cautiously, as the actual TGFβ-activity does not necessarily correspond with the presence of the protein, due to inactivating complex formation with other proteins and extracellular matrix [299]. Nevertheless, I was furthermore interested in what specific cell type(s) expresses TGFβ isoforms in the thymus. To this end, I established an intracellular cytokine staining for flow cytometry. Interestingly, analysis of young mice revealed a large fraction of DN and a smaller fraction of both TEC and non-TEC stromal cells demonstrating immunoreactivity, whereas the largest fraction of other thymocyte subpopulations did

not react with the antibody. This is in line with earlier findings of TGFβ-production by thymocytes and cultured thymic epithelium [216,228,281,300,301]. It remains to be shown however, if there is a change in the expression pattern in aged mice.

4.2 TEC respond to TGFβ in vitro

Due to scarcity of epithelial cells within the thymic compartment, the rapid loss of TEC-specific functions in culture as well as their inclination for apoptosis when removed from their three-dimensional network hampers the study of primary adult TEC. Yet, I tried to get an idea about the effects of TGFβ on TEC using two different systems. On the one hand, established TEC lines (derived from neonatal thymi [302]) on the other hand thymocyte-depleted fetal lobes (containing 60-70% epithelial cells) were exposed to TGFβ. As demonstrated in Figure 2Ai and ii, TEC lines (results shown for TEC1.2) rapidly activate the canonical TGFβ-signaling pathway as demonstrated by phosphorylated Smad2, which translocates to the nucleus. The cellular effects observed are inhibition of proliferation and for some TEC lines activation of apopototic pathways. The most reproducible transcriptional changes imposed by TGFβ on TEC is the down-regulation of c-myc transcription. In fact, whereas c-myc was consistently repressed in all TEC lines tested within 24-48 hours, transcript levels for cell cycle regulators such as the CDKs p16, p21 and p27 showed a great variability depending on the time point after stimulation used for analysis. In addition, the serum concentration within the culture medium correlated with the anti-proliferative and partially pro-apoptotic effects of TGFβ, indicating an antagonizing factor in the animal serum. Therefore TEC lines were routinely starved overnight in medium without serum prior to stimulation to achieve the most prominent and consistent effect. A slightly more physiological situation is found in d-Guo depleted fetal thymic lobes, whereby the three-dimensional meshwork of TEC is retained despite the absence of thymocytes. This 'empty stromal bag' expresses cytokines and surface molecules required for thymocyte development [303]. Addition of TGFβ to the cultures induced drastic numeric reduction of the epithelial– in particular the MHCII^{high} – fraction within 36 hours, at least partially induced by reduction of proliferation. TGFβ was previously reported to induce down-regulation of MHCII via repression of CIITA [304,305]. In our system it is however unlikely, that TGFβ exerts the reduction of MHCII^{high} cells via targeting of CIITA, as the absolute number of MHCII^{low} cells remained constant during this relatively short culture period. Interstingly, the non-epithelial fraction was not significantly reduced, indicating that TGFβ preferentially affects thymic epithelium. On the other hand, an indirect effect of TGFβ via non-epithelial stromal cells cannot be excluded (e.g. down-regulation of growth factors provided by mesenchymal cells). This in vitro model provides a suitable tool to examine the effects of TGFβ on ligand-induced TEC differentiation and proliferation, as well as on their production of cytokines or chemokines.

4.3 Elucidating the role of TGFβ-signaling in TEC in vivo

The contribution of TGFβ to TEC development and function under steady-state conditions can only be studied using conditional ablation of a vital signaling component with a high specificity for TGFβ. TGFβRII is the most suitable target to date, as it initiates the signaling cascade by complexing the ligand with the TGFβRI. As TGFβRII^{null} mice die around E10.5, i.e. prior to the formation of the thymus, TEC-specific inactivation of the TGFβRII is required. Conditional ablation of this receptor was successfully demonstrated [294]. Yet, prior to crossing TGFβRII$^{lox/lox}$ mice to Cre-expressing mice, the different Cre-drivers, i.e. Foxn1-Cre, Hoxa3-Cre and Lefty-Cre, had to be tested for the specificity, timing and reliability of Cre-expression.

4.4 Characterisation of Cre-mediated deletion using different Cre-drivers

To test the timing and specificity of the Cre recombinase under different promoters, I analysed crossings to the GFP- and LacZ-reporter strains, which express either GFP or β-galactosidase in the cell type where Cre recombinase has successfully excised the floxed sequence. The transcription factor Foxn1 is specifically expressed in thymic epithelium early during development and in keratinocytes. Cre expression under the transcriptional control of Foxn1 should therefore target recombination specifically to these cell types. This was demonstrated for the E12.5 thymus using the LacZ-reporter strain (S. Zyklus, in press). However, I wished to know the recombination efficiency at later time points and on a single-cell level, which is best achieved by FACS analysis. Therefore I analyzed thymi derived from GFP-reporter::Foxn1-Cre+ and Cre- E15 embryos and adult mice. E15 TEC showed a high recombination efficiency of roughly 85%. The results derived from embryonic TEC are in line with the observations by Itoi et al.[8], demonstrating a roughly 80% expression of Foxn1 in cytokeratin-positive TEC at E13. Foxn1 expression was shown to be non-redundant for maturation of TEC in a cell-autonomous manner [5], meaning that all MHCII-expressing TEC should have - at one point during their maturation – expressed Foxn1. However, by flowcytometric analysis only about 60-70% of MHCII$^{high/intermediate}$ TEC derived from adult GFP-reporter::Foxn1-Cre+ mice gave a GFP signal. Different scenarios could explain this finding:

(A) technical difficulties including loss of GFP during the isolation procedure or inefficient reporter activity are unlikely, as GFP-reporter::Hoxa3-Cre+ would demonstrate a similar finding which is not the case (see below).

(B) Inefficient Cre-expression and/or –activity are again unlikely as detection of deletion in the TGFβRII$^{lox/lox}$::Foxn1-Cre crossing showed a high recombination efficiency of the floxed allele, although locus accessibility might play a role.

(C) Delayed expression of the reporter construct or in contrast silencing thereof might account for this finding and cannot be completely ruled out.

I therefore tried another approach to identify Cre-expressing cells by flow cytometry, namely direct detection of the protein using anti-Cre antibody. As positive control served TEC derived from Aire-Cre mice, which demonstrate Cre-immunoreactivity in a subpopulation of MHCII^{high} TEC (Figure 4B, right

panel). TEC obtained from adult Foxn1-Cre-expressing mice however did show – if any – only a slight immunoreactivity, which suggests very low levels of protein expressed. Retrospectively, this is however not surprising, as only a small fraction of TEC express Foxn1 at this stage[8] and its promoter activity might be very weak. In addition, kinetics of Cre-protein turnover might be high, leading to low protein levels.

Characterization of Hoxa3-Cre-expressing mice was somewhat less puzzling. Surprisingly however was the finding, that at E14 and also at E19 of the thymic cell populations only epithelial cells showed a high level of recombination, whereas mesenchymal cells and thymocytes recombined only in a small fraction of cells. This unexpectedly high specificity of Cre-expression for TEC together with the fact that a large proportion of cells in the third pouch area has recombined by 10.25 (Figure 5A, middle and lower panel) provides a useful tool to conditionally ablate genes in TEC-precursors during the inductive phase of thymic development. Its use is only limited by the fact that Hoxa3 shows a wide tissue distribution outside the 3rd pouch area during midgestation (Figure 5A, upper panel). This particular problem was encountered in the context of homozygosity for either the Smad4^{lox} or the TGFβRII^{lox} allele and Hoxa3-Cre expression, which both resulted in early fetal lethality (Figure 5C and 7B, respectively).

Mesenchymal-epithelial interactions through secreted molecules or membrane-bound receptors play crucial roles during organ induction, which was demonstrated for early thymic organogenesis [306]. Conditional ablation of genes in either compartment will therefore reveal their respective contribution to organ development. The lefty-Cre mouse was generated in the lab of Anne Moon, Salt Lake City and proposed to show mesenchymal specificity (personal communication). However, analysis of Cre-expression in thymic cell populations using the described reporter strains revealed recombination mostly in thymocytes, but only in a small fraction of mesenchymal cells (Figure 6). This mouse was therefore not used for further studies.

4.5   Lack of TGFβRII in Foxn1 expressing cells does not lead to skin or lactation defects

Foxn1 is expressed in the matrix, cortex and outer root sheet of the hair and in suprabasal layers of the epidermis [13]. Consecutively, Cre-mediated recombination was detected in the skin of LacZ-reporter::Foxn1-Cre mice. TGFβRII$^{lox/lox}$::Foxn1-Cre mice did however not show an obvious skin phenotype with regards to stability, keratinization problems or hair or nail loss. Detailed analysis was not performed and TGFβRII$^{lox/lox}$::Foxn1-Cre mice might be a valuable tool for analyzing the contribution of TGFβ-signals to skin homeostasis, wound healing and (induced) carcinogenesis.

Since the first description of the nude mouse it was appreciated that Foxn1-deficient mice (i.e. nude mice) were unable to maintain a litter, despite normal fertility. This was attributed to their reduced capacity to lactate. The expression pattern of this transcription factor or its exact contribution to initiate or maintain a functional mammary gland has not been described. The Foxn1-Cre mouse provides a valuable tool to elucidate the expression pattern of Foxn1 in the murine mammary gland and to

conditionally ablate or activate genes to study their role in physiological (pregnancy, lactation, regression) as well as pathological conditions (e.g. breast cancer). Preliminary data obtained in Rosa26lacZ::Foxn1-Cre female mice indicate, that Foxn1 is expressed during differentiation of the mammary epithelium in pregnancy, whereas no β-galactosidase staining is detected in the mammary gland during puberty or under adult steady-state conditions. TGFβ plays a multifaceted role during branching, specification and carcinogenesis of mammary epithelium [307]. However, TGFβRII[lox/lox]::Foxn1-Cre female mice were routinely used for breeding and they sustained normal litter sizes. This indicates no immediate deleterious influence of perturbed TGFβ signaling on the lactating mammary gland. However, detailed histological analysis of mammary glands was not performed and further studies of the absence of TGFβ signaling on involution of the mammary gland after involution or upon transforming agents should be stimulated.

4.6 Cre-mediated deletion of TGFβRII[lox/lox] in thymic epithelium at different stages is efficient but results only in a minor thymic phenotype in young mice

Considering the expression pattern of TGFβ and its receptors in the developing thymus at all stages tested, it came as a surprise, that thymic development as well as TEC maturation proceeded unhindered when TGFβRII was deleted from thymic epithelium, and resulted in a microenvironment that supported normal T cell development. Insufficient deletion efficiency could be ruled out as the underlying cause in embryonic and adult TEC (Figure 7). Cre-activation in TEC beyond a stage with indispensable requirement for TGFβ-signaling could also be excluded, driving Cre under control of a promoter active prior to TEC commitment (ref. 14 and Figure 5A). Whereas other studies tried to address this issue studying mice deficient for TGFβ isoforms [282] – thus not ruling out (partial) redundancy between the isoforms as well as trans-placental transfer [230] – this work is the first to exclude a non-redundant role of TGFβ-signaling in TEC via TGFβRII for induction and migration of the thymic anlage as well as for attraction of thymocyte precursors and their further maturation (Figures 8, 10, 11 and 13).

An important and complex role has been assigned to TGF-β signaling for regulating the expansion, activation and effector functions of mature T cells in peripheral lymphoid organs and target tissues during an adaptive immune response [224], whereas intrathymic TGFβ-requirement for normal T cell development is debated [287-289].

Which cell type(s) therefore rely on the presence of TGFβ during thymic organogenesis? The formation of the pharyngeal apparatus involves coordinated actions between neural crest cells and cells of ectodermal, endodermal and mesodermal origin [308]. Moreover, TGF-β signaling may be required in the 3rd pharyngeal arch for non-epithelial cells that influence TEC development and function. Indeed, neural crest stem cells are responsive to TGF-β family members [54-56]. Ablation of TGFβRII-mediated signaling in neural crest cells alters their post-migratory differentiation, consequently reducing the peri-thymic condensation of mesenchyme and diminishing the detection of neural crest-derived cells in the established thymic cortex [65]. Interestingly, these morphological changes correlate with a significant decrease in thymus size and other defects and are consistent with a proposed role of neural crest cells in

thymus organogenesis [65, 46]. Thus, the requirement for TGFβ during thymus organogenesis is independent of direct signaling to TECs but appears to be indirect via the involvement of neural crest cells and mesenchymal-epithelial cross-talk during thymus organogenesis [309].

4.7   TGFβ-signaling in TEC contributes to thymic involution

The molecular mechanisms operational in the process of senescence-related thymic involution are not precisely known despite their relevance for the loss of immunological competence in the aged. Indications that TGF-β signaling may be involved in this process have been largely correlative, such as increased TGF-β steady state mRNA levels in the ageing human thymus [174], without evidence for a causative role. More recently, haploinsufficiency for TGF-β2 was shown to be associated with a decreased rate of thymic involution. Although this observation has been attributed to the action of TGFβ on early thymopoiesis, bone marrow transplantation experiments suggest that the decrease in thymic involution was at least in part the consequence of altered functions of the thymic stroma [154]. The data presented in this study are clearly in support of the view that TGFβ signaling in TECs is directly associated with the phenomenon of thymic involution. Although the absence of TGFβRII in TEC did not prevent involution, its onset was delayed and the progression mitigated (Figure 11A&B). Delayed involution was furthermore associated with reduced frequency of CD44^{high} – i.e. activated/memory T cells – and slightly increased numbers of TREC^{+} cells in the periphery of old TGFβRII$^{lox/lox}$::Foxn1-Cre mice (Figure 20A). Differences in TCRVβ usage in one-year old mice were however not seen between the groups, indicative that thymi in either group still showed significant output (Figure 20B). It remains to be tested whether such differences would occur in older animals (≥ 2 years old). These findings in TGFβRII$^{lox/lox}$::Foxn1-Cre mice are supported by the dramatically increased cellularity observed in grafted thymic derived from TGFβRII$^{lox/lox::}$Hoxa3-Cre embryos (Figure 12B).

Interestingly, the frequency and absolute numbers of ETP as well as developmentally more advanced DN thymocytes in aged experimental animals were comparable to controls (Figure 13B), ruling out enhanced attraction of precursors by TGFβRII$^{lox/lox}$::Foxn1-Cre mice as the underlying cause for mitigated involution.

Consistent with the role of TGFβ in negatively regulating cell cycle [300] TECs deficient in TGF-β signaling retain a higher proliferative capacity (Figure 21C) which correlates with an increased representation of these cells in TGFβRII$^{lox/lox}$::Foxn1-Cre mice (Figure 21A). Yet, the overall structure of the thymic microenvironment was unaffected despite the lack of TGF-β signaling in TEC (Figure 22). Therefore, the observation of a mitigated thymic involution in the mutant mice suggests that the enlarged stromal compartment is able to host an increased number of thymocytes. Nevertheless, the thymocyte-to-TEC ratio decreased with age in both mouse strains (data not shown) arguing for the fact that TGFβ signaling in TEC is not uniquely responsible for the phenomenon of thymic involution.

4.8 Subtle changes in thymocyte development induced by the absence of functional TGFβ signaling in TEC

The corollary of the loss of TGFβ signaling in TEC on thymocyte development is subtle but causes a consistent and significant accumulation of mature single positive thymocytes. This increase is unlikely to be caused by T cells re-circulating from the periphery to the thymus but is rather reflective of an accumulation of mature post-selection thymocytes, because these cells are low in their expression of CD24, CD69 and CD44 but display high surface concentrations of CD62L [139]. The sphingosine-1-phosphate receptor 1 (S1P1) is rapidly up-regulated by mature thymocytes and facilitates egress. However, no differences are detected between CD24$^{low/neg}$ SP thymocytes between the groups (Figure 19).

A higher proliferative rate of mature thymocytes which would have accounted for their increased frequency could also be excluded, suggesting a local retention of these mature cells within the thymic microenvironment. In support of this conclusion are three additional observations: the increased detection of these phenotypically mature thymocytes in TGFβRII$^{lox/lox}$::Foxn1-Cre mice as young as 5 days of life (Table 2), the lower frequency and absolute numbers of peripheral T cells 3 days post-natally (Figure 18) and the significantly smaller fraction of mature thymocytes that are exported to the periphery in young adult TGFβRII$^{lox/lox}$::Foxn1-Cre mice. The observed alterations in the composition and size of the thymic microenvironment might provide an explanation for these changes in thymopoiesis in TGFβRII$^{lox/lox}$::Foxn1-Cre mice because an enlarged (and possibly functionally altered) stromal scaffold is likely to accommodate more and possibly different thymocytes. In fact, the relative and absolute expansion of UEA-1^{+}MHCII^{high} TEC – i.e. a medullary subpopulation – in TGFβRII$^{lox/lox}$::Foxn1-Cre (and TGFβRII$^{lox/lox}$::Hoxa3-Cre) mice in comparison to control littermates is associated with this increase in mature thymocytes. As thymocytes at different maturational stages are located to specific 'zones' within the thymus [310], one could thus hypothesize, that the enlarged medullary stromal compartment will be filled up with thymocytes restricted to this area, leading to an increased pool of medullary i.e. SP thymocytes, without any functional relevance. In line with this hypothesis is the finding, that the fraction of mature thymocytes in TGFβRII$^{lox/lox}$::Foxn1-Cre does not show a steady increase over time, but levels off and actually reaches in old animals levels comparable to control mice, concurrent with a reduction of medullary epithelium in TGFβRII$^{lox/lox}$::Foxn1-Cre mice.

4.9 Enhanced thymic reconstitution in TGFβRII$^{lox/lox}$::Foxn1-Cre mice following γ-irradiation and BMT

Irradiation has a negative impact on thymic cellularity, concerning mostly thymocytes but also epithelial cells in a dose-dependent fashion [214,215]. Following irradiation, thymocytes release high concentrations of TGFβ resulting in an immunosuppressive milieu *in vitro* [216]. This mechanism might well be operational *in vivo*, and not only affect thymocyte differentiation directly but also influence stromal cell types. Indeed, exposure of thymic epithelia to TGFβ modulates the production of

cytokines important for T cell development [186]. We demonstrate here, that TGFβ1 transcript and protein levels are dramatically increased following irradiation in normal thymi. Whereas thymocytes might release a large portion of prestored protein, thymic stromal cells in general and TEC in particular are responsible for the de novo production (Figure 23C) of active protein, as indicated by lack of LAP-staining. The presence of active TGFβ is furthermore supported by increased levels of phosphorylated Smad2 in irradiated thymi. As previously demonstrated [214,215], thymic epithelial cell numbers are drastically reduced within 6 days after irradiation (Figure 23F). In particular, damage to the MHCII^{high} population is most extensive. This negative impact of irradiation on TEC and total thymic cellularity was dampened in the absence of TGFβ-signaling in TEC (Figure 24 and 25), with a more rapid recovery following the insult in TGFβRII$^{lox/lox}$::Foxn1-Cre mice. Whereas decreased cell loss following irradiation might account for the rapid recovery in TGFβRII$^{lox/lox}$::Foxn1-Cre mice, intrathymically produced TGFβ might indirectly affect on thymocyte development via inhibition of the production of cyto- and chemokines. Interestingly, 48 hours following irradiation there was a 2.5 fold increase in SCF expression in thymi derived from TGFβRII$^{lox/lox}$::Foxn1-Cre mice (Figure 25B), whereas the cellular composition of thymi did not differ between the groups. One might hypothesize, that increased levels of SCF at this early time point might enhance the proliferation (and survival) of residual and DN1 and DN2, which is in line with preliminary data showing enhanced proliferation of these cells early after irradiation in TGFβRII$^{lox/lox}$::Foxn1-Cre mice. In addition, TEC apoptosis and proliferation following irradiation in the absence of TGFβ-signaling remains to be demonstrated. TGFβ is amenable to exogenous inhibition using specific antibodies or small molecule inhibitors [311], a principle which was tested with some limited success - with regards to thymocyte cellularity and TEC numbers - in the context of thymic reconstitution following lethal irradiation (Figure 26). Changes in timing and dosing or the use of small molecule inhibitors might prove more effective. A direct effect on thymocyte development by these compounds cannot be excluded. One experimental approach to exclude a direct effect of TGFβ on thymocyte development in this system lies in the transfer of TGFβRII-deficient bone marrow into lethally irradiated host with consecutive analysis of the speed of immune reconstitution.

Smad4 is an essential molecule involved in canonical TGFβ-signaling, yet lacks specificity for TGFβ-mediated signals, as other TGFβ-family members also rely on Smad4. Interestingly, Smad4-deficiency in TEC led to a protracted reconstitution following irradiation in conjunction with drastic increases in the fraction of FSC^{low}SSC^{high} – indicative of apoptosis – and DN thymocytes in thymi from irradiated Smad4$^{lox/lox}$::Foxn1-Cre mice (Figure 27). These findings might imply that (A) signals of other TGFβ-family members in TEC are essential or (B) an imbalance between canonical and non-canonical pathways in TEC is deleterious for T cell development under these circumstances. This issue is currently addressed using conditional inactivation as well as conditional activation of the BMP receptor Alk2 in TEC for reconstitution experiments. C-myc down-regulation is recognized as a critical event in the cell cycle arrest response of epithelial cells to TGFβ-stimulation, and therefore might be a potential target molecule of TGFβ in TEC affecting their proliferation and consequently T cell reconstitution following γ-irradiation. Yet surprisingly, TEC-specific deletion of c-myc did not show a negative effect on T cell reconstitution. The fact that conditional ablation of c-myc in TEC results in an increased

thymocyte/TEC ratio, which is even more pronounced after irradiation and reconstitution (data not shown) indicate qualitatively superior epithelium in the absence of c-myc. Although the underlying molecular mechanisms remain to be demonstrated, this adds a new facet to TEC biology.

Keratinocyte growth factor (KGF) stimulates proliferation and function of thymic epithelium and was shown to enhance thymopoiesis via protection of TEC in the context of irradiation/BMT [312][313]. On the other hand, TGFβ and KGF demonstrate antagonistic activities [314,315]. In fact, a synergistic effect was seen between the absence of TGFβ-signaling in TEC and KGF treatment. Its effectiveness in the context of post-irradiation reconstitution is part of ongoing studies.

Although there is a wealth of information concerning the effect of TGF-β signaling on T cell development, only relatively little is known regarding the *in vivo* role of TGF-β for TEC development and function. The present study presents insight into the contributions of TGF-β signaling under both steady state conditions and after lethal irradiation. Here, we demonstrate that the loss of TGF-β signaling in TECs is not essential for thymus organogenesis but affects (i) total thymocyte cellularity as a function of age, (ii) the pool of mature thymocytes, (iii) the phenotype, proliferation and cellular composition of the thymic epithelial compartment, and (iv) the capacity of TEC to support early reconstitution of thymopoiesis following irradiation.

4.10 Negative regulation of TGFβ-signaling by Ski and its involvement in TEC and T cell biology

As a complementary approach to conditional deletion of TGFβ-signaling in TEC I wished to assess whether uninhibited TGFβ-signaling in the same cell type would demonstrate phenotypic and functional alterations. Ski is considered a potent transcriptional repressor of TGFβ-signaling. Ski-deficient animals die prior to or immediately after birth due to craniofacial abnormalities and failure of neuropore closure[316]. Thymic analysis has to be undertaken similarly to the one in TGFβRII[lox/lox]::Hoxa3-Cre. Thymi of embryos beyond E13 were smaller in size but showed a regular localization in situ. Although cultured Ski-/- lobes demonstrated regular thymocyte development, thymocyte cellularity was drastically reduced in comparison to wildtype lobes. Analysis of TEC in E18 lobes revealed aberrant phenotypical changes with loss of the reticular pattern of cytokeratin staining and forming of small epithelial islets in Ski-/- thymi. However, when Ski-deficient, thymocyte depleted E14 thymic lobes were transplanted into *nude* recipients an inconspicuous architecture and similar T cell numbers were seen 8-10 weeks after transplantation in comparison to transplanted wildtype lobes. The discrepancy between the embryonic findings and the grafted thymi might be explained by defective support of TEC by mesenchymal cells [316]. Of interest was the finding that transplantation of Ski-deficient fetal liver precursors into irradiated hosts led to a small but significant reduction of thymic cellularity in comparison to recipients of wildtype fetal liver. This was attributable to a significant decrease of Ski-/- DP. In contrast, there was a significant increase of CD8 SP in recipients of Ski-/- fetal liver. This difference was 'exported' to the peripheral lymphoid organs of these mice, with a significant relative increase in CD8+ T cells. These findings prompted me to analyse Ski protein

levels in the different thymocyte populations and peripheral T cells of wildtype mice. Ski protein is very abundant in the thymus, mostly attributable to DP thymocytes, whereas DN and SP show low levels of the protein. This correlated directly with Smad-2 posphorylation. Indeed, besides its role in negatively regulating Smad2-dependent transcription recent reports suggest a direct role for Ski in the de-phosphorylation of Smad2 [317,318]. Recent reports using conditional inactivation of TGFβRII in developing T cells have shown a reverse pattern of thymocyte frequencies, with a decrease of mature CD8SP thymocytes [289].

Collectively, these findings demonstrate a minor – if any – role for Ski in TEC development and function. However, the tight regulation of Ski protein expression during T cell development with high expression levels at the DP stage imply a specific role for this molecule, possibly during CD4/CD8 lineage decision or positive selection. The Ski-deficient mouse provides an exciting new model in order to study the potential regulatory role of TGFβ in thymocyte development.

5   Conclusions

- Cre recombinase expression under the control of either the Hoxa3 or the Foxn1 promoter provide reliable and relatively specific tools to conditionally inactivate genes of interest in thymic epithelial cells at different stages of development in order to study inductive events (in the case of Hoxa3-Cre mice) and steady-state conditions (in the case of Foxn1-Cre mice).

- TGFβRII expression in thymic epithelial cells is not required for thymic epithelial cell development, as it does not affect maturation into the different TEC subpopulations. Nevertheless, they demonstrate an enlarged pool of medullary epithelial cells. Although permitting essentially normal T cell development, this results in an increase of medullary T cell numbers and a decreased export of mature T cells into the periphery, relative to the number of intrathymic T cells.

- TGFβ-signaling in thymic epithelium plays a role in promoting thymic involution with respect to onset and progression. Inactivation of TGFβ signaling in TEC is associated in delayed loss of TEC over time and positively influences the proliferative capacity of thymic epithelium.

- TGFβ is prestored in and released by thymocytes following γ-irradiation. As a consequence, the cytokine has detrimental effects on thymic reconstitution early after γ-irradiation. Abolishion of TGFβ-signaling protects TEC from radiation-induced cell death. In addition, the proliferative capacity of TEC in response to irradiation is enhanced in the absence of TGFβ-singaling. TGFβ also acts as a negative regulator of 'thymostimulatory' cytokines such as SCF, which are required for proliferation and survival of thymocyte precursors. Preliminary data furthermore suggest, that keratinocyte growth factor – currently explored as a TEC-protective factor in the context of hematopoetic stem cell transplantation – acts synergistically with inhibition of TGFβ-singnaling. Recent advances in the development of clinically useful small molecule inhibitors for TGFβ signaling provide an impetus for further studies in this field.

- TEC development is marginally affected by TGFβ. This is further underscored by the finding, that the absence of Ski – a potent negative regulator of TGFβ-induced transcription – in thymic epithelium does not influence TEC development. However, although recent work indicates that the absence of TGFβ-signaling in thymocytes is redundant, our studies using Ski-deficient hematopoietic precursors suggest a role for TGFβ signaling in the lineage decision of CD4+CD8+ double-positive thymocytes and peripheral homeostasis of CD8+ T cells.

6   References

1. Donskoy E, Goldschneider I. Thymocytopoiesis is maintained by blood-borne precursors throughout postnatal life. A study in parabiotic mice. J Immunol. 1992;148:1604-1612.

2. Boehm T, Bleul CC. The evolutionary history of lymphoid organs. Nat Immunol. 2007;8:131-135.

3. Gordon J, Wilson VA, Blair NF, Sheridan J, Farley A, et al. Functional evidence for a single endodermal origin for the thymic epithelium. Nat Immunol. 2004;5:546-553.

4. Gordon J, Bennett AR, Blackburn CC, Manley NR. Gcm2 and Foxn1 mark early parathyroid- and thymus-specific domains in the developing third pharyngeal pouch. Mech Dev. 2001;103:141-143.

5. Blackburn CC, Augustine CL, Li R, Harvey RP, Malin MA, et al. The nu gene acts cell-autonomously and is required for differentiation of thymic epithelial progenitors. Proc Natl Acad Sci U S A. 1996;93:5742-5746.

6. Nehls M, Kyewski B, Messerle M, Waldschütz R, Schüddekopf K, et al. Two genetically separable steps in the differentiation of thymic epithelium. Science. 1996;272:886-889.

7. Bleul CC, Corbeaux T, Reuter A, Fisch P, Mönting JS, Boehm T. Formation of a functional thymus initiated by a postnatal epithelial progenitor cell. Nature. 2006;441:992-996.

8. Itoi M, Tsukamoto N, Amagai T. Expression of Dll4 and CCL25 in Foxn1-negative epithelial cells in the post-natal thymus. Int Immunol. 2006;19:127-132.

9. Bleul CC, Boehm T. Chemokines define distinct microenvironments in the developing thymus. Eur J Immunol. 2000;30:3371-3379.

10. Meier N, Dear TN, Boehm T. Whn and mHa3 are components of the genetic hierarchy controlling hair follicle differentiation. Mech Dev. 1999;89:215-221.

11. Baxter RM, Brissette JL. Role of the nude gene in epithelial terminal differentiation. J Invest Dermatol. 2002;118:303-309.

12. Köpf-Maier P, Mboneko VF, Merker HJ. Nude mice are not hairless. A morphological study. Acta Anat (Basel). 1990;139:178-190.

13. Li J, Baxter RM, Weiner L, Goetinck PF, Calautti E, Brissette JL. Foxn1 promotes keratinocyte differentiation by regulating the activity of protein kinase C. Differentiation. 2007;75:694-701.

14. Macatee TL, Hammond BP, Arenkiel BR, Francis L, Frank DU, Moon AM. Ablation of specific expression domains reveals discrete functions of ectoderm- and endoderm-derived FGF8 during cardiovascular and pharyngeal development. Development. 2003;130:6361-6374.

15. Kameda Y, Arai Y, Nishimaki T, Chisaka O. The role of Hoxa3 gene in parathyroid gland organogenesis of the mouse. J Histochem Cytochem. 2004;52:641-651.

16. Manley NR, Capecchi MR. The role of Hoxa-3 in mouse thymus and thyroid development. Development. 1995;121:1989-2003.

17. Mulder GB, Manley N, Maggio-Price L. Retinoic acid-induced thymic abnormalities in the mouse are associated with altered pharyngeal morphology, thymocyte maturation defects, and altered expression of Hoxa3 and Pax1. Teratology. 1998;58:263-275.

18. Mulder GB, Manley N, Grant J, Schmidt K, Zeng W, et al. Effects of excess vitamin A on development of cranial neural crest-derived structures: a neonatal and embryologic study. Teratology. 2000;62:214-226.

19. Dietrich S, Gruss P. undulated phenotypes suggest a role of Pax-1 for the development of vertebral and extravertebral structures. Dev Biol. 1995;167:529-548.

20. Su DM, Manley NR. Hoxa3 and pax1 transcription factors regulate the ability of fetal thymic epithelial cells to promote thymocyte development. J Immunol. 2000;164:5753-5760.

21. Wallin J, Eibel H, Neubüser A, Wilting J, Koseki H, Balling R. Pax1 is expressed during development of the thymus epithelium and is required for normal T-cell maturation. Development. 1996;122:23-30.

22. Wehr R, Gruss P. Pax and vertebrate development. Int J Dev Biol. 1996;40:369-377.

23. Hetzer-Egger C, Schorpp M, Haas-Assenbaum A, Balling R, Peters H, Boehm T. Thymopoiesis requires Pax9 function in thymic epithelial cells. Eur J Immunol. 2002;32:1175-1181.

24. Neubüser A, Koseki H, Balling R. Characterization and developmental expression of Pax9, a paired-box-containing gene related to Pax1. Dev Biol. 1995;170:701-716.

25. Peters H, Neubüser A, Kratochwil K, Balling R. Pax9-deficient mice lack pharyngeal pouch derivatives and teeth and exhibit craniofacial and limb abnormalities. Genes Dev. 1998;12:2735-2747.

26. Lang D, Powell SK, Plummer RS, Young KP, Ruggeri BA. PAX genes: roles in development, pathophysiology, and cancer. Biochem Pharmacol. 2007;73:1-14.

27. Nabarra B, Andrianarison I. Ultrastructural studies of thymic reticulum: I. Epithelial [corrected] component. Thymus. 1987;9:95-121.

28. Moraux-Moyson A, Scheiff JM, Haumont S. Thymus histogenesis in C3H mice. Thymus. 1988;12:89-109.

29. Kampinga J, Berges S, Boyd RL, Brekelmans P, Colić M, et al. Thymic epithelial antibodies: immunohistological analysis and introduction of nomenclature. Thymus. 1989;13:165-173.

30. Klug DB, Carter C, Crouch E, Roop D, Conti CJ, Richie ER. Interdependence of cortical thymic epithelial cell differentiation and T-lineage commitment. Proc Natl Acad Sci U S A. 1998;95:11822-11827.

31. Müller EJ, Williamson L, Kolly C, Suter MM. Outside-in signaling through integrins and cadherins: a central mechanism to control epidermal growth and differentiation? J Invest Dermatol. 2008;128:501-516.

32. Kutlesa S, Wessels JT, Speiser A, Steiert I, Müller CA, Klein G. E-cadherin-mediated interactions of thymic epithelial cells with CD103+ thymocytes lead to enhanced thymocyte cell proliferation. J Cell Sci. 2002;115:4505-4515.

33. Lee MG, Sharrow SO, Farr AG, Singer A, Udey MC. Expression of the homotypic adhesion molecule E-cadherin by immature murine thymocytes and thymic epithelial cells. J Immunol. 1994;152:5653-5659.

34. Müller KM, Luedecker CJ, Udey MC, Farr AG. Involvement of E-cadherin in thymus organogenesis and thymocyte maturation. Immunity. 1997;6:257-264.

35. Lucas B, Germain RN. Opening a window on thymic positive selection: developmental changes in the influence of cosignaling by integrins and CD28 on selection events induced by TCR engagement. J Immunol. 2000;165:1889-1895.

36. Paessens LC, Singh SK, Fernandes RJ, van Kooyk Y. Vascular cell adhesion molecule-1 (VCAM-1) and intercellular adhesion molecule-1 (ICAM-1) provide co-stimulation in positive selection along with survival of selected thymocytes. Mol Immunol. 2008;45:42-48.

37. Martinic MM, van den Broek MF, Rülicke T, Huber C, Odermatt B, et al. Functional CD8+ but not CD4+ T cell responses develop independent of thymic epithelial MHC. Proc Natl Acad Sci U S A. 2006;103:14435-14440.

38. Holländer GA, Wang B, Nichogiannopoulou A, Platenburg PP, van Ewijk W, et al. Developmental control point in induction of thymic cortex regulated by a subpopulation of prothymocytes. Nature. 1995;373:350-353.

39. Anderson G, Jenkinson EJ. Lymphostromal interactions in thymic development and function. Nat Rev Immunol. 2001;1:31-40.

40. Penit C, Lucas B, Vasseur F, Rieker T, Boyd RL. Thymic medulla epithelial cells acquire specific markers by post-mitotic maturation. Dev Immunol. 1996;5:25-36.

41. Shores EW, Van Ewijk W, Singer A. Disorganization and restoration of thymic medullary epithelial cells in T cell receptor-negative scid mice: evidence that receptor-bearing lymphocytes influence maturation of the thymic microenvironment. Eur J Immunol. 1991;21:1657-1661.

42. Jenkinson WE, Rossi SW, Jenkinson EJ, Anderson G. Development of functional thymic epithelial cells occurs independently of lymphostromal interactions. Mech Dev. 2005;122:1294-1299.

43. Jiang X, Rowitch DH, Soriano P, McMahon AP, Sucov HM. Fate of the mammalian cardiac neural crest. Development. 2000;127:1607-1616.

44. Veitch E, Begbie J, Schilling TF, Smith MM, Graham A. Pharyngeal arch patterning in the absence of neural crest. Curr Biol. 1999;9:1481-1484.

45. Anderson G, Jenkinson EJ, Moore NC, Owen JJ. MHC class II-positive epithelium and mesenchyme cells are both required for T-cell development in the thymus. Nature. 1993;362:70-73.

46. Bockman DE, Kirby ML. Dependence of thymus development on derivatives of the neural crest. Science. 1984;223:498-500.

47. Anderson G, Anderson KL, Tchilian EZ, Owen JJ, Jenkinson EJ. Fibroblast dependency during early thymocyte development maps to the CD25+ CD44+ stage and involves interactions with fibroblast matrix molecules. Eur J Immunol. 1997;27:1200-1206.

48. Banwell CM, Partington KM, Jenkinson EJ, Anderson G. Studies on the role of IL-7 presentation by mesenchymal fibroblasts during early thymocyte development. Eur J Immunol. 2000;30:2125-2129.

49. Revest JM, Suniara RK, Kerr K, Owen JJ, Dickson C. Development of the thymus requires signaling through the fibroblast growth factor receptor R2-IIIb. J Immunol. 2001;167:1954-1961.

50. Jenkinson WE, Rossi SW, Parnell SM, Jenkinson EJ, Anderson G. PDGFR{alpha}-expressing mesenchyme regulates thymus growth and the availability of intrathymic niches. Blood. 2006;109:954-960.

51. Barembaum M, Bronner-Fraser M. Early steps in neural crest specification. Semin Cell Dev Biol. 2005;16:642-646.

52. Steventon B, Carmona-Fontaine C, Mayor R. Genetic network during neural crest induction: from cell specification to cell survival. Semin Cell Dev Biol. 2005;16:647-654.

53. Watari N, Kameda Y, Takeichi M, Chisaka O. Hoxa3 regulates integration of glossopharyngeal nerve precursor cells. Dev Biol. 2001;240:15-31.

54. Hagedorn L, Suter U, Sommer L. P0 and PMP22 mark a multipotent neural crest-derived cell type that displays community effects in response to TGF-beta family factors. Development. 1999;126:3781-3794.

55. Hagedorn L, Floris J, Suter U, Sommer L. Autonomic neurogenesis and apoptosis are alternative fates of progenitor cell communities induced by TGFbeta. Dev Biol. 2000;228:57-72.

56. Shah NM, Groves AK, Anderson DJ. Alternative neural crest cell fates are instructively promoted by TGFbeta superfamily members. Cell. 1996;85:331-343.

57. Fuchs S, Sommer L. The neural crest: understanding stem cell function in development and disease. Neurodegener Dis. 2007;4:6-12.

58. Dudas M, Sridurongrit S, Nagy A, Okazaki K, Kaartinen V. Craniofacial defects in mice lacking BMP type I receptor Alk2 in neural crest cells. Mech Dev. 2004;121:173-182.

59. Kaartinen V, Dudas M, Nagy A, Sridurongrit S, Lu MM, Epstein JA. Cardiac outflow tract defects in mice lacking ALK2 in neural crest cells. Development. 2004;131:3481-3490.

60. Stottmann RW, Choi M, Mishina Y, Meyers EN, Klingensmith J. BMP receptor IA is required in mammalian neural crest cells for development of the cardiac outflow tract and ventricular myocardium. Development. 2004;131:2205-2218.

61. Choudhary B, Ito Y, Makita T, Sasaki T, Chai Y, Sucov HM. Cardiovascular malformations with normal smooth muscle differentiation in neural crest-specific type II TGFbeta receptor (Tgfbr2) mutant mice. Dev Biol. 2006;289:420-429.

62. Wang J, Nagy A, Larsson J, Dudas M, Sucov HM, Kaartinen V. Defective ALK5 signaling in the neural crest leads to increased postmigratory neural crest cell apoptosis and severe outflow tract defects. BMC Dev Biol. 2006;6:51.

63. Jia Q, McDill BW, Li SZ, Deng C, Chang CP, Chen F. Smad signaling in the neural crest regulates cardiac outflow tract remodeling through cell autonomous and non-cell autonomous effects. Dev Biol. 2007;311:172-184.

64. Ko SO, Chung IH, Xu X, Oka S, Zhao H, et al. Smad4 is required to regulate the fate of cranial neural crest cells. Dev Biol. 2007;312:435-447.

65. Wurdak H, Ittner LM, Lang KS, Leveen P, Suter U, et al. Inactivation of TGFbeta signaling in neural crest stem cells leads to multiple defects reminiscent of DiGeorge syndrome. Genes Dev. 2005;19:530-535.

66. Goldschneider I, Komschlies KL, Greiner DL. Studies of thymocytopoiesis in rats and mice. I. Kinetics of appearance of thymocytes using a direct intrathymic adoptive transfer assay for thymocyte precursors. J Exp Med. 1986;163:1-17.

67. Lind EF, Prockop SE, Porritt HE, Petrie HT. Mapping precursor movement through the postnatal thymus reveals specific microenvironments supporting defined stages of early lymphoid development. J Exp Med. 2001;194:127-134.

68. Rossi FM, Corbel SY, Merzaban JS, Carlow DA, Gossens K, et al. Recruitment of adult thymic progenitors is regulated by P-selectin and its ligand PSGL-1. Nat Immunol. 2005;6:626-634.

69. Uehara S, Grinberg A, Farber JM, Love PE. A role for CCR9 in T lymphocyte development and migration. J Immunol. 2002;168:2811-2819.

70. Misslitz A, Pabst O, Hintzen G, Ohl L, Kremmer E, et al. Thymic T cell development and progenitor localization depend on CCR7. J Exp Med. 2004;200:481-491.

71. Wilkinson B, Owen JJ, Jenkinson EJ. Factors regulating stem cell recruitment to the fetal thymus. J Immunol. 1999;162:3873-3881.

72. Liu C, Ueno T, Kuse S, Saito F, Nitta T, et al. The role of CCL21 in recruitment of T-precursor cells to fetal thymi. Blood. 2005;105:31-39.

73. Nagasawa T, Hirota S, Tachibana K, Takakura N, Nishikawa S, et al. Defects of B-cell lymphopoiesis and bone-marrow myelopoiesis in mice lacking the CXC chemokine PBSF/SDF-1. Nature. 1996;382:635-638.

74. Zou YR, Kottmann AH, Kuroda M, Taniuchi I, Littman DR. Function of the chemokine receptor CXCR4 in haematopoiesis and in cerebellar development. Nature. 1998;393:595-599.

75. Tachibana K, Hirota S, Iizasa H, Yoshida H, Kawabata K, et al. The chemokine receptor CXCR4 is essential for vascularization of the gastrointestinal tract. Nature. 1998;393:591-594.

76. Ma Q, Jones D, Borghesani PR, Segal RA, Nagasawa T, et al. Impaired B-lymphopoiesis, myelopoiesis, and derailed cerebellar neuron migration in CXCR4- and SDF-1-deficient mice. Proc Natl Acad Sci U S A. 1998;95:9448-9453.

77. Ara T, Itoi M, Kawabata K, Egawa T, Tokoyoda K, et al. A role of CXC chemokine ligand 12/stromal cell-derived factor-1/pre-B cell growth stimulating factor and its receptor CXCR4 in fetal and adult T cell development in vivo. J Immunol. 2003;170:4649-4655.

78. Plotkin J, Prockop SE, Lepique A, Petrie HT. Critical role for CXCR4 signaling in progenitor localization and T cell differentiation in the postnatal thymus. J Immunol. 2003;171:4521-4527.

79. Porritt HE, Gordon K, Petrie HT. Kinetics of steady-state differentiation and mapping of intrathymic-signaling environments by stem cell transplantation in nonirradiated mice. J Exp Med. 2003;198:957-962.

80. Shortman K, Egerton M, Spangrude GJ, Scollay R. The generation and fate of thymocytes. Semin Immunol. 1990;2:3-12.

81. Wang H, Pierce LJ, Spangrude GJ. Distinct roles of IL-7 and stem cell factor in the OP9-DL1 T-cell differentiation culture system. Exp Hematol. 2006;34:1730-1740.

82. Radtke F, Wilson A, Stark G, Bauer M, van Meerwijk J, et al. Deficient T cell fate specification in mice with an induced inactivation of Notch1. Immunity. 1999;10:547-558.

83. Radtke F, Wilson A, MacDonald HR. Notch signaling in T- and B-cell development. Curr Opin Immunol. 2004;16:174-179.

84. Wolfer A, Wilson A, Nemir M, MacDonald HR, Radtke F. Inactivation of Notch1 impairs VDJbeta rearrangement and allows pre-TCR-independent survival of early alpha beta Lineage Thymocytes. Immunity. 2002;16:869-879.

85. Tanigaki K, Tsuji M, Yamamoto N, Han H, Tsukada J, et al. Regulation of alphabeta/gammadelta T cell lineage commitment and peripheral T cell responses by Notch/RBP-J signaling. Immunity. 2004;20:611-622.

86. Egerton M, Scollay R, Shortman K. Kinetics of mature T-cell development in the thymus. Proc Natl Acad Sci U S A. 1990;87:2579-2582.

87. Shortman K, Vremec D, Egerton M. The kinetics of T cell antigen receptor expression by subgroups of CD4+8+ thymocytes: delineation of CD4+8+3(2+) thymocytes as post-selection intermediates leading to mature T cells. J Exp Med. 1991;173:323-332.

88. Ernst B, Surh CD, Sprent J. Thymic selection and cell division. J Exp Med. 1995;182:961-971.

89. Hare KJ, Jenkinson EJ, Anderson G. Specialisation of thymic epithelial cells for positive selection of CD4+8+ thymocytes. Cell Mol Biol (Noisy-le-grand). 2001;47:119-127.

90. Starr TK, Jameson SC, Hogquist KA. Positive and negative selection of T cells. Annu Rev Immunol. 2003;21:139-176.

91. Liu YJ. A unified theory of central tolerance in the thymus. Trends Immunol. 2006;27:215-221.

92. Yasutomo K, Lucas B, Germain RN. TCR signaling for initiation and completion of thymocyte positive selection has distinct requirements for ligand quality and presenting cell type. J Immunol. 2000;165:3015-3022.

93. Witt CM, Raychaudhuri S, Schaefer B, Chakraborty AK, Robey EA. Directed migration of positively selected thymocytes visualized in real time. PLoS Biol. 2005;3:e160.

94. Scollay R, Godfrey DI. Thymic emigration: conveyor belts or lucky dips? Immunol Today. 1995;16:268-73; discussion 273-4.

95. Ramsdell F, Jenkins M, Dinh Q, Fowlkes BJ. The majority of CD4+8- thymocytes are functionally immature. J Immunol. 1991;147:1779-1785.

96. Gabor MJ, Godfrey DI, Scollay R. Recent thymic emigrants are distinct from most medullary thymocytes. Eur J Immunol. 1997;27:2010-2015.

97. Lucas B, Vasseur F, Penit C. Production, selection, and maturation of thymocytes with high surface density of TCR. J Immunol. 1994;153:53-62.

98. Chen W. The late stage of T cell development within mouse thymus. Cell Mol Immunol. 2004;1:3-11.

99. Ge Q, Chen WF. Phenotypic identification of the subgroups of murine T-cell receptor alphabeta+ CD4+ CD8- thymocytes and its implication in the late stage of thymocyte development. Immunology. 1999;97:665-671.

100. Sheard MA, Liu C, Takahama Y. Developmental status of CD4-CD8+ and CD4+CD8- thymocytes with medium expression of CD3. Eur J Immunol. 2004;34:25-35.

101. Ceredig R, Glasebrook AL, MacDonald HR. Phenotypic and functional properties of murine thymocytes. I. Precursors of cytolytic T lymphocytes and interleukin 2-producing cells are all contained within a subpopulation of "mature" thymocytes as analyzed by monoclonal antibodies and flow microfluorometry. J Exp Med. 1982;155:358-379.

102. Reichert RA, Weissman IL, Butcher EC. Phenotypic analysis of thymocytes that express homing receptors for peripheral lymph nodes. J Immunol. 1986;136:3521-3528.

103. Kishimoto H, Sprent J. Negative selection in the thymus includes semimature T cells. J Exp Med. 1997;185:263-271.

104. Laufer TM, DeKoning J, Markowitz JS, Lo D, Glimcher LH. Unopposed positive selection and autoreactivity in mice expressing class II MHC only on thymic cortex. Nature. 1996;383:81-85.

105. Kishimoto H, Sprent J. Several different cell surface molecules control negative selection of medullary thymocytes. J Exp Med. 1999;190:65-73.

106. Kishimoto H, Surh CD, Sprent J. A role for Fas in negative selection of thymocytes in vivo. J Exp Med. 1998;187:1427-1438.

107. Lucas B, Stefanová I, Yasutomo K, Dautigny N, Germain RN. Divergent changes in the sensitivity of maturing T cells to structurally related ligands underlies formation of a useful T cell repertoire. Immunity. 1999;10:367-376.

108. Eck SC, Zhu P, Pepper M, Bensinger SJ, Freedman BD, Laufer TM. Developmental Alterations in Thymocyte Sensitivity Are Actively Regulated by MHC Class II Expression in the Thymic Medulla. J Immunol. 2006;176:2229-2237.

109. Tarakhovsky A, Kanner SB, Hombach J, Ledbetter JA, Müller W, et al. A role for CD5 in TCR-mediated signal transduction and thymocyte selection. Science. 1995;269:535-537.

110. Hare KJ, Wilkinson RW, Jenkinson EJ, Anderson G. Identification of a developmentally regulated phase of postselection expansion driven by thymic epithelium. J Immunol. 1998;160:3666-3672.

111. Hare KJ, Jenkinson EJ, Anderson G. An essential role for the IL-7 receptor during intrathymic expansion of the positively selected neonatal T cell repertoire. J Immunol. 2000;165:2410-2414.

112. Le Campion A, Vasseur F, Pénit C. Regulation and kinetics of premigrant thymocyte expansion. Eur J Immunol. 2000;30:738-746.

113. Le Campion A, Lucas B, Dautigny N, Léaument S, Vasseur F, Pénit C. Quantitative and qualitative adjustment of thymic T cell production by clonal expansion of premigrant thymocytes. J Immunol. 2002;168:1664-1671.

114. Uehara S, Song K, Farber JM, Love PE. Characterization of CCR9 expression and CCL25/thymus-expressed chemokine responsiveness during T cell development: CD3(high)CD69+ thymocytes and gammadeltaTCR+ thymocytes preferentially respond to CCL25. J Immunol. 2002;168:134-142.

115. Kurobe H, Liu C, Ueno T, Saito F, Ohigashi I, et al. CCR7-dependent cortex-to-medulla migration of positively selected thymocytes is essential for establishing central tolerance. Immunity. 2006;24:165-177.

116. Matloubian M, Lo CG, Cinamon G, Lesneski MJ, Xu Y, et al. Lymphocyte egress from thymus and peripheral lymphoid organs is dependent on S1P receptor 1. Nature. 2004;427:355-360.

117. Ushiki T. A scanning electron-microscopic study of the rat thymus with special reference to cell types and migration of lymphocytes into the general circulation. Cell Tissue Res. 1986;244:285-298.

118. Kato S. Thymic microvascular system. Microsc Res Tech. 1997;38:287-299.

119. Chaffin KE, Perlmutter RM. A pertussis toxin-sensitive process controls thymocyte emigration. Eur J Immunol. 1991;21:2565-2573.

120. Tashiro K, Tada H, Heilker R, Shirozu M, Nakano T, Honjo T. Signal sequence trap: a cloning strategy for secreted proteins and type I membrane proteins. Science. 1993;261:600-603.

121. Poznansky MC, Olszak IT, Evans RH, Wang Z, Foxall RB, et al. Thymocyte emigration is mediated by active movement away from stroma-derived factors. J Clin Invest. 2002;109:1101-1110.

122. Aiuti A, Webb IJ, Bleul C, Springer T, Gutierrez-Ramos JC. The chemokine SDF-1 is a chemoattractant for human CD34+ hematopoietic progenitor cells and provides a new mechanism to explain the mobilization of CD34+ progenitors to peripheral blood. J Exp Med. 1997;185:111-120.

123. Vianello F, Kraft P, Mok YT, Hart WK, White N, Poznansky MC. A CXCR4-dependent chemorepellent signal contributes to the emigration of mature single-positive CD4 cells from the fetal thymus. J Immunol. 2005;175:5115-5125.

124. Ueno T, Hara K, Willis MS, Malin MA, Höpken UE, et al. Role for CCR7 ligands in the emigration of newly generated T lymphocytes from the neonatal thymus. Immunity. 2002;16:205-218.

125. Wurbel MA, Philippe JM, Nguyen C, Victorero G, Freeman T, et al. The chemokine TECK is expressed by thymic and intestinal epithelial cells and attracts double- and single-positive thymocytes expressing the TECK receptor CCR9. Eur J Immunol. 2000;30:262-271.

126. Campbell JJ, Pan J, Butcher EC. Cutting edge: developmental switches in chemokine responses during T cell maturation. J Immunol. 1999;163:2353-2357.

127. Uldrich AP, Berzins SP, Malin MA, Bouillet P, Strasser A, et al. Antigen challenge inhibits thymic emigration. J Immunol. 2006;176:4553-4561.

128. Boehm T, Scheu S, Pfeffer K, Bleul CC. Thymic medullary epithelial cell differentiation, thymocyte emigration, and the control of autoimmunity require lympho-epithelial cross talk via LTbetaR. J Exp Med. 2003;198:757-769.

129. Savino W, Mendes-Da-Cruz DA, Smaniotto S, Silva-Monteiro E, Villa-Verde DM. Molecular mechanisms governing thymocyte migration: combined role of chemokines and extracellular matrix. J Leukoc Biol. 2004;75:951-961.

130. Savino W, Mendes-da-Cruz DA, Silva JS, Dardenne M, Cotta-de-Almeida V. Intrathymic T-cell migration: a combinatorial interplay of extracellular matrix and chemokines? Trends Immunol. 2002;23:305-313.

131. Vivinus-Nebot M, Rousselle P, Breittmayer JP, Cenciarini C, Berrih-Aknin S, et al. Mature human thymocytes migrate on laminin-5 with activation of metalloproteinase-14 and cleavage of CD44. J Immunol. 2004;172:1397-1406.

132. Boursalian TE, Golob J, Soper DM, Cooper CJ, Fink PJ. Continued maturation of thymic emigrants in the periphery. Nat Immunol. 2004;5:418-425.

133. Jin R, Zhang J, Chen W. Thymic output: influence factors and molecular mechanism. Cell Mol Immunol. 2006;3:341-350.

134. Berzins SP, Godfrey DI, Miller JF, Boyd RL. A central role for thymic emigrants in peripheral T cell homeostasis. Proc Natl Acad Sci U S A. 1999;96:9787-9791.

135. Gabor MJ, Scollay R, Godfrey DI. Thymic T cell export is not influenced by the peripheral T cell pool. Eur J Immunol. 1997;27:2986-2993.

136. Berzins SP, Boyd RL, Miller JF. The role of the thymus and recent thymic migrants in the maintenance of the adult peripheral lymphocyte pool. J Exp Med. 1998;187:1839-1848.

137. Hale JS, Boursalian TE, Turk GL, Fink PJ. Thymic output in aged mice. Proc Natl Acad Sci U S A. 2006;103:8447-8452.

138. Berzins SP, Uldrich AP, Sutherland JS, Gill J, Miller JF, et al. Thymic regeneration: teaching an old immune system new tricks. Trends Mol Med. 2002;8:469-476.

139. Agus DB, Surh CD, Sprent J. Reentry of T cells to the adult thymus is restricted to activated T cells. J Exp Med. 1991;173:1039-1046.

140. Surh CD, Sprent J, Webb SR. Exclusion of circulating T cells from the thymus does not apply in the neonatal period. J Exp Med. 1993;177:379-385.

141. Jamieson BD, Douek DC, Killian S, Hultin LE, Scripture-Adams DD, et al. Generation of functional thymocytes in the human adult. Immunity. 1999;10:569-575.

142. Taub DD, Longo DL. Insights into thymic aging and regeneration. Immunol Rev. 2005;205:72-93.

143. Aspinall R, Andrew D, Pido-Lopez J. Age-associated changes in thymopoiesis. Springer Semin Immunopathol. 2002;24:87-101.

144. Aspinall R, Andrew D. Thymic involution in aging. J Clin Immunol. 2000;20:250-256.

145. Mackall CL, Bare CV, Granger LA, Sharrow SO, Titus JA, Gress RE. Thymic-independent T cell regeneration occurs via antigen-driven expansion of peripheral T cells resulting in a repertoire that is limited in diversity and prone to skewing. J Immunol. 1996;156:4609-4616.

146. Hobbs MV, Ernst DN, Torbett BE, Glasebrook AL, Rehse MA, et al. Cell proliferation and cytokine production by CD4+ cells from old mice. J Cell Biochem. 1991;46:312-320.

147. Malaguarnera L, Ferlito L, Imbesi RM, Gulizia GS, Di Mauro S, et al. Immunosenescence: a review. Arch Gerontol Geriatr. 2001;32:1-14.

148. Haynes L, Swain SL. Why aging T cells fail: implications for vaccination. Immunity. 2006;24:663-666.

149. Cho RH, Sieburg HB, Muller-Sieburg CE. A new mechanism for the aging of hematopoietic stem cells: aging changes the clonal composition of the stem cell compartment but not individual stem cells. Blood. 2008;111:5553-5561.

150. Schwarz BA, Bhandoola A. Circulating hematopoietic progenitors with T lineage potential. Nat Immunol. 2004;5:953-960.

151. Zediak VP, Maillard I, Bhandoola A. Multiple prethymic defects underlie age-related loss of T progenitor competence. Blood. 2007;110:1161-1167.

152. Gui J, Zhu X, Dohkan J, Cheng L, Barnes PF, Su DM. The aged thymus shows normal recruitment of lymphohematopoietic progenitors but has defects in thymic epithelial cells. Int Immunol. 2007;19:1201-1211.

153. Zhu X, Gui J, Dohkan J, Cheng L, Barnes PF, Su DM. Lymphohematopoietic progenitors do not have a synchronized defect with age-related thymic involution. Aging Cell. 2007;6:663-672.

154. Kumar R, Langer JC, Snoeck HW. Transforming growth factor-beta2 is involved in quantitative genetic variation in thymic involution. Blood. 2006;107:1974-1979.

155. Sharp A, Kukulansky T, Globerson A. In vitro analysis of age-related changes in the developmental potential of bone marrow thymocyte progenitors. Eur J Immunol. 1990;20:2541-2546.

156. Donskoy E, Foss D, Goldschneider I. Gated importation of prothymocytes by adult mouse thymus is coordinated with their periodic mobilization from bone marrow. J Immunol. 2003;171:3568-3575.

157. Goldschneider I. Cyclical mobilization and gated importation of thymocyte progenitors in the adult mouse: evidence for a thymus-bone marrow feedback loop. Immunol Rev. 2006;209:58-75.

158. Kenins L, Gill JW, Boyd RL, Holländer GA, Wodnar-Filipowicz A. Intrathymic expression of Flt3 ligand enhances thymic recovery after irradiation. J Exp Med. 2008;205:523-531.

159. Min H, Montecino-Rodriguez E, Dorshkind K. Reduction in the developmental potential of intrathymic T cell progenitors with age. J Immunol. 2004;173:245-250.

160. Hirokawa K. Thymic involution: effect on T cell differentiation. The Journal of Immunology. 1975;114:1659-1664.

161. Mackall CL, Punt JA, Morgan P, Farr AG, Gress RE. Thymic function in young/old chimeras: substantial thymic T cell regenerative capacity despite irreversible age-associated thymic involution. Eur J Immunol. 1998;28:1886-1893.

162. Farr AG, Sidman CL. Reduced expression of Ia antigens by thymic epithelial cells of aged mice. J Immunol. 1984;133:98-103.

163. Gray DH, Seach N, Ueno T, Milton MK, Liston A, et al. Developmental kinetics, turnover and stimulatory capacity of thymic epithelial cells. Blood. 2006;108:3777-3785.

164. Yang SJ, Ahn S, Park CS, Holmes KL, Westrup J, et al. The quantitative assessment of MHC II on thymic epithelium: implications in cortical thymocyte development. Int Immunol. 2006;18:729-739.

165. Ortman CL, Dittmar KA, Witte PL, Le PT. Molecular characterization of the mouse involuted thymus: aberrations in expression of transcription regulators in thymocyte and epithelial compartments. Int Immunol. 2002;14:813-822.

166. Yajima N, Sakamaki K, Yonehara S. Age-related thymic involution is mediated by Fas on thymic epithelial cells. Int Immunol. 2004;16:1027-1035.

167. Robles AI, Larcher F, Whalin RB, Murillas R, Richie E, et al. Expression of cyclin D1 in epithelial tissues of transgenic mice results in epidermal hyperproliferation and severe thymic hyperplasia. Proc Natl Acad Sci U S A. 1996;93:7634-7638.

168. Klug DB, Crouch E, Carter C, Coghlan L, Conti CJ, Richie ER. Transgenic expression of cyclin D1 in thymic epithelial precursors promotes epithelial and T cell development. J Immunol. 2000;164:1881-1888.

169. Andrew D, Aspinall R. Il-7 and not stem cell factor reverses both the increase in apoptosis and the decline in thymopoiesis seen in aged mice. J Immunol. 2001;166:1524-1530.

170. Phillips JA, Brondstetter TI, English CA, Lee HE, Virts EL, Thoman ML. IL-7 gene therapy in aging restores early thymopoiesis without reversing involution. J Immunol. 2004;173:4867-4874.

171. Peschon JJ, Morrissey PJ, Grabstein KH, Ramsdell FJ, Maraskovsky E, et al. Early lymphocyte expansion is severely impaired in interleukin 7 receptor-deficient mice. J Exp Med. 1994;180:1955-1960.

172. von Freeden-Jeffry U, Vieira P, Lucian LA, McNeil T, Burdach SE, Murray R. Lymphopenia in interleukin (IL)-7 gene-deleted mice identifies IL-7 as a nonredundant cytokine. J Exp Med. 1995;181:1519-1526.

173. Andrew D, Aspinall R. Age-associated thymic atrophy is linked to a decline in IL-7 production. Exp Gerontol. 2002;37:455-463.

174. Sempowski GD, Hale LP, Sundy JS, Massey JM, Koup RA, et al. Leukemia inhibitory factor, oncostatin M, IL-6, and stem cell factor mRNA expression in human thymus increases with age and is associated with thymic atrophy. J Immunol. 2000;164:2180-2187.

175. Fry TJ, Moniuszko M, Creekmore S, Donohue SJ, Douek DC, et al. IL-7 therapy dramatically alters peripheral T-cell homeostasis in normal and SIV-infected nonhuman primates. Blood. 2003;101:2294-2299.

176. Fry TJ, Mackall CL. Interleukin-7: from bench to clinic. Blood. 2002;99:3892-3904.

177. Dixit VD, Yang H, Sun Y, Weeraratna AT, Youm YH, et al. Ghrelin promotes thymopoiesis during aging. J Clin Invest. 2007;117:2778-2790.

178. French RA, Broussard SR, Meier WA, Minshall C, Arkins S, et al. Age-associated loss of bone marrow hematopoietic cells is reversed by GH and accompanies thymic reconstitution. Endocrinology. 2002;143:690-699.

179. Koo GC, Huang C, Camacho R, Trainor C, Blake JT, et al. Immune enhancing effect of a growth hormone secretagogue. J Immunol. 2001;166:4195-4201.

180. Montecino-Rodriguez E, Clark R, Dorshkind K. Effects of insulin-like growth factor administration and bone marrow transplantation on thymopoiesis in aged mice. Endocrinology. 1998;139:4120-4126.

181. Murphy WJ, Durum SK, Longo DL. Role of neuroendocrine hormones in murine T cell development. Growth hormone exerts thymopoietic effects in vivo. J Immunol. 1992;149:3851-3857.

182. Gruver AL, Hudson LL, Sempowski GD. Immunosenescence of ageing. J Pathol. 2007;211:144-156.

183. Shen MM, Skoda RC, Cardiff RD, Campos-Torres J, Leder P, Ornitz DM. Expression of LIF in transgenic mice results in altered thymic epithelium and apparent interconversion of thymic and lymph node morphologies. EMBO J. 1994;13:1375-1385.

184. Hsu HC, Zhang HG, Li L, Yi N, Yang PA, et al. Age-related thymic involution in C57BL/6J x DBA/2J recombinant-inbred mice maps to mouse chromosomes 9 and 10. Genes Immun. 2003;4:402-410.

185. Li L, Hsu HC, Stockard CR, Yang P, Zhou J, et al. IL-12 inhibits thymic involution by enhancing IL-7- and IL-2-induced thymocyte proliferation. J Immunol. 2004;172:2909-2916.

186. Schluns KS, Cook JE, Le PT. TGF-beta differentially modulates epidermal growth factor-mediated increases in leukemia-inhibitory factor, IL-6, IL-1 alpha, and IL-1 beta in human thymic epithelial cells. J Immunol. 1997;158:2704-2712.

187. Henderson J. On the relationship of the thymus to the sexual organs: I. The influence of castration on the thymus. J Physiol. 1904;31:222-229.

188. Utsuyama M, Hirokawa K. Hypertrophy of the thymus and restoration of immune functions in mice and rats by gonadectomy. Mech Ageing Dev. 1989;47:175-185.

189. Olsen NJ, Watson MB, Henderson GS, Kovacs WJ. Androgen deprivation induces phenotypic and functional changes in the thymus of adult male mice. Endocrinology. 1991;129:2471-2476.

190. Kumar N, Shan LX, Hardy MP, Bardin CW, Sundaram K. Mechanism of androgen-induced thymolysis in rats. Endocrinology. 1995;136:4887-4893.

191. Olsen NJ, Olson G, Viselli SM, Gu X, Kovacs WJ. Androgen receptors in thymic epithelium modulate thymus size and thymocyte development. Endocrinology. 2001;142:1278-1283.

192. Olsen NJ, Viselli SM, Fan J, Kovacs WJ. Androgens accelerate thymocyte apoptosis. Endocrinology. 1998;139:748-752.

193. Barr IG, Pyke KW, Pearce P, Toh BH, Funder JW. Thymic sensitivity to sex hormones develops post-natally; an in vivo and an in vitro study. J Immunol. 1984;132:1095-1099.

194. Min H, Montecino-Rodriguez E, Dorshkind K. Reassessing the role of growth hormone and sex steroids in thymic involution. Clin Immunol. 2006;118:117-123.

195. Heng TS, Goldberg GL, Gray DH, Sutherland JS, Chidgey AP, Boyd RL. Effects of castration on thymocyte development in two different models of thymic involution. J Immunol. 2005;175:2982-2993.

196. Goldberg GL, Sutherland JS, Hammet MV, Milton MK, Heng TS, et al. Sex steroid ablation enhances lymphoid recovery following autologous hematopoietic stem cell transplantation. Transplantation. 2005;80:1604-1613.

197. Olsen NJ, Zhou P, Ong H, Kovacs WJ. Testosterone induces expression of transforming growth factor-beta 1 in the murine thymus. J Steroid Biochem Mol Biol. 1993;45:327-332.

198. Olsen NJ, Gu X, Kovacs WJ. Bone marrow stromal cells mediate androgenic suppression of B lymphocyte development. J Clin Invest. 2001;108:1697-1704.

199. Yoon G, Kim JY, Choi YK, Won YS, Lim IK. Direct activation of TGF-beta1 transcription by androgen and androgen receptor complex in Huh7 human hepatoma cells and its tumor in nude mice. J Cell Biochem. 2006;97:393-411.

200. Bertho JM, Demarquay C, Moulian N, Van Der Meeren A, Berrih-Aknin S, Gourmelon P. Phenotypic and immunohistological analyses of the human adult thymus: evidence for an active thymus during adult life. Cell Immunol. 1997;179:30-40.

201. Douek DC, McFarland RD, Keiser PH, Gage EA, Massey JM, et al. Changes in thymic function with age and during the treatment of HIV infection. Nature. 1998;396:690-695.

202. Douek DC. The contribution of the thymus to immune reconstitution after hematopoietic stem-cell transplantation. Cytotherapy. 2002;4:425-426.

203. Haynes BF, Markert ML, Sempowski GD, Patel DD, Hale LP. The role of the thymus in immune reconstitution in aging, bone marrow transplantation, and HIV-1 infection. Annu Rev Immunol. 2000;18:529-560.

204. Mackall CL, Gress RE. Pathways of T-cell regeneration in mice and humans: implications for bone marrow transplantation and immunotherapy. Immunol Rev. 1997;157:61-72.

205. Peggs KS. Immune reconstitution following stem cell transplantation. Leuk Lymphoma. 2004;45:1093-1101.

206. Peggs KS, Mackinnon S. Immune reconstitution following haematopoietic stem cell transplantation. Br J Haematol. 2004;124:407-420.

207. Weinberg K, Blazar BR, Wagner JE, Agura E, Hill BJ, et al. Factors affecting thymic function after allogeneic hematopoietic stem cell transplantation. Blood. 2001;97:1458-1466.

208. Ceredig R, MacDonald HR. Phenotypic and functional properties of murine thymocytes. II. Quantitation of host- and donor-derived cytolytic T lymphocyte precursors in regenerating radiation bone marrow chimeras. J Immunol. 1982;128:614-620.

209. Huiskamp R, van Ewijk W. Repopulation of the mouse thymus after sublethal fission neutron irradiation. I. Sequential appearance of thymocyte subpopulations. J Immunol. 1985;134:2161-2169.

210. Huiskamp R, van Vliet E, van Ewijk W. Repopulation of the mouse thymus after sublethal fission neutron irradiation. II. Sequential changes in the thymic microenvironment. J Immunol. 1985;134:2170-2178.

211. Wiedmeier SE, Samlowski WE, Rasmussen CJ, Huang K, Daynes RA. Effect of ionizing radiation on thymic epithelial cell function. I. Radiation-spared thymic epithelial grafts expedite the recovery of T cell function in lethally irradiated and fetal liver reconstituted mice. J Immunol. 1988;140:21-29.

212. Randle-Barrett ES, Boyd RL. Thymic microenvironment and lymphoid responses to sublethal irradiation. Dev Immunol. 1995;4:101-116.

213. Popa I, Zubkova I, Medvedovic M, Romantseva T, Mostowski H, et al. Regeneration of the adult thymus is preceded by the expansion of K5+K8+ epithelial cell progenitors and by increased expression of Trp63, cMyc and Tcf3 transcription factors in the thymic stroma. Int Immunol. 2007.

214. Zubkova I, Mostowski H, Zaitseva M. Up-regulation of IL-7, stromal-derived factor-1 alpha, thymus-expressed chemokine, and secondary lymphoid tissue chemokine gene expression in the stromal cells in response to thymocyte depletion: implication for thymus reconstitution. J Immunol. 2005;175:2321-2330.

215. Chung B, Barbara-Burnham L, Barsky L, Weinberg K. Radiosensitivity of thymic interleukin-7 production and thymopoiesis after bone marrow transplantation. Blood. 2001;98:1601-1606.

216. Chen W, Frank ME, Jin W, Wahl SM. TGF-beta released by apoptotic T cells contributes to an immunosuppressive milieu. Immunity. 2001;14:715-725.

217. Tang J, Nuccie BL, Ritterman I, Liesveld JL, Abboud CN, Ryan DH. TGF-beta down-regulates stromal IL-7 secretion and inhibits proliferation of human B cell precursors. J Immunol. 1997;159:117-125.

218. Massagué J, Gomis RR. The logic of TGFbeta signaling. FEBS Lett. 2006;580:2811-2820.

219. Huang SS, Huang JS. TGF-beta control of cell proliferation. J Cell Biochem. 2005;96:447-462.

220. Sporn MB, Roberts AB. Transforming growth factor-beta: recent progress and new challenges. J Cell Biol. 1992;119:1017-1021.

UNKNOWN PUBLICATION TYPE

222. Aoki CA, Borchers AT, Li M, Flavell RA, Bowlus CL, et al. Transforming growth factor beta (TGF-beta) and autoimmunity. Autoimmun Rev. 2005;4:450-459.

223. Kemeny DM, Macary PA. The growing complexity of TGF-beta as a T-cell regulator. Immunology. 2005;114:459-460.

224. Letterio JJ. TGF-beta signaling in T cells: roles in lymphoid and epithelial neoplasia. Oncogene. 2005;24:5701-5712.

225. Yingling JM, Blanchard KL, Sawyer JS. Development of TGF-beta signalling inhibitors for cancer therapy. Nat Rev Drug Discov. 2004;3:1011-1022.

226. Roberts AB. Molecular and cell biology of TGF-beta. Miner Electrolyte Metab. 1998;24:111-119.

227. Millan FA, Denhez F, Kondaiah P, Akhurst RJ. Embryonic gene expression patterns of TGF beta 1, beta 2 and beta 3 suggest different developmental functions in vivo. Development. 1991;111:131-143.

228. Schmid P, Cox D, Bilbe G, Maier R, McMaster GK. Differential expression of TGF beta 1, beta 2 and beta 3 genes during mouse embryogenesis. Development. 1991;111:117-130.

229. Shull MM, Ormsby I, Kier AB, Pawlowski S, Diebold RJ, et al. Targeted disruption of the mouse transforming growth factor-beta 1 gene results in multifocal inflammatory disease. Nature. 1992;359:693-699.

230. Letterio JJ, Geiser AG, Kulkarni AB, Roche NS, Sporn MB, Roberts AB. Maternal rescue of transforming growth factor-beta 1 null mice. Science. 1994;264:1936-1938.

231. Sanford LP, Ormsby I, Gittenberger-de Groot AC, Sariola H, Friedman R, et al. TGFbeta2 knockout mice have multiple developmental defects that are non-overlapping with other TGFbeta knockout phenotypes. Development. 1997;124:2659-2670.

232. Proetzel G, Pawlowski SA, Wiles MV, Yin M, Boivin GP, et al. Transforming growth factor-beta 3 is required for secondary palate fusion. Nat Genet. 1995;11:409-414.

233. Dünker N, Krieglstein K. Tgfbeta2 -/- Tgfbeta3 -/- double knockout mice display severe midline fusion defects and early embryonic lethality. Anat Embryol (Berl). 2002;206:73-83.

234. Wipff PJ, Rifkin DB, Meister JJ, Hinz B. Myofibroblast contraction activates latent TGF-beta1 from the extracellular matrix. J Cell Biol. 2007;179:1311-1323.

235. Munger JS, Huang X, Kawakatsu H, Griffiths MJ, Dalton SL, et al. The integrin alpha v beta 6 binds and activates latent TGF beta 1: a mechanism for regulating pulmonary inflammation and fibrosis. Cell. 1999;96:319-328.

236. Yang Z, Mu Z, Dabovic B, Jurukovski V, Yu D, et al. Absence of integrin-mediated TGFbeta1 activation in vivo recapitulates the phenotype of TGFbeta1-null mice. J Cell Biol. 2007;176:787-793.

237. Travis MA, Reizis B, Melton AC, Masteller E, Tang Q, et al. Loss of integrin alpha(v)beta8 on dendritic cells causes autoimmunity and colitis in mice. Nature. 2007;449:361-365.

238. Puthawala K, Hadjiangelis N, Jacoby SC, Bayongan E, Zhao Z, et al. Inhibition of integrin alpha(v)beta6, an activator of latent transforming growth factor-beta, prevents radiation-induced lung fibrosis. Am J Respir Crit Care Med. 2008;177:82-90.

239. Ten Dijke P, Arthur HM. Extracellular control of TGFbeta signalling in vascular development and disease. Nat Rev Mol Cell Biol. 2007.

240. Barcellos-Hoff MH, Derynck R, Tsang ML, Weatherbee JA. Transforming growth factor-beta activation in irradiated murine mammary gland. J Clin Invest. 1994;93:892-899.

241. Ehrhart EJ, Segarini P, Tsang ML, Carroll AG, Barcellos-Hoff MH. Latent transforming growth factor beta1 activation in situ: quantitative and functional evidence after low-dose gamma-irradiation. FASEB J. 1997;11:991-1002.

242. Andarawewa KL, Paupert J, Pal A, Barcellos-Hoff MH. New rationales for using TGFbeta inhibitors in radiotherapy. Int J Radiat Biol. 2007;83:803-811.

243. Reish RG, Eriksson E. Scar treatments: preclinical and clinical studies. J Am Coll Surg. 2008;206:719-730.

244. Eickelberg O, Centrella M, Reiss M, Kashgarian M, Wells RG. Betaglycan inhibits TGF-beta signaling by preventing type I-type II receptor complex formation. Glycosaminoglycan modifications alter betaglycan function. J Biol Chem. 2002;277:823-829.

245. Yamashita H, Okadome T, Franzén P, ten Dijke P, Heldin CH, Miyazono K. A rat pituitary tumor cell line (GH3) expresses type I and type II receptors and other cell surface binding protein(s) for transforming growth factor-beta. J Biol Chem. 1995;270:770-774.

246. Wu HB, Kumar A, Tsai WC, Mascarenhas D, Healey J, Rechler MM. Characterization of the inhibition of DNA synthesis in proliferating mink lung epithelial cells by insulin-like growth factor binding protein-3. J Cell Biochem. 2000;77:288-297.

247. Massagué J, Seoane J, Wotton D. Smad transcription factors. Genes Dev. 2005;19:2783-2810.

248. Moustakas A, Souchelnytskyi S, Heldin CH. Smad regulation in TGF-beta signal transduction. J Cell Sci. 2001;114:4359-4369.

249. Tsukazaki T, Chiang TA, Davison AF, Attisano L, Wrana JL. SARA, a FYVE domain protein that recruits Smad2 to the TGFbeta receptor. Cell. 1998;95:779-791.

250. Brown JD, DiChiara MR, Anderson KR, Gimbrone MA, Topper JN. MEKK-1, a component of the stress (stress-activated protein kinase/c-Jun N-terminal kinase) pathway, can selectively activate Smad2-mediated transcriptional activation in endothelial cells. J Biol Chem. 1999;274:8797-8805.

251. Luukko K, Ylikorkala A, Mäkelä TP. Developmentally regulated expression of Smad3, Smad4, Smad6, and Smad7 involved in TGF-beta signaling. Mech Dev. 2001;101:209-212.

252. Derynck R, Zhang YE. Smad-dependent and Smad-independent pathways in TGF-beta family signalling. Nature. 2003;425:577-584.

253. Arora K, Warrior R. A new Smurf in the village. Dev Cell. 2001;1:441-442.

254. Itoh S, Itoh F, Goumans MJ, Ten Dijke P. Signaling of transforming growth factor-beta family members through Smad proteins. Eur J Biochem. 2000;267:6954-6967.

255. Denissova NG, Pouponnot C, Long J, He D, Liu F. Transforming growth factor beta -inducible independent binding of SMAD to the Smad7 promoter. Proc Natl Acad Sci U S A. 2000;97:6397-6402.

256. Li X, Ionescu AM, Schwarz EM, Zhang X, Drissi H, et al. Smad6 is induced by BMP-2 and modulates chondrocyte differentiation. J Orthop Res. 2003;21:908-913.

257. Kavsak P, Rasmussen RK, Causing CG, Bonni S, Zhu H, et al. Smad7 binds to Smurf2 to form an E3 ubiquitin ligase that targets the TGF beta receptor for degradation. Mol Cell. 2000;6:1365-1375.

258. Ebisawa T, Fukuchi M, Murakami G, Chiba T, Tanaka K, et al. Smurf1 interacts with transforming growth factor-beta type I receptor through Smad7 and induces receptor degradation. J Biol Chem. 2001;276:12477-12480.

259. Pulaski L, Landström M, Heldin CH, Souchelnytskyi S. Phosphorylation of Smad7 at Ser-249 does not interfere with its inhibitory role in transforming growth factor-beta-dependent signaling but affects Smad7-dependent transcriptional activation. J Biol Chem. 2001;276:14344-14349.

260. Ulloa L, Doody J, Massagué J. Inhibition of transforming growth factor-beta/SMAD signalling by the interferon-gamma/STAT pathway. Nature. 1999;397:710-713.

261. Baugé C, Attia J, Leclercq S, Pujol JP, Galéra P, Boumédiene K. Interleukin-1beta up-regulation of Smad7 via NF-kappaB activation in human chondrocytes. Arthritis Rheum. 2008;58:221-226.

262. Janknecht R, Wells NJ, Hunter T. TGF-beta-stimulated cooperation of smad proteins with the coactivators CBP/p300. Genes Dev. 1998;12:2114-2119.

263. Wotton D, Lo RS, Lee S, Massagué J. A Smad transcriptional corepressor. Cell. 1999;97:29-39.

264. Luo K. Ski and SnoN: negative regulators of TGF-beta signaling. Curr Opin Genet Dev. 2004;14:65-70.

265. Stroschein SL, Bonni S, Wrana JL, Luo K. Smad3 recruits the anaphase-promoting complex for ubiquitination and degradation of SnoN. Genes Dev. 2001;15:2822-2836.

266. Tokitou F, Nomura T, Khan MM, Kaul SC, Wadhwa R, et al. Viral ski inhibits retinoblastoma protein (Rb)-mediated transcriptional repression in a dominant negative fashion. J Biol Chem. 1999;274:4485-4488.

267. He W, Dorn DC, Erdjument-Bromage H, Tempst P, Moore MA, Massagué J. Hematopoiesis controlled by distinct TIF1gamma and Smad4 branches of the TGFbeta pathway. Cell. 2006;125:929-941.

268. Yu L, Hébert MC, Zhang YE. TGF-beta receptor-activated p38 MAP kinase mediates Smad-independent TGF-beta responses. EMBO J. 2002;21:3749-3759.

269. Ozdamar B, Bose R, Barrios-Rodiles M, Wang HR, Zhang Y, Wrana JL. Regulation of the polarity protein Par6 by TGFbeta receptors controls epithelial cell plasticity. Science. 2005;307:1603-1609.

270. Foletta VC, Lim MA, Soosairajah J, Kelly AP, Stanley EG, et al. Direct signaling by the BMP type II receptor via the cytoskeletal regulator LIMK1. J Cell Biol. 2003;162:1089-1098.

271. Tachibana I, Imoto M, Adjei PN, Gores GJ, Subramaniam M, et al. Overexpression of the TGFbeta-regulated zinc finger encoding gene, TIEG, induces apoptosis in pancreatic epithelial cells. J Clin Invest. 1997;99:2365-2374.

272. Siegel PM, Massagué J. Cytostatic and apoptotic actions of TGF-beta in homeostasis and cancer. Nat Rev Cancer. 2003;3:807-821.

273. Derynck R, Akhurst RJ. Differentiation plasticity regulated by TGF-beta family proteins in development and disease. Nat Cell Biol. 2007;9:1000-1004.

274. Ristow HJ. BSC-1 growth inhibitor/type beta transforming growth factor is a strong inhibitor of thymocyte proliferation. Proc Natl Acad Sci U S A. 1986;83:5531-5533.

275. Ellingsworth LR, Nakayama D, Segarini P, Dasch J, Carrillo P, Waegell W. Transforming growth factor-beta s are equipotent growth inhibitors of interleukin-1-induced thymocyte proliferation. Cell Immunol. 1988;114:41-54.

276. Chantry D, Turner M, Feldmann M. Interleukin 7 (murine pre-B cell growth factor/lymphopoietin 1) stimulates thymocyte growth: regulation by transforming growth factor beta. Eur J Immunol. 1989;19:783-786.

277. Suda T, Zlotnik A. In vitro induction of CD8 expression on thymic pre-T cells. I. Transforming growth factor-beta and tumor necrosis factor-alpha induce CD8 expression on CD8- thymic subsets including the CD25+CD3-CD4-CD8- pre-T cell subset. J Immunol. 1992;148:1737-1745.

278. Suda T, Zlotnik A. In vitro induction of CD8 expression on thymic pre-T cells. II. Characterization of CD3-CD4-CD8 alpha + cells generated in vitro by culturing CD25+CD3-CD4-CD8- thymocytes with T cell growth factor-beta and tumor necrosis factor-alpha. J Immunol. 1992;149:71-76.

279. Takahama Y, Letterio JJ, Suzuki H, Farr AG, Singer A. Early progression of thymocytes along the CD4/CD8 developmental pathway is regulated by a subset of thymic epithelial cells expressing transforming growth factor beta. J Exp Med. 1994;179:1495-1506.

280. Plum J, De Smedt M, Leclercq G, Vandekerckhove B. Influence of TGF-beta on murine thymocyte development in fetal thymus organ culture. J Immunol. 1995;154:5789-5798.

281. Mossalayi MD, Mentz F, Ouaaz F, Dalloul AH, Blanc C, et al. Early human thymocyte proliferation is regulated by an externally controlled autocrine transforming growth factor-beta 1 mechanism. Blood. 1995;85:3594-3601.

282. Chen W, Jin W, Tian H, Sicurello P, Frank M, et al. Requirement for transforming growth factor beta1 in controlling T cell apoptosis. J Exp Med. 2001;194:439-453.

283. Larsson J, Goumans MJ, Sjöstrand LJ, van Rooijen MA, Ward D, et al. Abnormal angiogenesis but intact hematopoietic potential in TGF-beta type I receptor-deficient mice. EMBO J. 2001;20:1663-1673.

284. Larsson J, Blank U, Helgadottir H, Björnsson JM, Ehinger M, et al. TGF-beta signaling-deficient hematopoietic stem cells have normal self-renewal and regenerative ability in vivo despite increased proliferative capacity in vitro. Blood. 2003;102:3129-3135.

285. Gorelik L, Flavell RA. Abrogation of TGFβ Signaling in T Cells Leads to Spontaneous T Cell Differentiation and Autoimmune Disease. Immunity. 2000;12:171-181.

286. Lucas PJ, Kim SJ, Melby SJ, Gress RE. Disruption of T cell homeostasis in mice expressing a T cell-specific dominant negative transforming growth factor beta II receptor. J Exp Med. 2000;191:1187-1196.

287. Levéen P, Carlsén M, Makowska A, Oddsson S, Larsson J, et al. TGF-beta type II receptor-deficient thymocytes develop normally but demonstrate increased CD8+ proliferation in vivo. Blood. 2005;106:4234-4240.

288. Marie JC, Liggitt D, Rudensky AY. Cellular mechanisms of fatal early-onset autoimmunity in mice with the T cell-specific targeting of transforming growth factor-beta receptor. Immunity. 2006;25:441-454.

289. Li MO, Sanjabi S, Flavell RA. Transforming growth factor-beta controls development, homeostasis, and tolerance of T cells by regulatory T cell-dependent and -independent mechanisms. Immunity. 2006;25:455-471.

290. Kasai M, Kominami E, Mizuochi T. The antigen presentation pathway in medullary thymic epithelial cells, but not that in cortical thymic epithelial cells, conforms to the endocytic pathway. Eur J Immunol. 1998;28:1867-1876.

291. Mizuochi T, Kasai M, Kokuho T, Kakiuchi T, Hirokawa K. Medullary but not cortical thymic epithelial cells present soluble antigens to helper T cells. J Exp Med. 1992;175:1601-1605.

292. Jeker LT, Barthlott T, Keller MP, Zuklys S, Hauri-Hohl M, et al. Maintenance of a normal thymic microenvironment and T cell homeostasis require Smad4-mediated signalling in thymic epithelial cells. Blood. 2008.

293. Jenkinson WE, Jenkinson EJ, Anderson G. Differential requirement for mesenchyme in the proliferation and maturation of thymic epithelial progenitors. J Exp Med. 2003;198:325-332.

294. Cazac BB, Roes J. TGF-beta receptor controls B cell responsiveness and induction of IgA in vivo. Immunity. 2000;13:443-451.

295. Massagué J. How cells read TGF-beta signals. Nat Rev Mol Cell Biol. 2000;1:169-178.

296. Heine U, Munoz EF, Flanders KC, Ellingsworth LR, Lam HY, et al. Role of transforming growth factor-beta in the development of the mouse embryo. J Cell Biol. 1987;105:2861-2876.

297. Ellingsworth LR, Brennan JE, Fok K, Rosen DM, Bentz H, et al. Antibodies to the N-terminal portion of cartilage-inducing factor A and transforming growth factor beta. Immunohistochemical localization and association with differentiating cells. J Biol Chem. 1986;261:12362-12367.

298. Schmierer B, Hill CS. TGFbeta-SMAD signal transduction: molecular specificity and functional flexibility. Nat Rev Mol Cell Biol. 2007;8:970-982.

299. Munger JS, Harpel JG, Gleizes PE, Mazzieri R, Nunes I, Rifkin DB. Latent transforming growth factor-beta: structural features and mechanisms of activation. Kidney Int. 1997;51:1376-1382.

300. Meilin A, Shoham J, Schreiber L, Sharabi Y. The role of thymocytes in regulating thymic epithelial cell growth and function. Scand J Immunol. 1995;42:185-190.

301. Schluns KS, Grutkoski PS, Cook JE, Engelmann GL, Le PT. Human thymic epithelial cells produce TGF-beta 3 and express TGF-beta receptors. Int Immunol. 1995;7:1681-1690.

302. Kasai M, Hirokawa K, Kajino K, Ogasawara K, Tatsumi M, et al. Difference in antigen presentation pathways between cortical and medullary thymic epithelial cells. Eur J Immunol. 1996;26:2101-2107.

303. Erickson M, Morkowski S, Lehar S, Gillard G, Beers C, et al. Regulation of thymic epithelium by keratinocyte growth factor. Blood. 2002;100:3269-3278.

304. Nandan D, Reiner NE. TGF-beta attenuates the class II transactivator and reveals an accessory pathway of IFN-gamma action. J Immunol. 1997;158:1095-1101.

305. O'Keefe GM, Nguyen VT, Benveniste EN. Class II transactivator and class II MHC gene expression in microglia: modulation by the cytokines TGF-beta, IL-4, IL-13 and IL-10. Eur J Immunol. 1999;29:1275-1285.

306. Graham A. Development of the pharyngeal arches. Am J Med Genet A. 2003;119:251-256.

307. Lanigan F, O'Connor D, Martin F, Gallagher WM. Molecular links between mammary gland development and breast cancer. Cell Mol Life Sci. 2007;64:3159-3184.

308. Graham A. The development and evolution of the pharyngeal arches. J Anat. 2001;199:133-141.

309. Holländer G, Gill J, Zuklys S, Iwanami N, Liu C, Takahama Y. Cellular and molecular events during early thymus development. Immunol Rev. 2006;209:28-46.

310. Petrie HT, Zúñiga-Pflücker JC. Zoned out: functional mapping of stromal signaling microenvironments in the thymus. Annu Rev Immunol. 2007;25:649-679.

311. Pinkas J, Teicher BA. TGF-beta in cancer and as a therapeutic target. Biochem Pharmacol. 2006;72:523-529.

312. Rossi SW, Jeker LT, Ueno T, Kuse S, Keller MP, et al. Keratinocyte growth factor (KGF) enhances postnatal T- cell development via enhancements in proliferation and function of thymic epithelial cells. Blood. 2007;109:3803-3811.

313. Kelly RM, Highfill SL, Panoskaltsis-Mortari A, Taylor PA, Boyd RL, et al. Keratinocyte growth factor and androgen blockade work in concert to protect against conditioning regimen-induced thymic epithelial damage and enhance T-cell reconstitution after murine bone marrow transplantation. Blood. 2008;111:5734.

314. Pereira CT, Herndon DN, Rocker R, Jeschke MG. Liposomal gene transfer of keratinocyte growth factor improves wound healing by altering growth factor and collagen expression. J Surg Res. 2007;139:222-228.

315. Zhang F, Nielsen LD, Lucas JJ, Mason RJ. Transforming growth factor-beta antagonizes alveolar type II cell proliferation induced by keratinocyte growth factor. Am J Respir Cell Mol Biol. 2004;31:679-686.

316. Berk M, Desai SY, Heyman HC, Colmenares C. Mice lacking the ski proto-oncogene have defects in neurulation, craniofacial, patterning, and skeletal muscle development. Genes Dev. 1997;11:2029-2039.

317. Prunier C, Pessah M, Ferrand N, Seo SR, Howe P, Atfi A. The oncoprotein Ski acts as an antagonist of transforming growth factor-beta signaling by suppressing Smad2 phosphorylation. J Biol Chem. 2003;278:26249-26257.

318. Heider TR, Lyman S, Schoonhoven R, Behrns KE. Ski promotes tumor growth through abrogation of transforming growth factor-beta signaling in pancreatic cancer. Ann Surg. 2007;246:61-68.

7 Materials and Methods

Mice

LacZ-reporter mice: B6;129-Gt(Rosa)26Sor<tm1Sho> were purchased from Jackson laboratories, stock number 003504

GFP-reporter mice: B6;129-Tg(CAG-Bgeo/GFP)21Lbe/J were purchased from Jackson laboratories, Stock Number 003920

Foxn1-Cre mice: Foxn1-Cre mice were produced as PAC transgenic animals (S. Zyklus, G.A.Holländer, in revision). Briefly, the cds for iCre (for eukaryotes codon usage optimized version of the bacteriophage p1 cre recombinase) was inserted into PAC clone RPCI21-436p24. Successfully modified BACs were purified and injected into C57Bl/6xBDF1 pronuclei by the transgenic mouse core facility (TCMF) of the Biozentrum at the University of Basel. Offspring was screened for transgene integration by PCR.

TGFβRII^{lox/lox} mice: TGFβRII conditional knockout mice were a kind gift of Dr. J. Roes at the Windeyer Institute of Medical Sciences, University College, London. Generation of the mice is described in [294].

Rag2-/- mice were a kind gift of Prof. A. Rolink, Zentrum für Biomedizin, Universität Basel.

C57Bl/6 mice were purchased from RCC Ltd, Füllinsdorf

C57Bl/6-Ly5.1 mice: B6.SJL-PtprcaPep3b/BoyJ mice were obtained from Jackson Laboratories (Bar Harbor, ME, USA)

B6.Foxn1^{nu/nu} mice were obtained from Jackson Laboratories (Bar Harbor, ME, USA)

Thymic epithelial cell lines

TEC1.2, TEC1.4, TEC2.3, TECC6, TECC9 were a kind gift from Dr. M. Kasai (Tokyo, Japan). They were cultured in IMDM-2% and detached if appropriate using Trypsin 0.25% (Gibco).

Buffers

Medium for cell cultures
> IMDM (Gibco, Lubio, Lucerne)
>> for TEC cultures: add 2% fetal calf serum
>> for T cell assays: add 10% fetal calf serum, 2-mercaptoethanol (Gibco, Lubio, Lucerne)

Antibiotics

in all cultures Kanamycin sulphate 100x (Gibco, Lubio, Lucerne), diluted in culture medium to 1x was used

FACS buffer (used for staining of cells for flow cytometry)

> Phosphate buffered saline, pH7.4, containing 2% fetal calf serum (Perbio, Lausanne)
> for stromal cell stainings 5mM EDTA (final concentration) was added (Invitrogen, Lubio, Lucerne)

Red blood cell lysis buffer
- 8.84g NH_4Cl
- 0.037g EDTA
- 1g $NaHCO_3$
- add H20 to 1l, sterile filter

PI solution for dead cell exclusion by FACS: 1mg/ml PI (Sigma-Aldrich, Buchs), used 1:500 in FACS buffer

LacZ staining solutions

0.5M EGTA
> 47.5g EGTA, add H2O to 200ml, adjust pH to 7.5 using NaOH (solubilizes only in neutral pH), add H2O to 250ml

LacZ Fix (50ml)
> 0.4ml 25% glutaraldehyde (Sigma-Aldrich, Buchs)

0.5ml 0.5M EGTA
5ml 1M MgCl2
44.1ml PBS (w/o MgCls/CaCl2, BioWhittaker)

lacZ Wash buffer (500ml)
1ml 1M MgCl2
5ml 1%T naDOC (final 0.01%)
5ml 2% Nonidet-P40 (final 0.02%, Roche)
489ml PBS (w/o MgCls/CaCl2, BioWhittaker)

LacZ stain (100ml)
95ml lacZ wash buffer
4ml 25mg/ml X-gal (dissolved in DMSO)
0.21g K-ferocyanide
0.16g K-ferricyanide

Fixation solution
PFA (1% - 4%) in PBS, dissolved at 55°C for 1 hour

Permeabilization
PBS containing 0.05% Tween20 (Sigma-Aldrich, Buchs)
PBS containing 0.1% Saponin (Sigma-Aldrich, Buchs)

Blocking of Biotin/Avidin in tissue sections
Vector labs-Kit

Blocking of endogenous peroxidases
PBS containing 0.3% NaN_3 + 0.1%H_2O_2

AEC buffer
37ml 0.2N acetic acid, 88ml 0.2 Na-acetate, 375ml H_2O, pH5.0

Tail lysis buffer
100mM Tris pH8.5, 5mM Na-EDTA, 0.2% SDS, 200mM NaCl, Proteinase K (100µg/ml, store at 4°C, add immediately prior to use)

Trypsin 0.25%/EDTA (Gibco, Lubio, Lucerne)

Molecular Biology
Isolation of genomic DNA from mouse tissue
Small tissue pieces (tip of tail, embryonic limb) was digested in 700µl of tail lysis buffer containing Proteinase K at 55°C for 2-12 hours in an Eppendorf Thermomixer shaker. Undigested tissue was pelleted in a tabletop mini centrifuge for 5 minutes at maximum speed. The supernatant was poured into an equal volume of isopropanol. DNA was precipitated by vortexing or inverting the tubes, thereafter pelleted by centrifugation at maximum speed, washed in 70% ethanol, again pelleted by centrifugation, the supernatant discarded and the DNA pellet air dried. TE buffer was added (200-400µl) and the pellet resuspended after incubation at 55° for 30 minutes. DNA was stored at +4°.

RNA isolation
RNA isolation was performed in an RNAse-free environment, wearing disposable gloves. Snap-frozen (using liquid nitrogen) tissue were homogenized in 1ml of TRI-reagent (Molecular Research Center Inc.) and homogenized with a Polytron homogenizer (Kinematica PT1200) for 30-60 seconds on ice, thereafter stored for 10' at RT. After adding of 100µl of bromochloropropanol (Molecular Research Center Inc.) the samples were vigorously vortexed for 10 seconds and incubated at RT for 10'. After centrifugation (Eppendorf Microcentrifuge, 14000rpm, 10 minutes, 4°C) the aqueous phase was transferred to a new Eppendorf tube into an equal volume of isopropanol (Sigma, Buchs), mixed and incubated in order to precipitate the RNA at RT for 30-60 minutes. After centrifugation (Eppendorf Microcentrifuge, 14000rpm, 30 minutes, 4°C) and aspiration of supernatant the pellet was vortexed in 1ml of freshly made 75% ethanol and centrifuged again for 10 minutes. The supernatant was

completely aspirated and the pellet air dried, thereafter dissolved in 10-30μl of ultra pure H2O. RNA concentration was measured with a Gene-Quant machine II (Pharmacia, ratio 260/280nm).

cDNA-synthesis from total RNA
4μg of total RNA was incubated in H2O containing 500μM dNTP, 10mM DTT, 1x 1st strand buffer and 10U RNAse-free DNAseI (final volume 18μl) for 30 minutes at 37°C, cooled on ice for 1 minute, 1μl each of oligo DT and random primers (dN6-G2) were added (final concentration 500nM), incubated 5 minutes at 70°C, cooled on ice for 1 minute. After addition of 1μl of Superscript RTIII (200U/μl) the mixture was incubated for 5 minutes at 25°, 60 minutes at 50°C and finally 15' at 70°. H2O was added to achieve the concentration of interest (~50ng/μl). Aliquots were stored at -80°.

Primer design
Oligonucleotides to be used as primers for PCR reactions were designed using Primer Express ™ across intron-exon boundaries where possible, which were searched by blasting genomic DNA versus mRNA. Selected primers were blasted to assure specificity. Primers were tested by qPCR and the product was run on an agarose gel.

PCR

genotyping of HoxA3-Cre and Foxn1-Cre mice

Primers (Hoxa3-Cre)
TM 2 ggctggaccaatgtaaatattgtc   sense
TM 4 ggtgggcaactctcctggct   antisense
TM 6 catggactacgggggcactg   sense
Expected product length
Hoxa3-Cre 280bp
WT 187bp

Primers (Foxn1-Cre)
     1621   ctc tcc tcc gag tat cca atc tg
     1622   ccc tca cat cct cag gtt cag

PCR reaction mix

10x Mg free Buffer (Promega)	2.2 ul
MgCl$_2$ (25 mM from Promega)	1.32 ul
dNTP mix (2.5 mM each dNTP)	1.32 ul
Primer mix	3.5 ul
Taq Polymerase (Promega)	0.18 ul
ddH$_2$0	11.7 ul
*DNA (boiled 5 min/iced 2 min)	1.0 ul
Total Volume	21 ul

PCR conditions

> Start - 1 minute at 61 degrees
> PCR cycle repeated 29 times:
> > 30 seconds at 72 degrees
> > 30 seconds at 94 degrees
> > 30 seconds at 60 degrees
> 7 minutes at 72 degrees
> Hold at 4 degrees

genotyping of TGFβRII$^{lox/lox}$ mice
Primers
Forward One 5'- GAA AGA GAT CTA CCA CCA TGT CTA CAA GGA TAG C -3'
Reverse One 5'- GGA ATC AAA TCT GAG AAG GGC AAG CAT GGA GC –3'

Reverse Two 5'- GCA AGA ATA TGA GTC CCA GTA GGA ACT CTT TGC C –3'

Mix One
- 100ng template DNA
- 20.5µl dH$_2$O
- 2.5µl 10X PCR

Mix Two
- 14.75µl dH$_2$O
- 2.5µl 10X PCR
- 3µl Mg^{2+} (50mM)
- 1µl Forward One (100µM)
- 2µl Reverse One (100µM)
- 1µl Reverse Two (100µM)
- 0.5µl dNTPs (20mM)
- 0.25µl taq polymerase (0.8 units/µl)

PCR conditions
96°C x 5min
80°C x 5min – add mix two

94°C x 30sec
65°C x 30sec   30 cycles
72°C x 30sec

72°C x 5min

primer sequences used for quantitative PCR (sequences 5'→3')

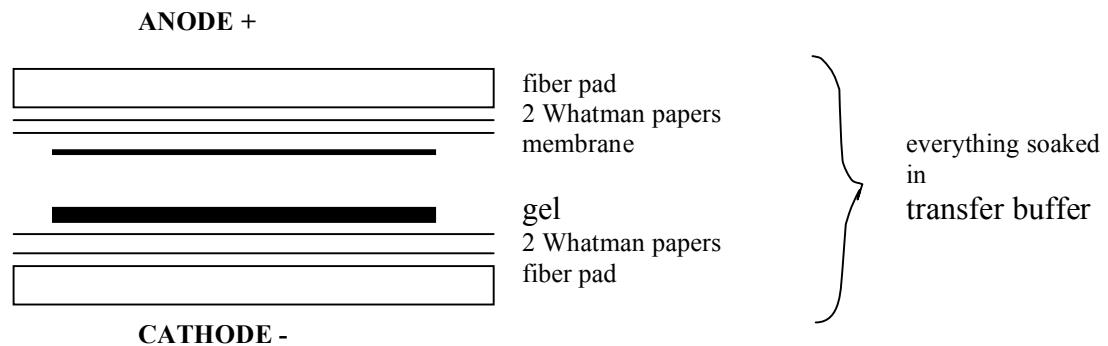|	forward	reverse
IL-7	gtgaggtatgagatgatggacac	gactctgaatcttcatagccttgc
IL-15	gtctccctaaaacagaggcca	gacagagtgctgtttgcaaggt
CCL21-c	tccaactcacaggcaaagagg	ctctaggtctaccccagggaa
CCL25	accttcactatgaaactgtggct	cctgtgctggtaacccaggcagca
CXCL12	AAATCCTCAACACTCCAAAC	GCTTTCTCCAGGTACTCTTG
c-Kit ligand	aaagaatctccgaagaggcca	cacagtcactagtgtcagatgcca
Ednra	tgagatggataagaaccggtg	gcttttggactggtgacaacag
Ednrb	caagacagccaaagattggtgg	agcttcaggatccggctgagg
Endothelin 1	cgcctggcacatttcagggag	gcaggggccagattctgtcatcct
Gata-2	aggactaaagtctccgtgggga	tgcatgcacttggagagctc
TGF-beta	tgacatgagctacctgggtc	ccacatgactcacactgacg

Western blotting

Lysis of tissue for Western blotting

Organs were harvested immediately after sacrificing the animal. 50-100mg of tissue was put in 1ml of RIPA buffer containing Proteinase-Inhibitor and homogenized using a Polytron homogenizer (Kinematica PT1200) for 30-60 seconds on ice. Alternatively, tissue was snap frozen in liquid nitrogen and pulverized with dry ice using a pre-cooled mortar and thereafter put in RIPA buffer containing Proteinase- and Phosphatase-Inhibitors. Protein concentration was measured using the Bradford assay in comparison to a previously established standard curve. Protein lysates were stored at -20° until further use.

SDS-PAGE GEL

Glass plates were assemble according to the Mini-Protean 3 Electrophoresis system (BIORAD). Gel solutions were prepared immediately prior to use. The separating gel was poured and overlayed with H2O and polymerized for 30 minutes. H2O was removed and
the stacking gel poured onto surface of polymerized separating gel, the comb inserted immediately therafter, trying to avoid air bubbles. The comb was removed after 30 minutes polymerization, and the gel mounted in the electrophoresis apparatus. 1x running buffer was added to the system and the wells briefly washed with running buffer using a pipet tip. Samples were prepared by heating them to 95°C for 5 minutes in 1x protein sample buffer. Protein was loaded (usually 20-40μg/well), one well was loaded with 2μl of marker (Caleidoscope, Biorad), empty wells were loaded with 1x loading buffer. The gel was run at 150V for appropriate time, thereafter the glass plates were removed and quickly washed in transfer buffer for 5 minutes. Nitrocellulose membranes were cut to the appropriate size and pre-wet in transfer buffer. A sandwich was done according to the following figure, preventing air bubbles between membrane and gel.

ANODE +

▭	fiber pad
═	2 Whatman papers
▬	membrane
▬	gel
═	2 Whatman papers
▭	fiber pad

everything soaked in
transfer buffer

CATHODE -

This gel-membrane sandwich was put in the transfer apparatus, filled with ice-cold 1x transfer buffer. Transfer was run at 100V for 1 hour. After transfer, the membrane was rinsed in TPBS and used for Western blotting.

WESTERN BLOT

Unspecific binding was blocked using Blotto for 1 hour at RT or overnight at 4°C on a shaking platform. Primary Antibody incubation was usually performed overnight at 4°C with shaking, diluted in Blotto, thereafter the membrane was washed 3-5 times 10 minutes in TPBS at RT.
2[ndary] Antibody (HRP-conjugated) incubation was done diluted in Blotto at RT for 45' on a shaking platform, thereafter washed 3-5 times 10min in TPBS at RT. The membrane was incubated for 5min with SuperSignal West Pico Chemiluminescent Substrat working solution (from PIERCE) (mix equal volumes of Luminol/Enhancer solution and Stable Peroxide solution) (*generated light should last up to 8hours*). The wet membrane was wrapped in plastic foil and an appropriately sized piece of Kodax BioMax Light film was usually exposed for 10 seconds to 15 minutes.

Preparation of single-cell suspensions
Organs were dissected immediately after sacrificing the animal and placed in ice-cold PBS-2 or IMDM-2. The organ was dissociated between two wet, appropriately sized 70μm pore-size meshes using a plunger. The resulting dissociated cells were harvested in (A) IMDM-10 (for culture purposes) or (B) in PBS-2.

Preparation of thymic stromal cell preparations
Organs were dissected immediately after sacrificing the animal and placed in ice-cold PBS-2 or IMDM-2. The lobes were separated and small cuts were made using small scissors. The thymic lobes were placed in digestion solution containing CollagenaseD and DNAse and placed in a waterbath pre-warmed to 37°C. Every 5 minutes the organs were gently pipetted up and down using a pipet tip with an appropriately sized opening (cut if necessary). For TEC quantification, the digest was continued until no more clumps were visible. For TEC enrichment, the supernatant was removed after 3-4 rounds

of pipetting and fresh Collagenase IV (1mg/ml)/DNAse (10μg/ml) solution was added. Usually two to three rounds were performed in this manner, resulting in a single-cell suspension. All further steps were performed using PBS-2 containing 5mM EDTA to prevent clumping and adherence of the cells. Cells were filtered through a 40μm mesh.

FACS staining
Staining of filtered cells was performed in PBS-2% on ice in 96-well round bottom plates or in 5ml FACS tubes. Antibodies were added at pre-titrated optimal dilutions, incubated on ice for 30 minutes, washed in PBS-2%. Appropriate secondary reagent was added where applicable. Flow cytometric acquisition was performed on a FACS Calibur (BD, Allschwil). Data was analysed using Cell Quest Pro Software (BD, Allschwil) or FlowJo 8.2 (Tree Star Inc., Stanford)

in vitro T cell proliferation
96-well tissue culture plates were pre-incubated at 37°C for 1 hour with a-CD3 and a-CD28 (4μg/ml) in 50μl PBS/well. Thereafter wells were washed and cells added at 5×10^4 /well in a final volume of 200μl IMDM-10%. After 48 hours 50μl of supernatant was removed and 1μCi/well of 3H-Thymidine was added. 24 hours later the cells were harvested and counted in a b-scintillation counter.

TGFβ-ELISA
ELISA was performed in a 96-well flat bottom high absorbance plate (ebioscience Inc., San Diego, CA, USA) according to the manufacturer. The ELISA plate was coated with 100 μl/well of capture antibody in Coating Buffer and the plate was sealed the plate and incubated overnight at 4°C. Thereafter washed 5 times with >250 μl/well Wash Buffer (diluted to 1X). Allowing time for soaking (~ 1 minute) during each wash step increases the effectiveness of the washes. Blot plate on absorbent paper to remove any residual buffer.
Dilute 1 part 5x concentrated Assay Diluent with 4 parts DI water. Block wells with 200 μl/well of 1x Assay Diluent. Incubate at room temperature for 1 hour. Aspirate/wash 5x
Acid Activation of Samples: To activate latent TGF-ß1 to the immunoreactive form, the samples (but not standards) must be acidified, and then neutralized. Animal serum used in culture media may contain high levels of latent TGF-ß1, so controls should be run to determine baseline concentrations of TGF-ß1 in culture media.
Tissue culture supernatants: Per 100 ul of sample, add 20 ul of 1N HCl; incubate 10 minutes at room temperature, then neutralize with 20 ul of 1N NaOH. [When calculating final sample concentration, correct to the dilution factor of 1.4.]
Serum or plasma: Dilute 1:5 in PBS, then treat as above for supernatants.
Using Assay Diluent, dilute standards as noted on the Certificate of Analysis (C of A). Add 100 μl/well of standard to the appropriate wells. Perform 2-fold serial dilutions of the top standards to make the standard curve. Add 100 μl/well of your acid-activated samples to the appropriate wells. Cover or seal the plate and incubate at room temperature for 2 hours (or overnight at 4°C for maximal sensitivity).
Wash 5 times as above.
Add 100 μl/well of detection antibody diluted in 1X Assay Diluent (dilute as noted on C of A). Seal the plate and incubate at room temperature for 1 hour.
Aspirate/wash. Repeat for a total of 5 washes.
Add 100 μl/well of Avidin-HRP diluted in 1X Assay Diluent. Seal the plate and incubate at room temperature for 30 minutes.
Aspirate and wash. In this wash step, soak wells in Wash Buffer for 1 to 2 minutes prior to aspiration. Repeat for a total of 7 washes.
Add 100 μl/well of Substrate Solution to each well. Incubate plate at room temperature for 15 minutes.
Add 50 μl of Stop Solution (2N H2SO4) to each well.
Read plate at 450 nm. If wavelength subtraction is available, subtract the values of 570 nm from those of 450 nm and analyze data.

Histology
Freshly dissected organs were embeddedin OCT compound (Medite, Switzerland) in Tissue-Tek Cryomolds (Miles Inc., Elkhart, USA). Tissues were frozen in methyl-butane pre-cooled with dry ice and then stored at -80°C until further use.
Alternatively the organ was fixed in 4% PFA/PBS overnight, washed in PBS an thereafter parafinized.

HE staining

OCT embedded tissues were cut at 5-10μm thickness usin a cryostat. Tissues were air dried for 30 minutes to overnight at RT, thein either frozen at -80°C (wrapped in aluminium foil) or processed directly, Sections were fixed in Delaunay's fixation solution for 1' rehydrated in a series of ethanol dilutions for 1 minute each (100% - 96% - 70% -50% - 0%), stained in Meyer's Hämalaun for 2 minutes, washed 3 minutes in warm water, stained in Erythrosin, washed again 2 minutes in water and dehydrated in increasing ethanol concentrations. After air drying the slides were covered with Pertex and cover slips.

Immunohistochemistry
5-10μm sections were fixed in 4% PFA/PBS at RT for 15 minutes or alternatively in pre-cooled Acetone (Sigma, Buchs) for 10' at -20°, thereafter incubated in PBS-Tween0.05% for 5 minutes. Unspecific binding was reduced by blocking with PBS-2% BSA-Tween0.05%, biotin/avidin block was used to block endogenous biotin. Incubation with primary antibody was performed in PBS-Tween0.05% for 2 hours up to overnight. Sections were washed thereafter 3 times in PBS-Tween0.05% 5 minutes each, and incubated with secondary antibody for 30' at RT of riwth SA-conjugated horseradish peroxidase. Sections were developed using AEC and counterstained with hemalaun. Alternatively, fluorochrome-labeled primary or secondary antibodies were used to detect the antigens of interest using a confocal microscope (Carl-Zeiss AG, Feldbach, Switzerland).

β-galactosidase staining

Tissue processing:
Embryos up to E14: whole mount possible, yet cutting into smaller pieces (e.g. removing head and limbs helps penetration of fixative and staining solution

Fixation in LacZ fixation solution:
Whole mount: depending on the size of the tissue 2-12 hours at 4°C gave adequate results.
wash with PBS at least 3x 5 minutes

X-gal staining
Whole mount: incubate in LacZ staining solution at 30-37° overnight
wash with PBS at least 3x 5 minutes
Fix again in 0.2% glutaraldehyde/PBS overnight at 4°C
wash with PBS at least 3x 5 minutes
proceed to paraffin embedding

staining for intracellular TGFβ1-3
Cells were stained for surface antigens for 30 minutes on ice in FACS buffer, washed, fixed in 2% PFA for 10 minutes at room temperature, washed in PBS-0.2% Saponin, and stained with Fluos-labelled a-TGFβ (clone 1D11)

BrdU staining for measurement of proliferation
Cells were stained for surface antigens for 30 minutes on ice in FACS buffer, washed, fixed in Cytofix/Cytoperm buffer (BD biosciences, Allschwil) for 30 minutes on ice, washed in Wash/Perm buffer (BD biosciences, Allschwil), resuspended in 10%DMSO/90% FCS and frozen at -80°C for at least 12 hours, thereafter thawed in 37°C waterbath, washed in FACS buffer, re-fixed in Cytofix/Cytoperm buffer for 10-15 minutes on ice, washed, incubated in 1x DNAse buffer containing RNAse-free DNAse (Roche Diagnostics, Basel) at 4U/ml in 37° C waterbath for 60 minutes, washed in Wash/Perm buffer, incubated with a-BrdU-FITC (BD Biosciences or ebioscience (clone PRB-1), washed in Wash/Perm buffer and finally analyse at a flow rate of 400 events/second. This method has the advantage of excellent preservation of FSC/SSC characteristics.

Fetal thymic organ culture and lymphocyte depletion
Fetal thymic lobes were placed on Nucleopore track-edge membrane filters (shiny side up), which was placed on the surface of medium in a 12- or 24-well plate. Lymphocyte depletion was performed prior to transplantation of the thymic grafts into nude recipients for a 5-day culture period using 2-deoxy-Guanosine (2dGuo) (Sigma-Aldrich, Buchs, Switzerland). Deoxy-Guanosine, final concentration 1.35mM in IMDM-10%FCS

In vivo **BrdU labeling**

To measure TEC proliferation, mice (12 – 18 weeks of age) were first injected with 1mg BrdU (Sigma-Aldrich, Buchs, Switzerland) and, thereafter, fed with BrdU-containing drinking water (0.8mg/ml). On day 14, thymic stromal cells were isolated as detailed above, stained for the expression of CD45 and MHCII, and analyzed for BrdU incorporation.

Intrathymic FITC injection for the detection of recent thymic emigrants

Anesthesized animals were injected in both thymic lobes wit 10µl of 125µg/ml FITC (Sigma, Buchs, Switzerland) diluted in PBS. 16-24 hours later the mice were analysed for FITC+ CD4+ or CD8+ cells in thymus and periphery.

Hematopoetic stem cell transplantation

Donors:

Bone marrow was flushed from femur and tibia using IMDM-10%. Cells were washed and filtered through a 40µm mesh. For T cell depletion anti-CD4 (clone RL172), anti-CD8 (clone 31M) and anti-Thy1.2 (clone H01349) supernatants were added to the cells. After washing T cell elimination was achieved using Low-Tox®-M rabbit complement lysis (Cedarlane, Bioreba AG, Switzerland).

Recipients:

Eight week old TGFbRII$^{lox/lox}$ and TGFbRII$^{lox/lox}$::Foxn1-Cre mice were lethally irradiated (9.5 Gy) using a ^{137}Cs source (0.81 Gy/min) and were subsequently intravenously infused with 10^7 T cell-depleted bone marrow cells derived from B6.CD45.1 mice in a total volume of 250µl HBSS. Transplanted mice were housed in single ventilated cages.

KGF treatment

Mice were injected intraperitoneally on 3 subsequent days with either HBSS or recombinant human KGF (kindly provided by Amgen, Thousand Oaks, CA, USA) at a dose of 5mg/kg per day. Analysis was performed 14 days after the last injection.
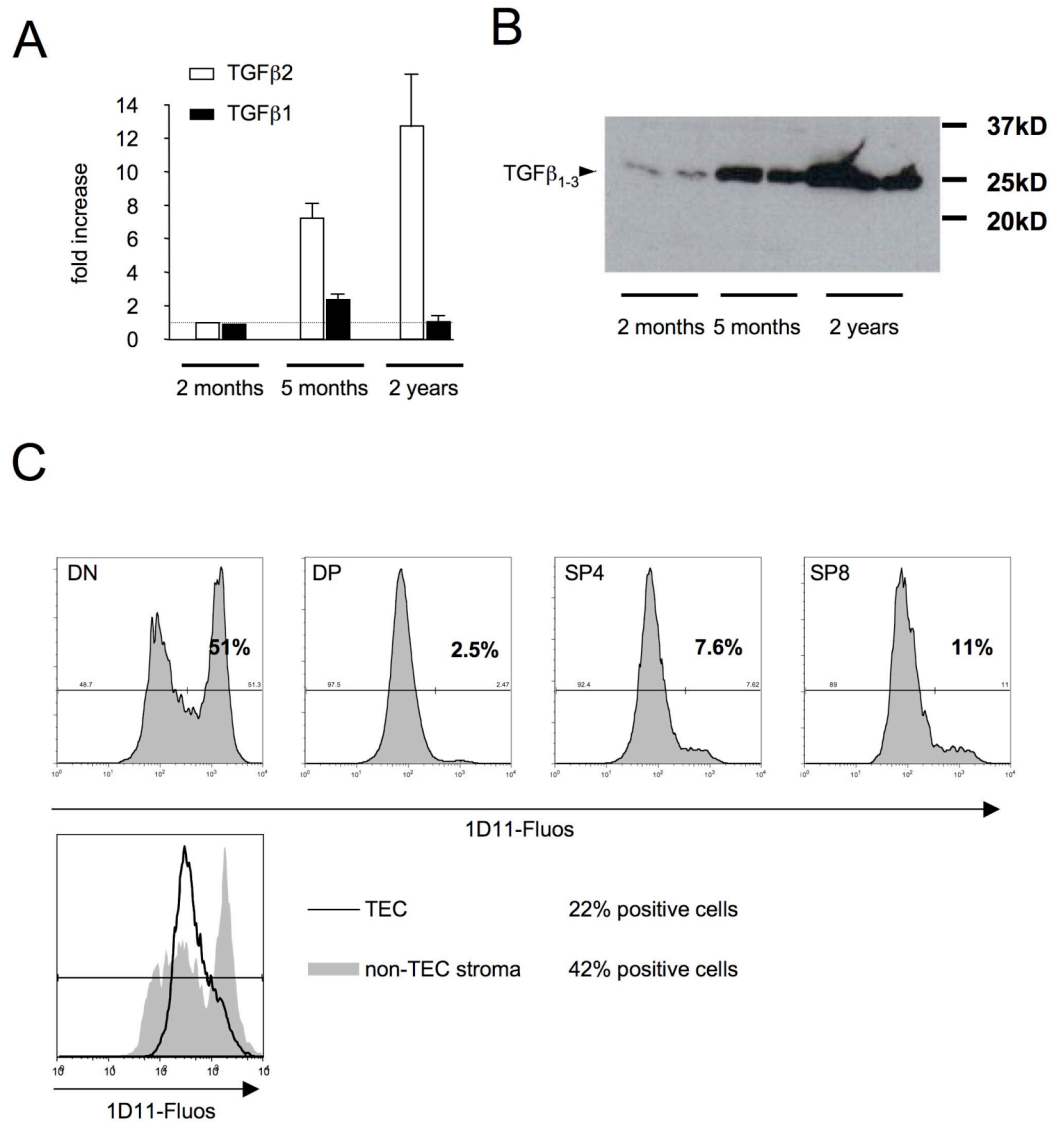
Figure 1

A

B

C

Figure 1. TGFβ expression in the thymus at different ages
(A) TGFβ1 and 2 transcript and (B) protein levels in thymi derived from mice at the indicated age. (C) Flowcytometric analysis for intracellular TGFβ1-3 in the indicated thymocyte populations in 8 week old wildtype animals.
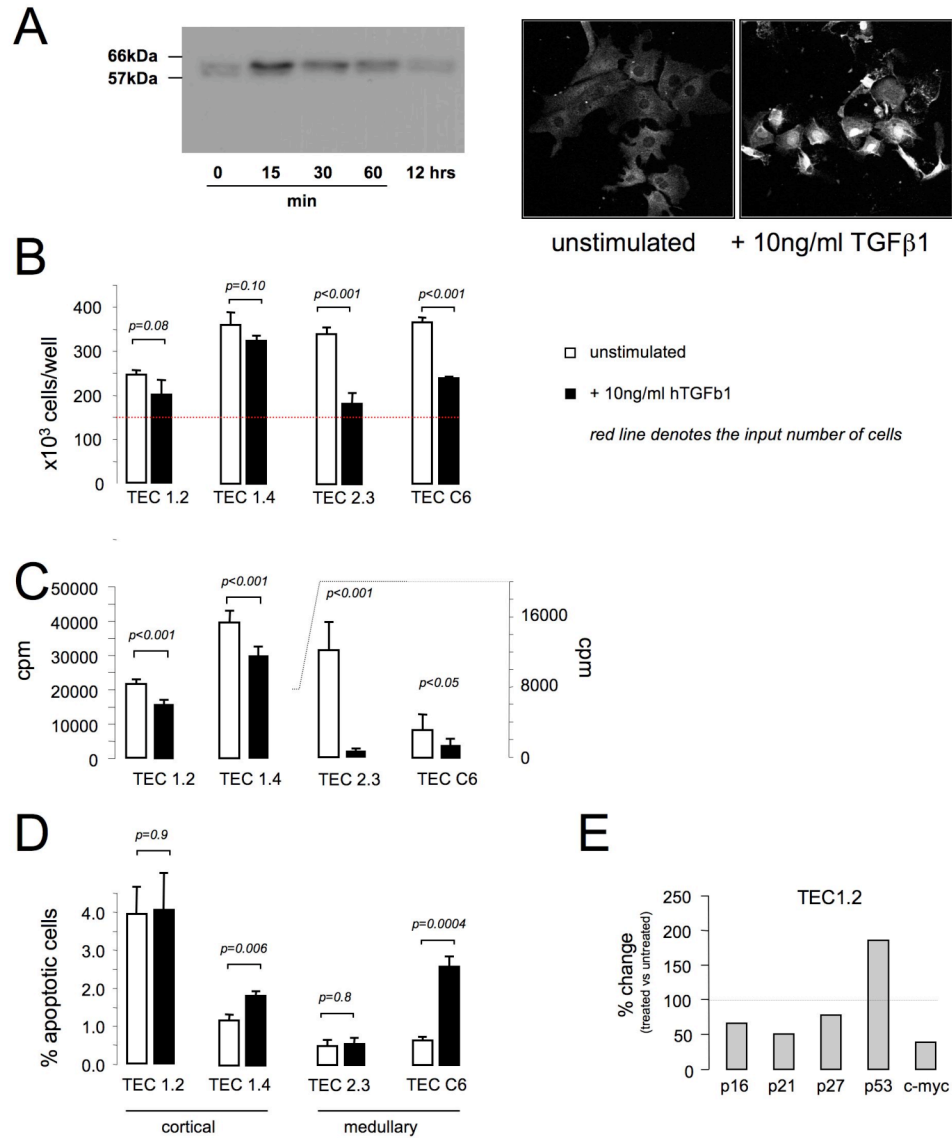
Figure 2

Figure 2. Responsiveness of TEC lines to TGFβ1

(A) Kinetics of Smad2 phosphorylation in the cortical TEC1.2 cell line at the indicated time points after stimulation with TGFβ1 (left panel) and Smad2 translocation 30 minutes after stimulation with TGFβ1 (right panel). (B) Cell recovery, (C) 3H-thymidine-incorporation and (D) apoptotic cells after 48 hours of stimulation with TGFβ1. (E) Transcriptional changes in TEC1.2 cells after 48 hours of stimulation with TGFb1.

Figure 3

A

B
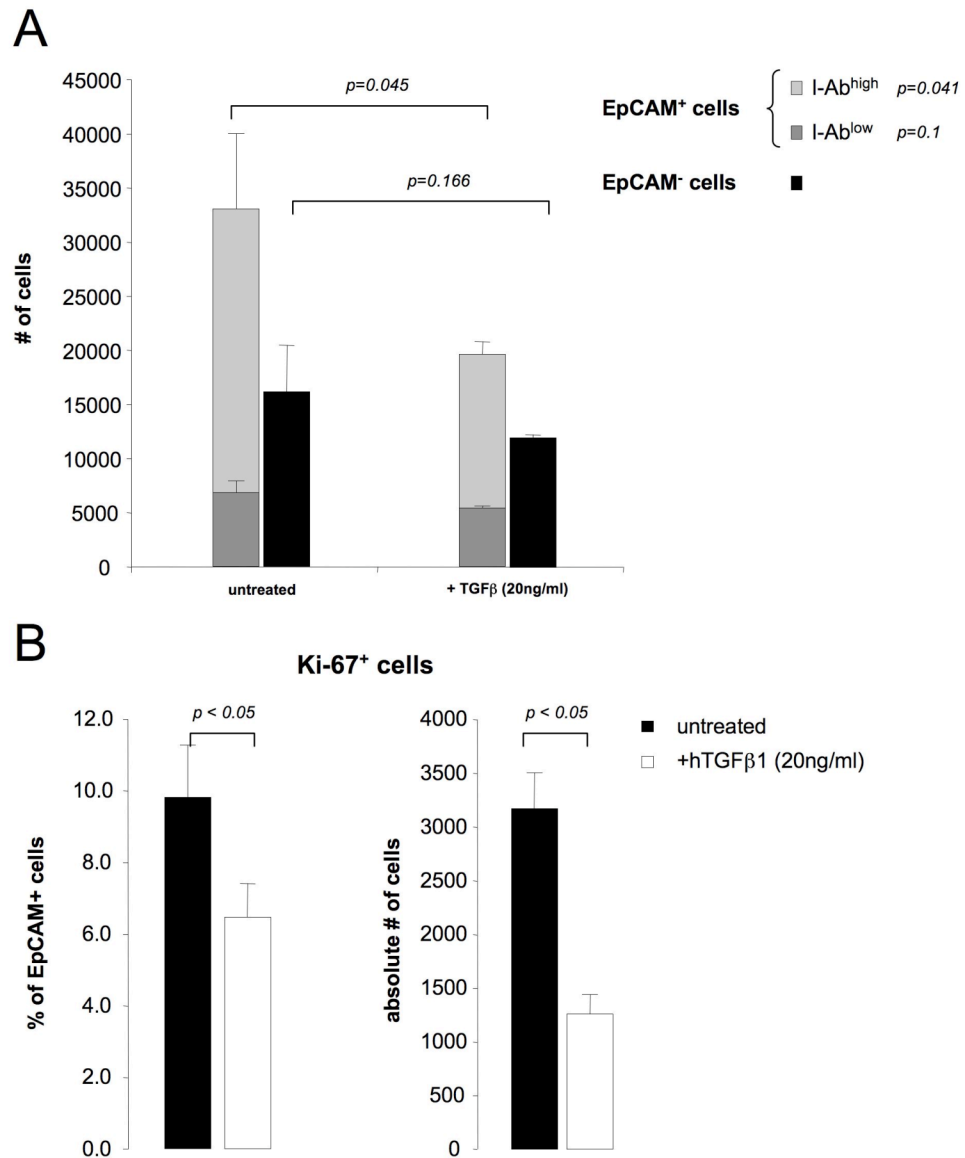
Figure 3. Responsiveness of primary TEC to TGFβ1
(A) Cell recovery of E15 fetal thymic lobes pretreated for 5 days with d-Guo and thereafter stimulated with TGFβ1(20ng/ml) (B) Frequency (left panel) and absolute cell numbers (right panel) or Ki-67-positive cells within the d-Guo treated lobes from (A).

Figure 4
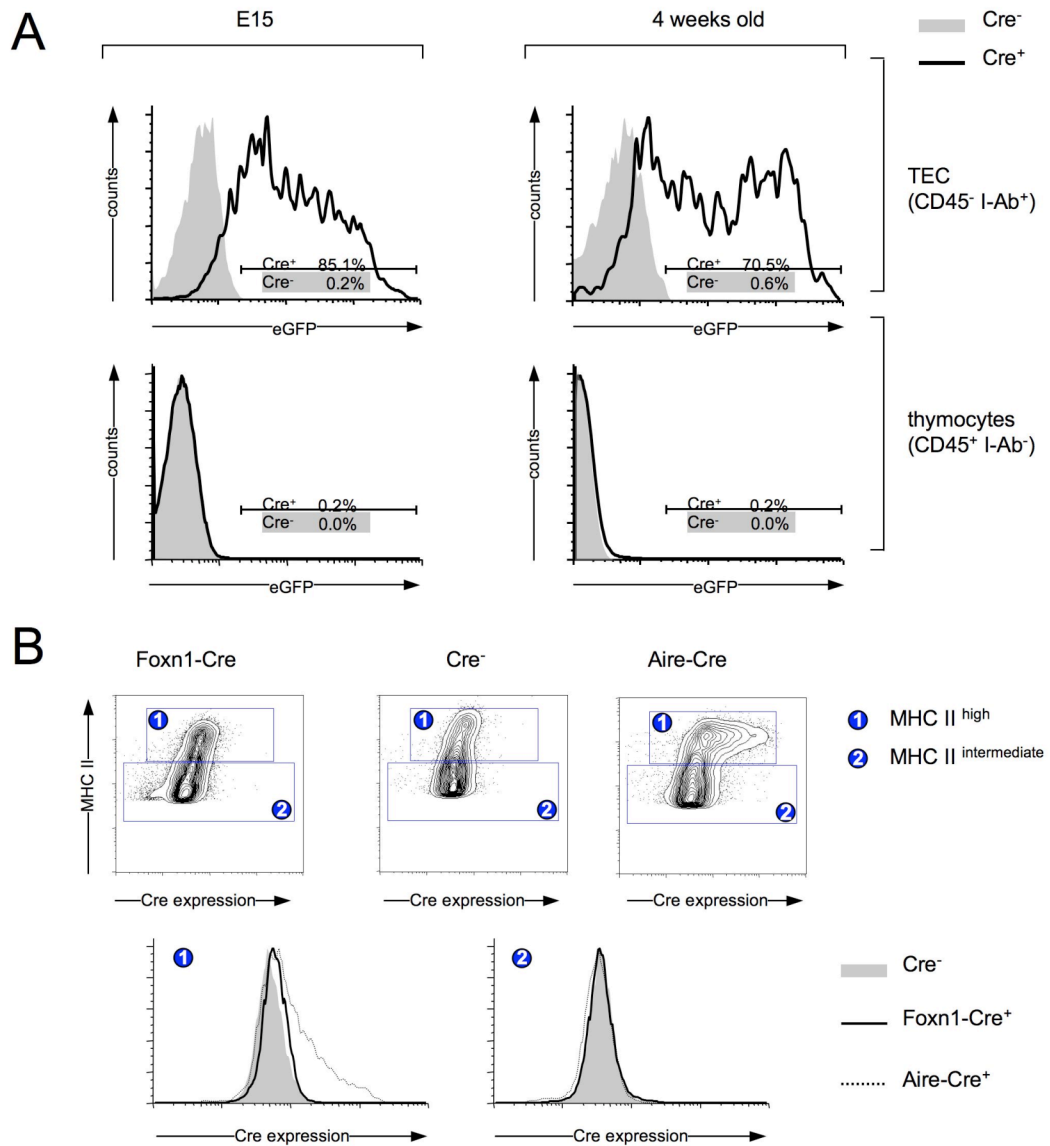
Figure 4. Effectiveness of Cre-mediated recombination in GFP-reporter::Foxn1-Cre mice

(A) GFP-fluorescence TEC and thymocytes derived from Cre+ and Cre- GFP-reporter mice at the indicated ages analysed (B) Detection of Cre-protein by flow cytometry in MHCII[high] and MHCII [intermediate] TEC populations in Foxn1-Cre, wildtype (negative control) and Aire-Cre (positive control) mice.

Figure 5
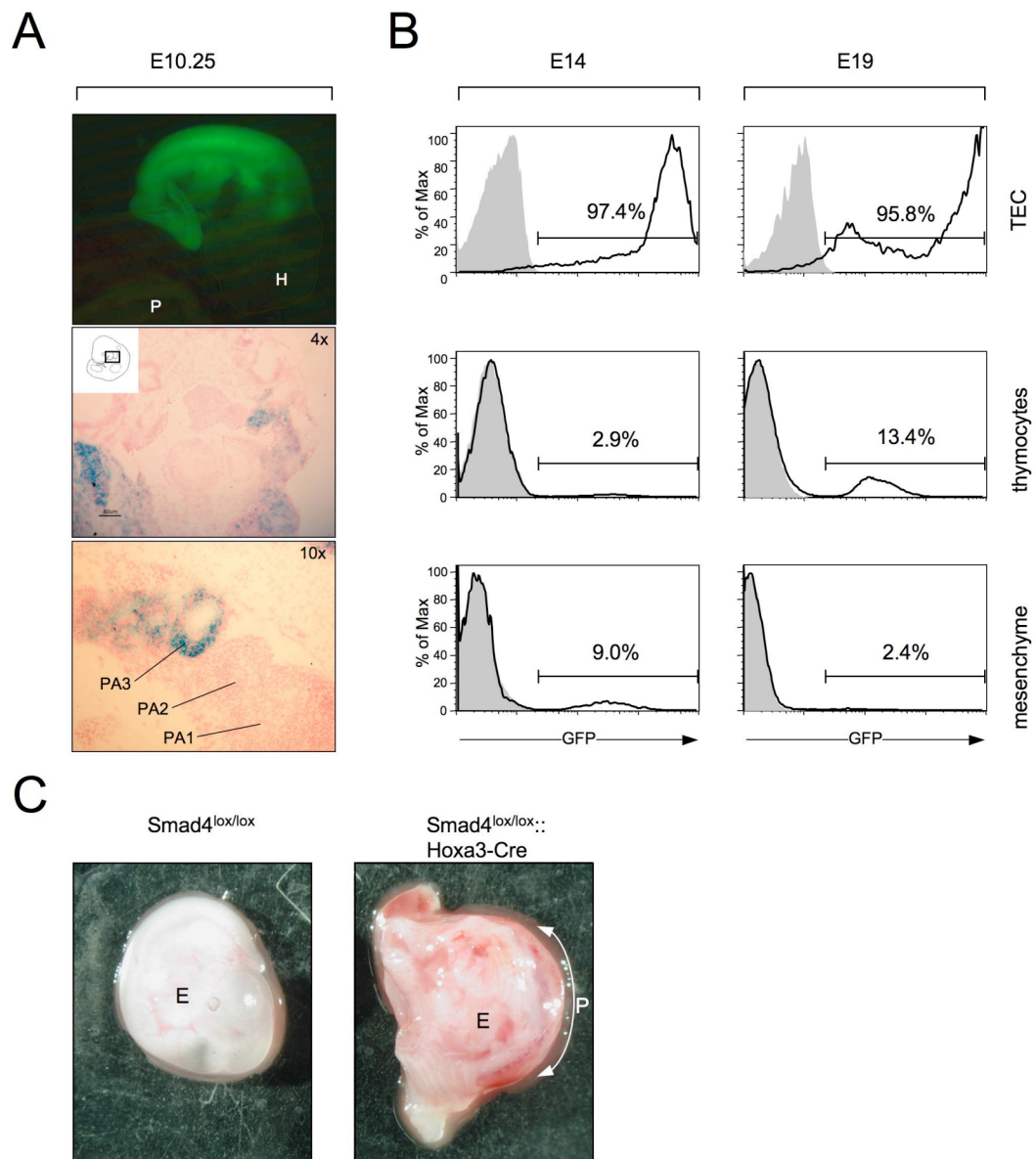
Figure 5. Effectiveness of Cre-mediated recombination in Hoxa3-Cre mice
(A) *upper panel* E10.25 GFP-reporter::Hoxa3-Cre embryo under the fluorescence microscope, *middle panel* 4x and *lower panel* 10x magnification of LacZ-reporter::Hoxa3-Cre stained for β-galactosidase expression.(B) Detection of GFP-fluorescence by flow cytometry in CD45-G8.8+ TEC, CD45+ thymocyte and CD45-G8.8- mesenchymal populations. Percentage shown indicates fraction of GFP-positive cells. (C) Smad4lox/lox and Smad4lox/lox::Hoxa3-Cre E11 embryos

Figure 6
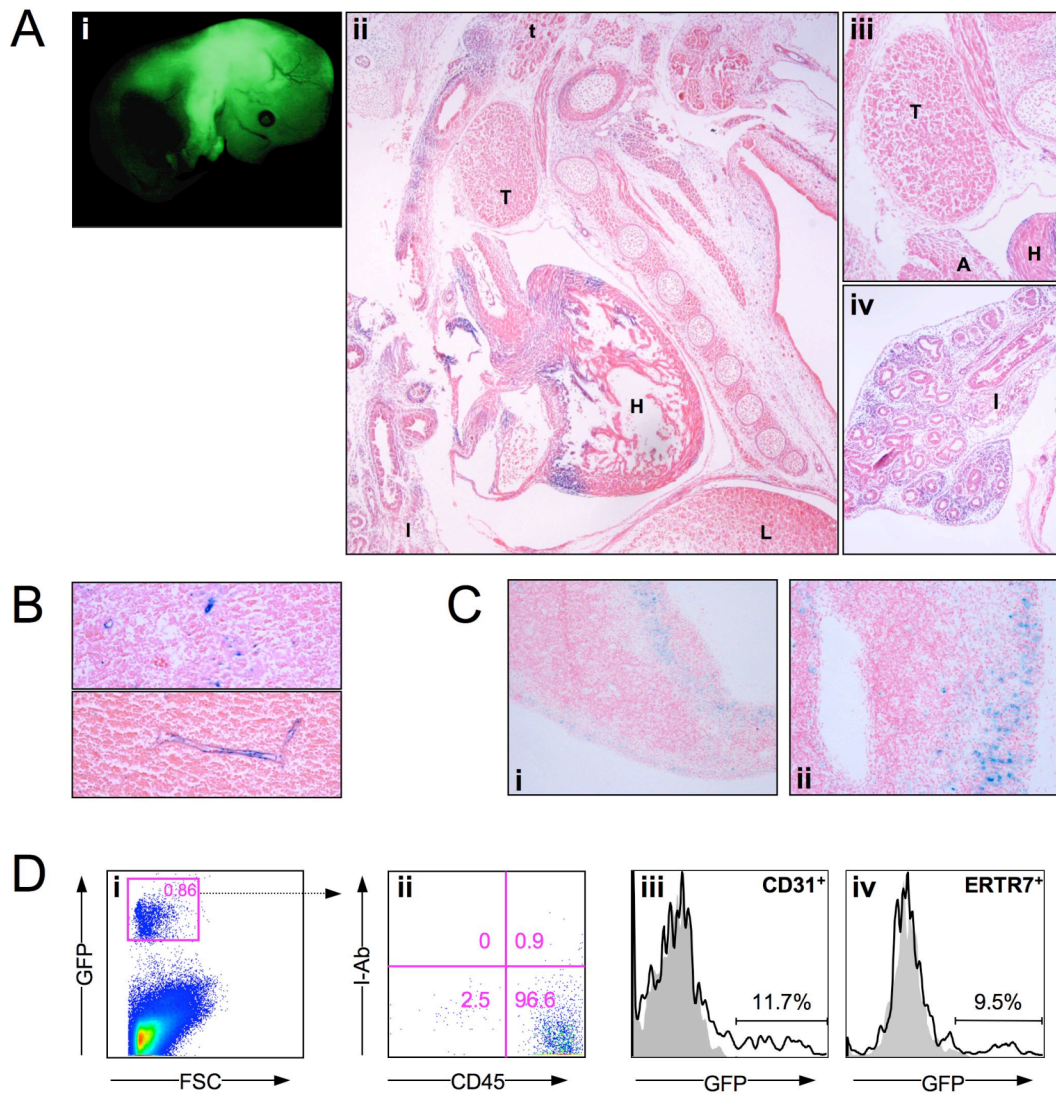
Figure 6. Characterization of Cre-mediated recombination in Lefty-Cre mice
(A) *i* E14 GFP-reporter::Lefty-Cre embryo under the fluorescence microscope, *ii 4*x
and *iii,iv* 10x magnification of LacZ-reporter::Lefty-Cre stained for β-galactosidase
activity; A aorta, H heart, L liver, l lungs, T thymus, t thyroid. (B) E17 embryonic
thymus section, 40x magnification and (C) i 20x, ii 40x newborn thymus section
stained for β-galactosidase activity. (C) Flowcytometric characterization of GFP
positive cells (i,ii); GFP-fluorescence in CD31+ endothelial (iii) and ERTR7+
fibroblast (iv) populations.

Figure 7

A

total offspring: 381	Foxn1-Cre⁺/⁻		Foxn1-Cre⁻/⁻	
	E	O	E	O
TGFβRII^lox/lox	190.5 (50%)	191 (50.1%)	190.5 (50%)	190 (49.9%)

E expected, O observed

B

	E	O			P
		E12	E13	E14	
Hoxa3-Cre⁻/⁻ TGFβRII^lox/lox	25%	25%	18%	0%	68%
Hoxa3-Cre⁻/⁻ TGFβRII^lox/wt	25%	25%	33%	71%	
Hoxa3-Cre⁺/⁻ TGFβRII^lox/wt	25%	25%	23%	14%	32%
Hoxa3-Cre⁺/⁻ TGFβRII^lox/lox	25%	25%	26%*1	14%*2	0%
		N=8	N=39	N=7	N=117

*1 smaller, delayed development compared to littermates
*2 smaller, protruded and translucent abdominal wall, otherwise normal aspect (head, limbs, tail)

E expected, O observed, P post-natal, ND not determined

Figure 7. Analysis of the frequency of Cre+ and Cre- offspring in TGFβ RII^lox/lox::Foxn1-Cre (A) and TGFβRII^lox/lox::Hoxa3-Cre (B) mice
E and O denotes the absolute number and relative frequency of the expected (mendelian) and observed genotype of the offspring. In (B) the percentage of observed genotypes is shown for the different time points prior to (E12, E13, E14) and after (P) birth; N denotes the number of animals genotyped.

Figure 8
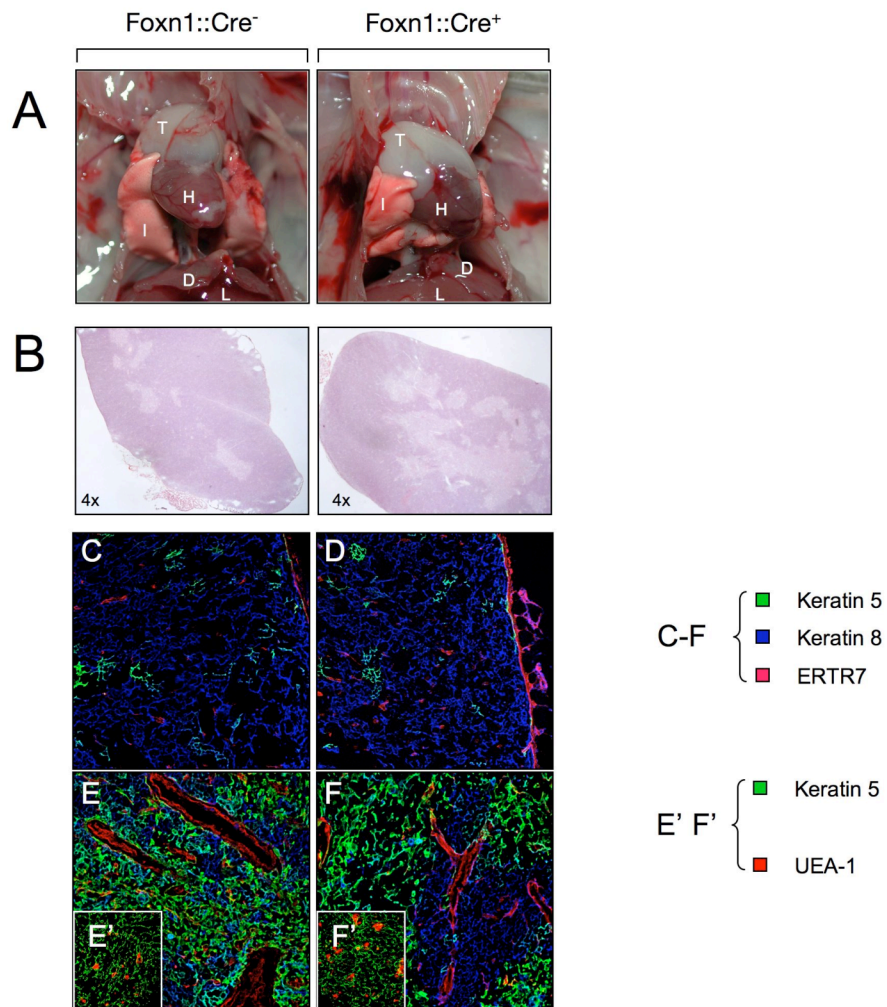
Figure 8. Gross morphology and thymic histology of 5 week old TGFβ RII[lox/lox]::Foxn1-Cre mice
(A) Aspect of upper thorax after removal of sternum and adjacent ribs; D diaphragm, H heart, l lungs, T thymus; (B) 4x magnifications of H&E staining of thymic sections (C)-(F') immunofluorescence analysis for thymic stromal components in thymic sections (magnification 40x)
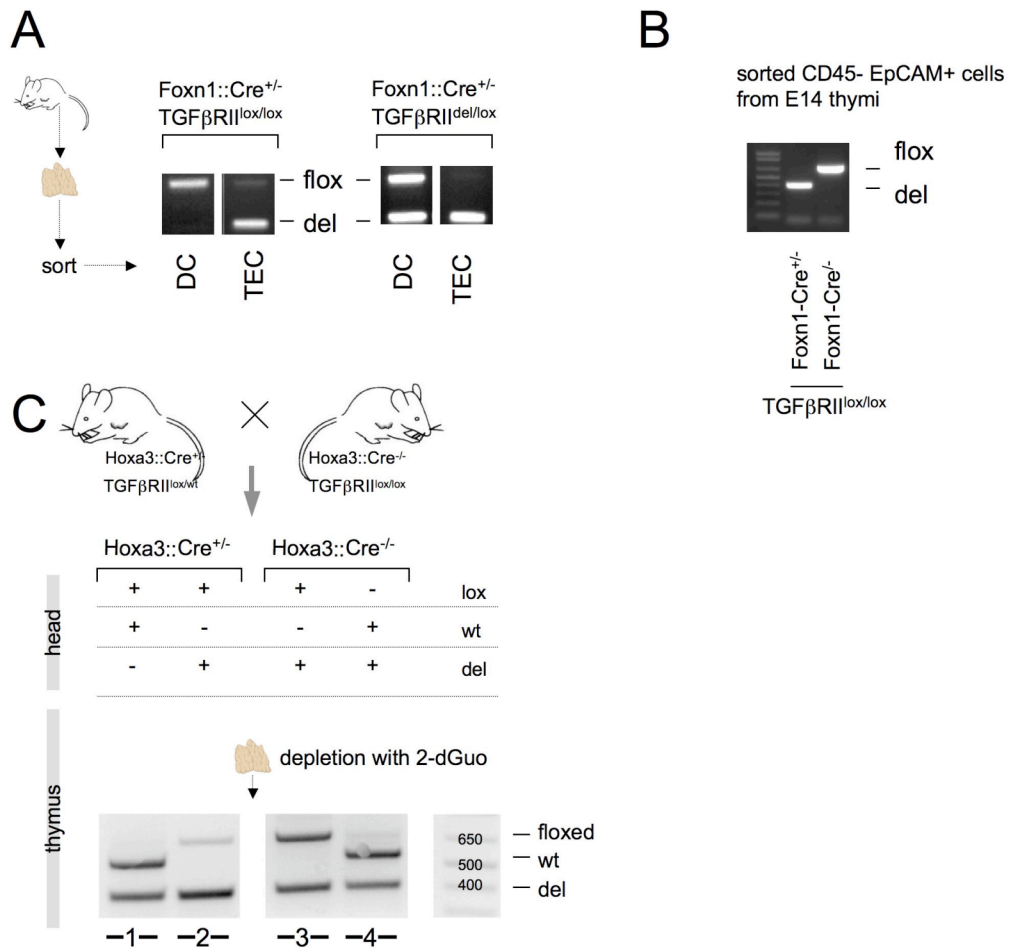
Figure 9

A

Foxn1::Cre$^{+/-}$
TGFβRII$^{lox/lox}$

Foxn1::Cre$^{+/-}$
TGFβRII$^{del/lox}$

— flox —
— del —

DC   TEC   DC   TEC

sort

B

sorted CD45- EpCAM+ cells
from E14 thymi

— flox
— del

Foxn1-Cre$^{+/-}$ Foxn1-Cre$^{-/-}$

TGFβRII$^{lox/lox}$

C

Hoxa3::Cre$^{+/-}$
TGFβRII$^{lox/wt}$

×

Hoxa3::Cre$^{-/-}$
TGFβRII$^{lox/lox}$

	Hoxa3::Cre$^{+/-}$		Hoxa3::Cre$^{-/-}$		
head	+	+	+	-	lox
	+	-	-	+	wt
	-	+	+	+	del

depletion with 2-dGuo

		650	— floxed
		500	— wt
		400	— del

—1— —2—   —3— —4—

**Figure 9. Analysis of Cre-mediated deletion of TGFβRII in TGFβP
II$^{lox/lox}$::Foxn1-Cre and TGFβRII$^{lox/lox}$::Hoxa3-Cre mice**
(A) genotyping PCR performed on FACS-sorted thymic dendritic cells (DC) or
epithelial cells (TEC) from indicated mice'flox' denotes the PCR product of the
floxed, non-deleted allele, 'del' denotes the product for the (B) sort purified TEC
derived from E14 thymic lobes from mice with the indicated genotype subjected to the
same analysis as in (A)(C) Genotyping of head and d-Guo depleted thymic lobes of
E13 embryos with the indicated genotype

Figure 10
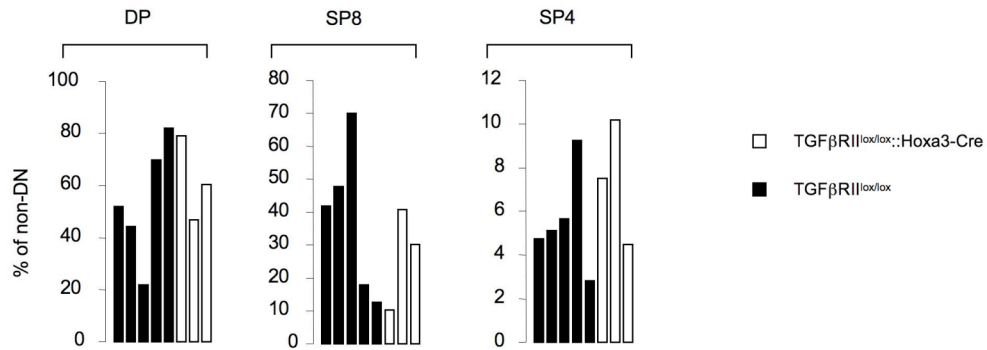
Figure 10. Thymocyte development in FTOC with E13 thymi from TGFβ RII^{lox/lox}::Hoxa3-Cre mice
Relative frequency of indicated thymocyte subpopulations in percent of non-DN. Each bar denotes the results of a pair of thymic lobes derived from a single mouse.
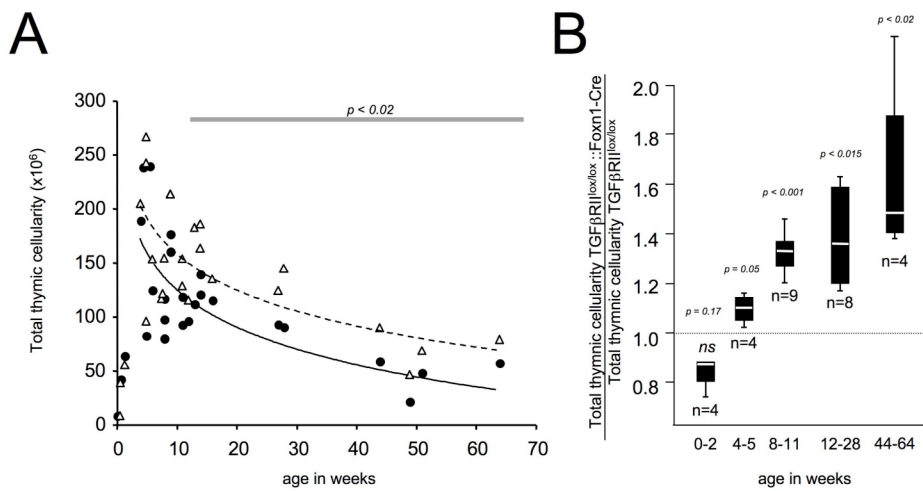
Figure 11

Figure 11. Increased thymocyte numbers in TGFβRII^{lox/lox}::Foxn1-Cre mice
(A) Absolute cell numbers of TGFβRII^{lox/lox}::Foxn1-Cre (open triangles) and wildtype littermates (filled circles) plotted against age in weeks.Each datapoint represents the average of at least 2 mice. A logarhythmic regression was plotted for each group, p value obtained using a paired t-test. (B) Same data as in (A) data is shown for TGFβRII^{lox/lox}::Foxn1-Cre mice, grouped for age groups and in relation to Cre-negative littermates.

Figure 12
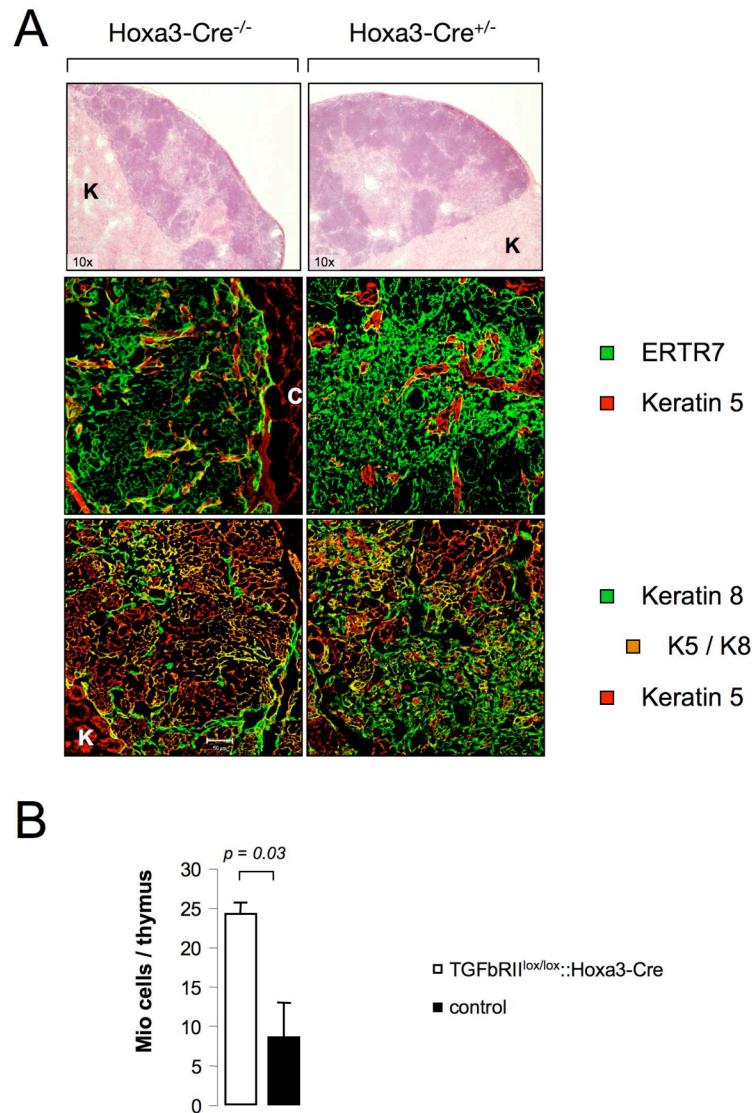
Figure 12. Thymic architecture and thymocyte numbers in TGFbRII^{lox/lox}::Hoxa3-Cre mice

(A) 10x magnification of H&E sections of thymic grafts 10 weeks after transplantation under the kidney capsule of *nu/nu* recipients (upper panels); 20x magnification of thymic sections stained for the indicated stromal markers and analysed by confocal microscopy; K kidney, C kidneycapsule (B) thymic cellularity of thymic grafts of the respective genotype 10 weeks after transplantation under the kidney capsule of *nu/nu* recipients.

Figure 13

A

B

C
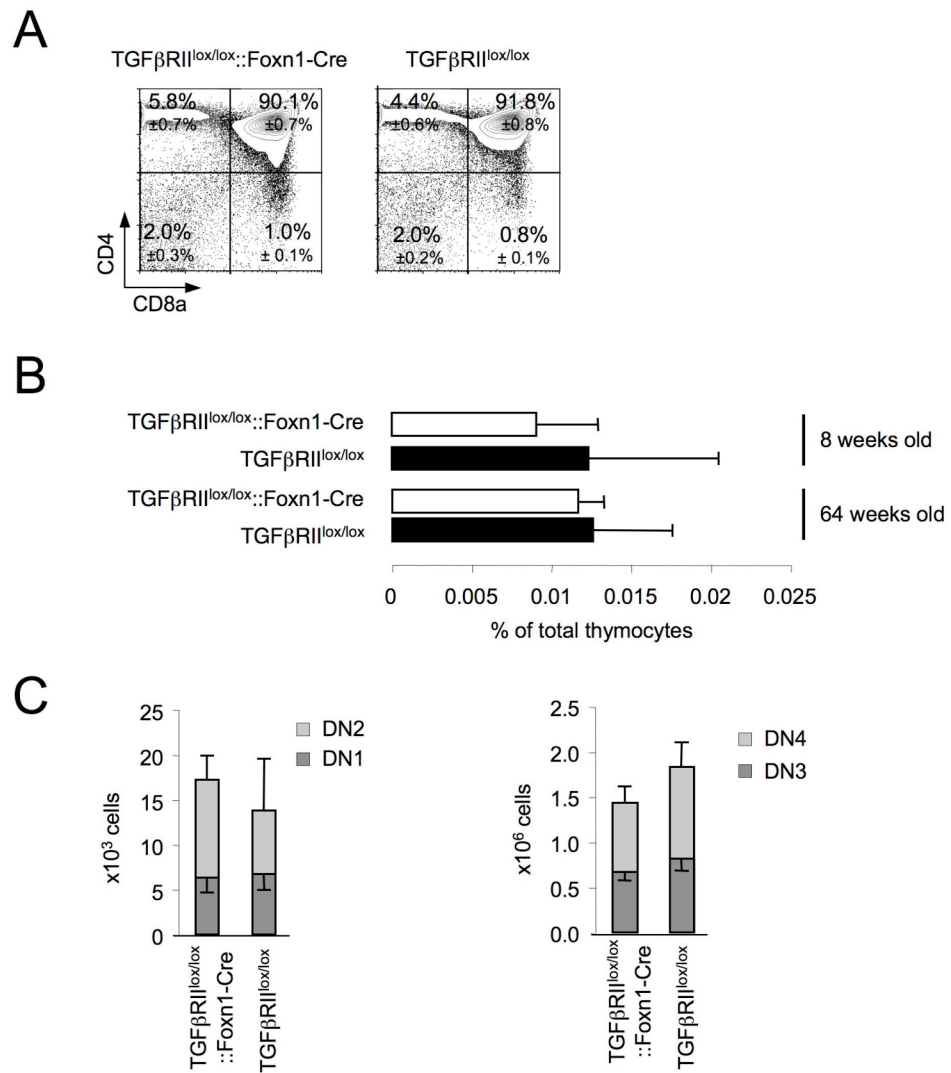
Figure 13. Thymocyte populations in TGFβRII$^{lox/lox}$::Foxn1-Cre mice

(A) FACS blot for CD4 and CD8 expression in thymi of 10 days old mice with the indicated genotype. (B) ETP (CD44+c-kit+Sca-1+lin-) frequencies in mice with the indicated genotype at the indicated age. (C) Absolute numbers of the different DN stages in 8 week old mice with the indicated genotype

Figure 14
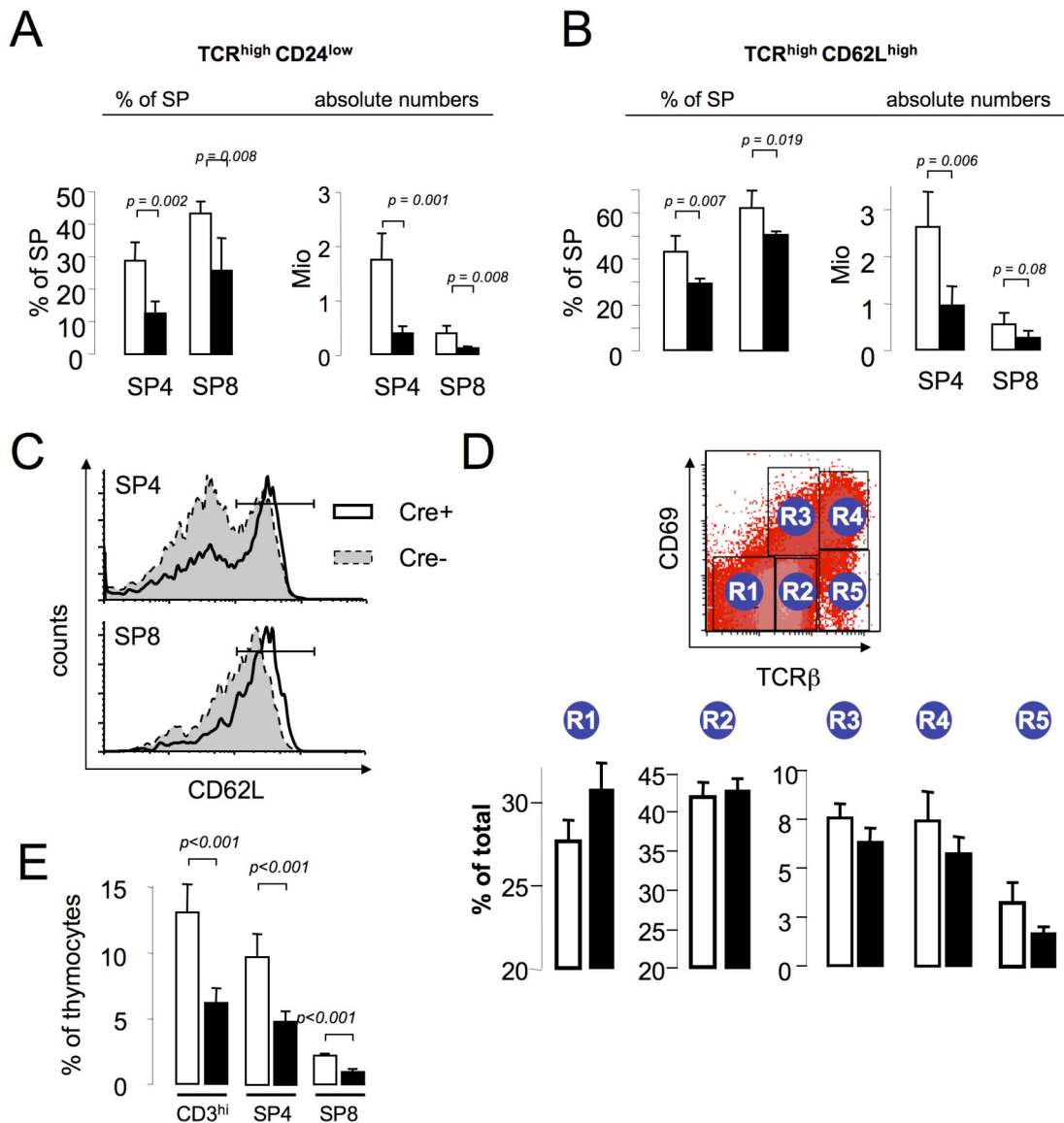
Figure 14. Increased frequency and numbers of mature thymocytes in TGFβ RII[lox/lox]::Foxn1-Cre

(A) frequency (left panel) and absolute numbers (right panel) of TCR^{high}CD24^{low} CD4 (SP4) or CD8 (SP8) thymocytes. (B) frequency (left panel) and absolute numbers (right panel) of TCR^{high}CD62L^{low} CD4 (SP4) or CD8 (SP8) thymocytes. (C) CD62L levels on TCR^{high} CD4 (SP4) or CD8 (SP8) thymocytes. (D) frequency of the indicated populations according to TCR and CD69 expression. (E) frequency of indicated populations inTGFβRII[lox/lox]::Hoxa3-Cre (black bar denotes wildtype, white bar denotes TGFβRII[lox/lox]::Foxn1-Cre)

Figure 15
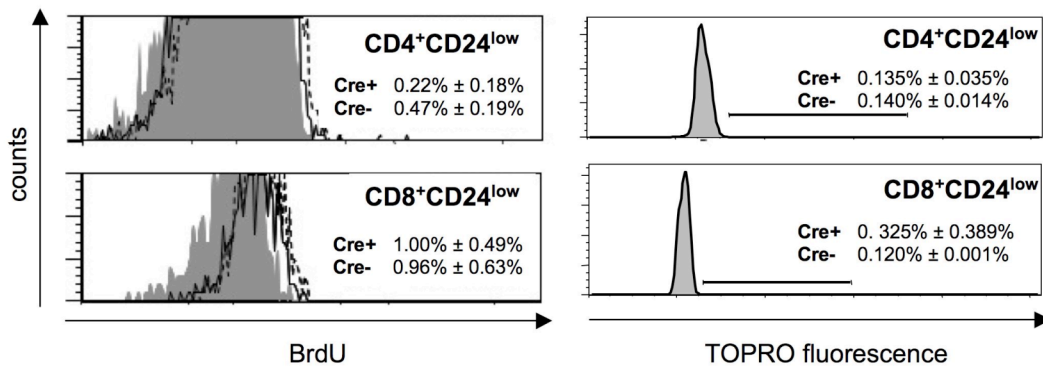
Figure 15. Proliferation analysis of mature thymocytes in TGFβRII$^{lox/lox}$::Foxn1-Cre and TGFβRII$^{lox/lox}$ mice

Mice were pulsed two times with 1mg BrdU each, 3 and 1 hour before analysis. Histograms of BrdU incorporation shown for mature CD4 (upper panels) and CD8 (lower panels), percentage BrdU+ cells indicated for the respective genotypes The right panels demonstrate DNA content visualized by TOPRO fluorescence of fixed and permeabilized thymocytes, gated on mature thymocytes, percentage of cells with DNA content >1

Figure 16
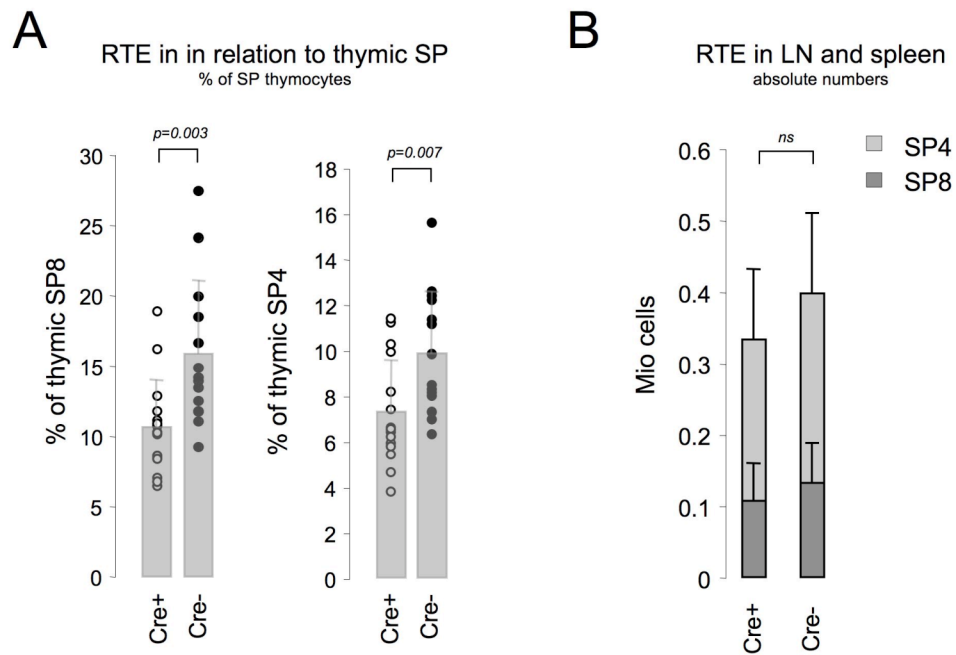
Figure 16. Recent thymic emigrants (RTE) in peripheral lymphoid organs 24 hours after intrathymic FITC-injection

Mice were injected intrathymically with $10\mu l$ each lobe of 250mg/ml FITC solution in PBS. RTE were quantified 24 hours later as FITC+ cells in the periphery and frequency calculated according to the formula

$$\frac{\text{abs. numbers of FITC+ cells in periphery}}{\text{abs. numbers of FITC+ cells in periphery + abs. numbers of FITC+ cells in thymus}}$$

(A) RTE shown for TGFβRII[lox/lox]::Foxn1-Cre (Cre+) and TGFβRII[lox/lox](Cre-) as percentage of thymic CD8 SP (left panel) and CD4 SP (right panel). (B) Absolute numbers of CD4+ and CD8+ RTE found in LN and spleen (same experiment as in A)
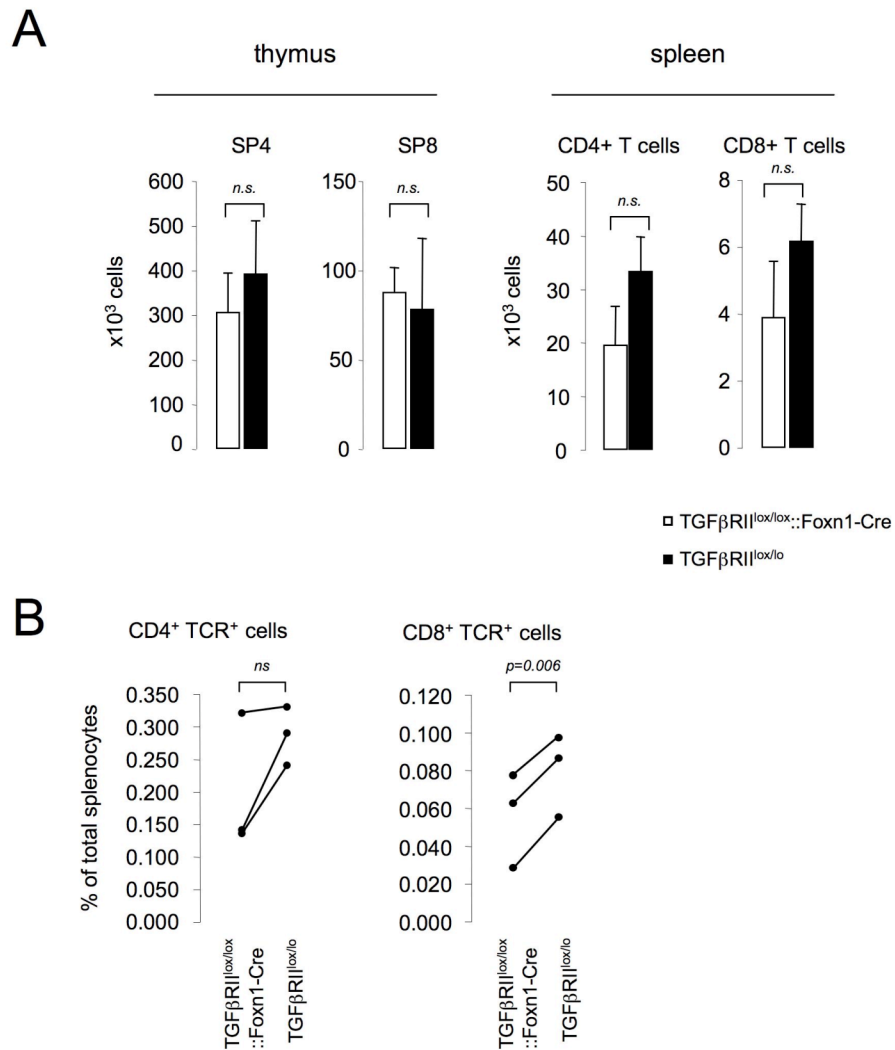
Figure 17

A

thymus

spleen

SP4   SP8

CD4+ T cells   CD8+ T cells

□ TGFβRII^lox/lox::Foxn1-Cre
■ TGFβRII^lox/lo

B

CD4⁺ TCR⁺ cells   CD8⁺ TCR⁺ cells

Figure 17. Occurrence of SP thymocytes and peripheral T cells 3 days postnatally
(A) 3 days old mice were sacrificed and TCR^high CD4+ or CD8+ cells in thymus and spleen quantified (B) shows the summary of 3 experiments for the frequency of peripheral CD4 and CD8 T cells dots denote the respective frequency, the line connects the dots of the same experiment. p values were obtained using a paired t test
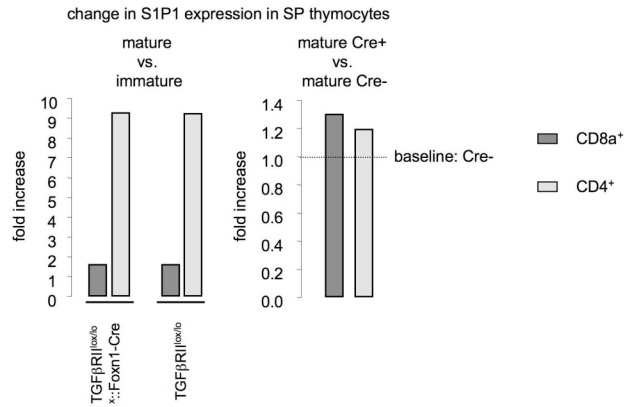
Figure 18

change in S1P1 expression in SP thymocytes

Figure 18. S1P1 expression in SP thymocytes

Sorted immature (CD24^{high}TCR^{high}) and mature (CD24^{low}TCR^{high}) CD4 and CD8 SP thymocytes from TGFβRII$^{lox/lox}$::Foxn1-Cre and control littermates were subjected to quantitative analysis of S1P1 expression. Expression levels of mature SP were compared to the levels in immature (left panel) SP. The right panel shows the relative expression of mature SP in Cre+ normalized to Cre-.
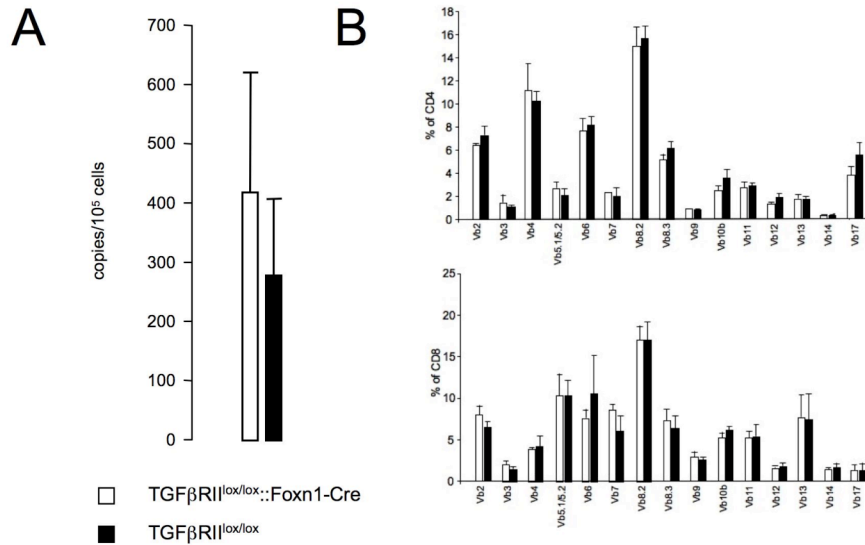
Figure 19

Figure 19. Thymic export and TCRVβ diversity in aged mice

(A) Quantification of T cell receptor excision circles in spleens of TGFβ RII$^{lox/lox}$::Foxn1-Cre and control mice, 1 out of 2 experiments with similar results shown. (B) TCRVβ usage in the two groups at the age of 12 months.

Figure 20

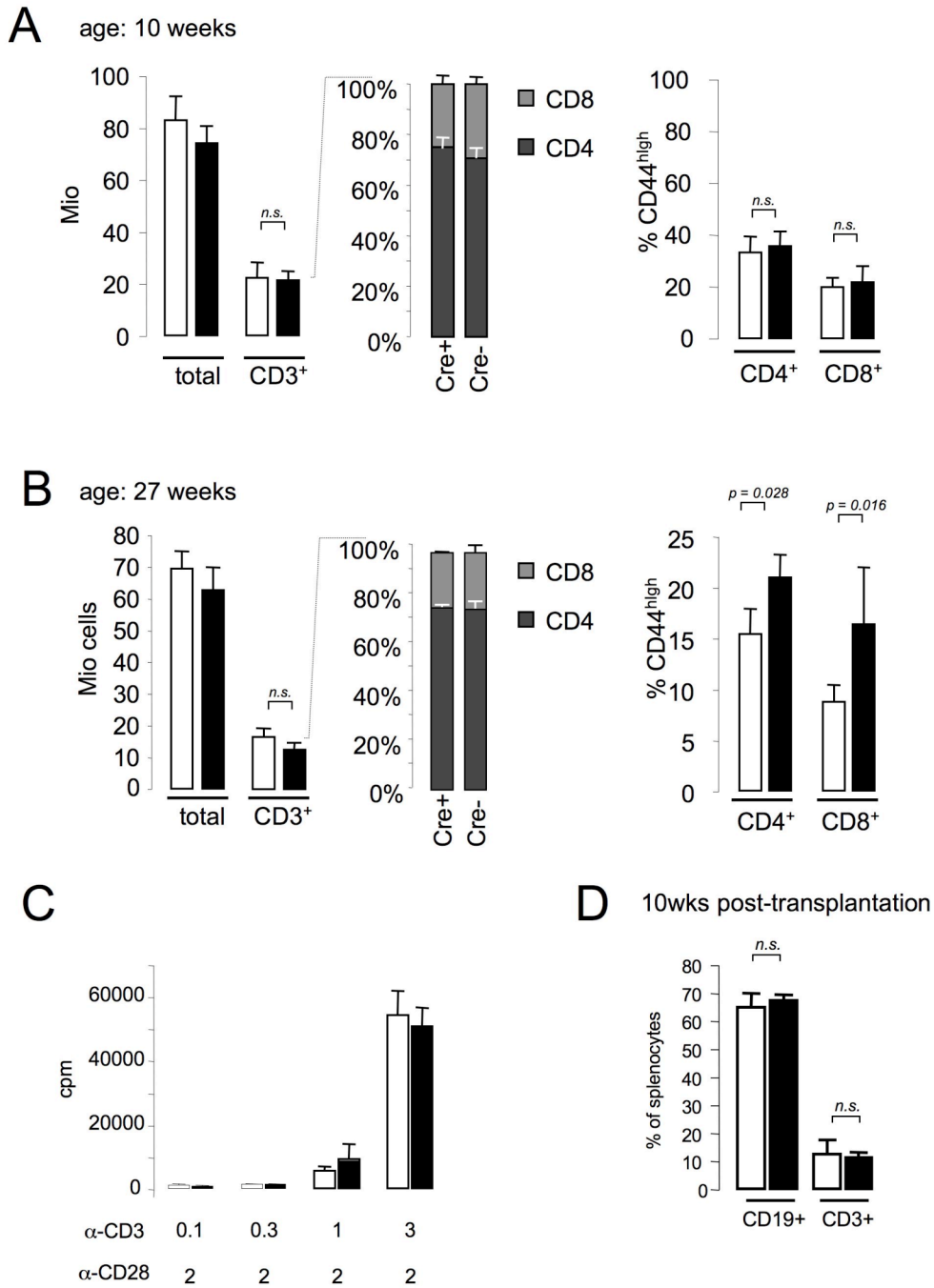**Figure 20. Analysis of peripheral T cells in TGFβRII$^{lox/lox}$::Foxn1-Cre and TGFβ RII$^{lox/lox}$::Hoxa3-Cre versus wildtype littermates**

(A,B) Absolute numbers of total and CD3+ splenocytes at 10 weeks (A) and 27 weeks (B) of age with relative distribution of CD4 and CD8+ T cells (left panel), the right panel shows the frequency of CD44^{high}cells among CD4+ or CD8+ TCRβ+ cells in the spleen. (C) 3H-thymidine uptake of 27 week old splenocytes of the respective genotype. (E) frequency of indicated populations in spleens of *nu/nu* recipients of TGFβRII$^{lox/lox}$::Hoxa3-Cre and wildtype thymic grafts. Black bar denotes wildtype, white bar denotes TGFβRII$^{lox/lox}$::Foxn1-Cre (A-C) and TGFβRII$^{lox/lox}$::Hoxa3-Cre (D)

Figure 21. Altered thymic epithelial phenotype in TGFβRII$^{lox/lox}$::Foxn1-Cre and -Hoxa3-Cre mice

(A) Absolute TEC numbers at different ages in the two groups measured as CD45-MHCII^{high} and MHC^{intermediate} cells (B) frequencies of different TEC populations according to UEA-1 reactivity and MHCII expression (C) BrdU incorporation in CD45- MHCII+ cells after 2 weeks of continuous labeling via drinking water (0.8mg BrdU/ml water)
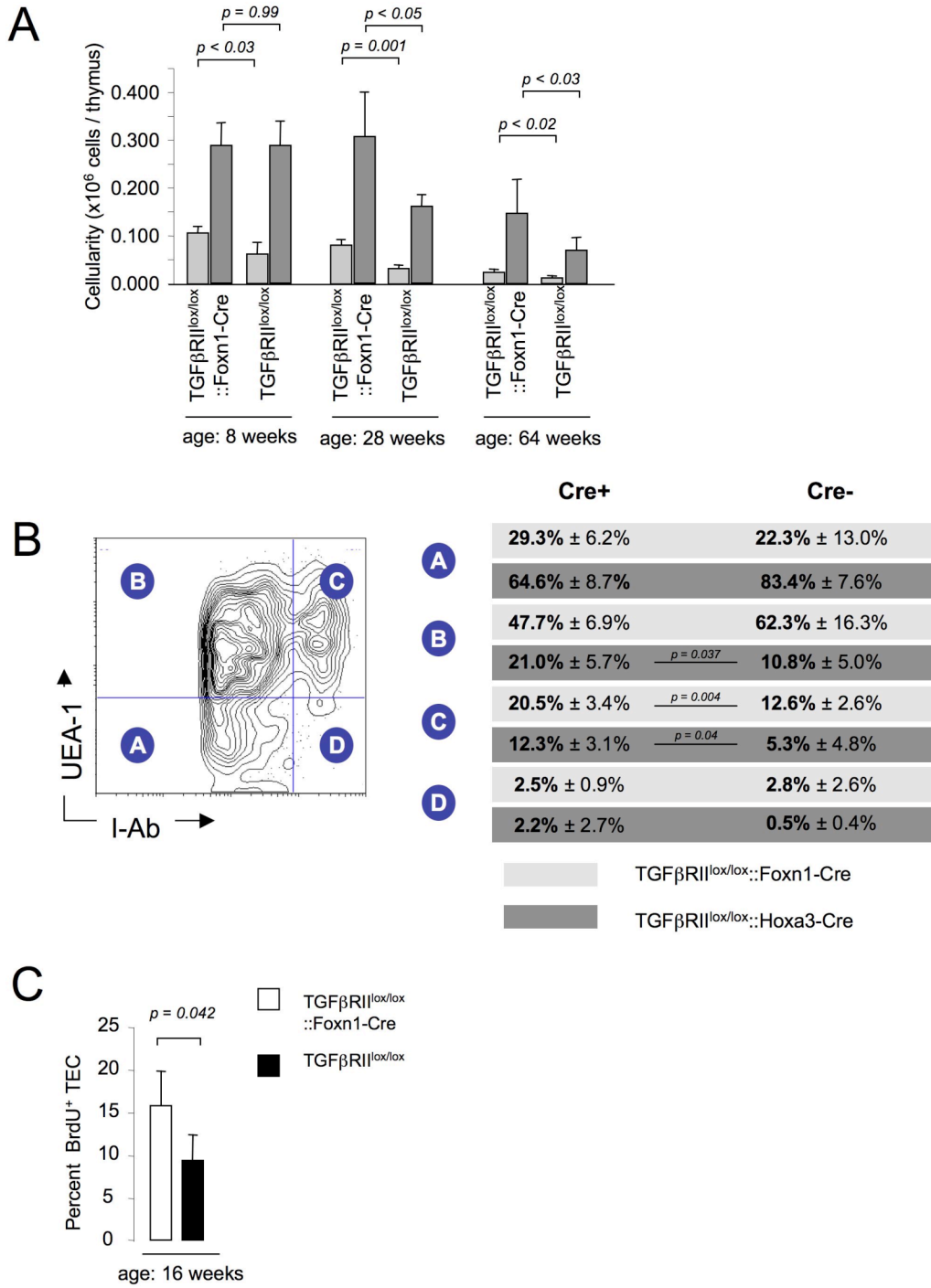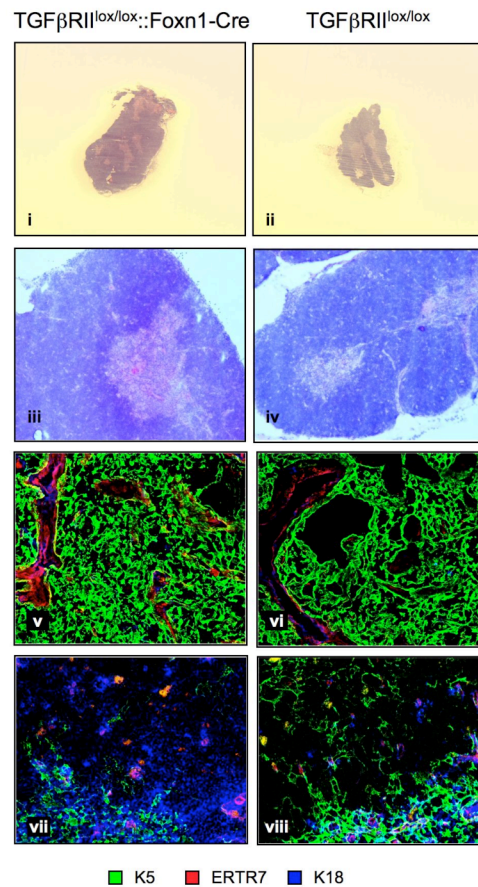
Figure 21

A

B

	Cre+	Cre-
A	**29.3%** ± 6.2%	**22.3%** ± 13.0%
	64.6% ± 8.7%	**83.4%** ± 7.6%
B	**47.7%** ± 6.9%	**62.3%** ± 16.3%
	21.0% ± 5.7% *p = 0.037*	**10.8%** ± 5.0%
C	**20.5%** ± 3.4% *p = 0.004*	**12.6%** ± 2.6%
	12.3% ± 3.1% *p = 0.04*	**5.3%** ± 4.8%
D	**2.5%** ± 0.9%	**2.8%** ± 2.6%
	2.2% ± 2.7%	**0.5%** ± 0.4%

TGFβRII$^{lox/lox}$::Foxn1-Cre

TGFβRII$^{lox/lox}$::Hoxa3-Cre

C

Figure 22

TGFβRII^lox/lox::Foxn1-Cre   TGFβRII^lox/lox

K5   ERTR7   K18

Figure 22. Thymic histology of aged TGFβRII^lox/lox::Foxn1-Cre and control mice
(i,ii) 1.5x and (iii,iv) 4x magnification of H&E sections of thymi (v-viii) 40x magnification, immunofluorescence analysis for the indicated stromal markers, v&vi showing medullary, vii &viii showing cortical regions

Figure 23. Irradiation-imposed changes in the thymus
(A) TGFβ1 protein levels in thymi at 12 and 24 hours after lethal (950rad) total body irradiation expressed as fold increase over non-irradiated controls. (B) TGFβ1 mRNA levels in thymi at 48 and 96 hours after lethal (950rad) total body irradiation expressed as fold increase over non-irradiated controls. (C) Fraction of 1D11-reactive thymic stromal cells by flow cytometric analysis derived from animals irradiated at the indicated time points.
(D) Immunoreactivity of active TGFβ1 (i, ii, v, vi) and LAP (iii, iv, vii, viii) in thymi derived from control (i-iv) and irradiated mice (v-viii), stained with AEC, counterstained with hemalaun. magnification 20x (i, iii, v, vii) and 40x (inserts)
(E) detection of phosphorylated Smad2 in lysates derived from non-irradiated control (left lane) and irradiated mice (right lane) 24 hours post-irradiation (950rad), arrowhead denotes the specific P-Smad2 signal
(F) Absolute TEC numbers in non-irradiated mice and irradiated mice (950rad, 6 days after irradiation)
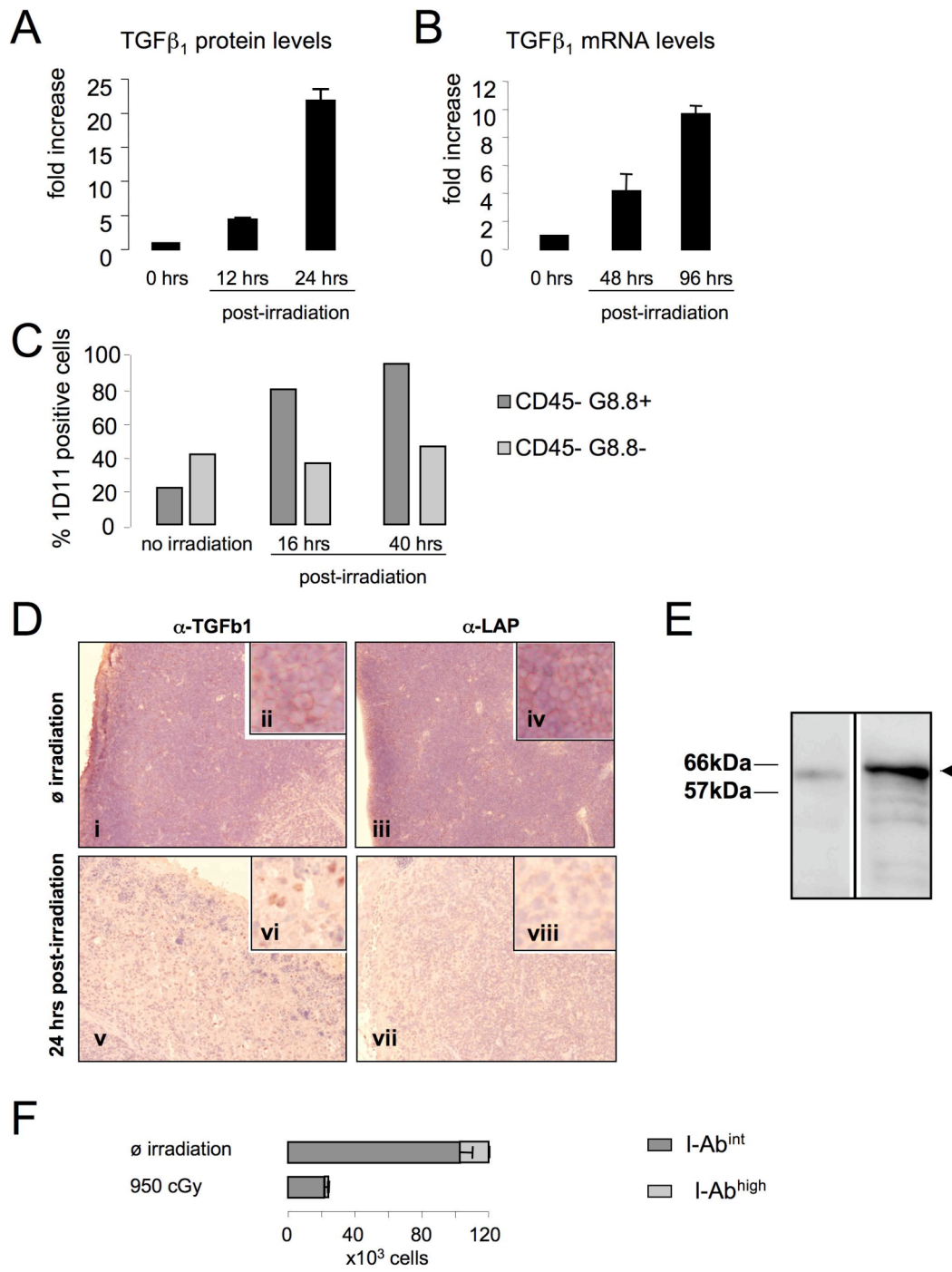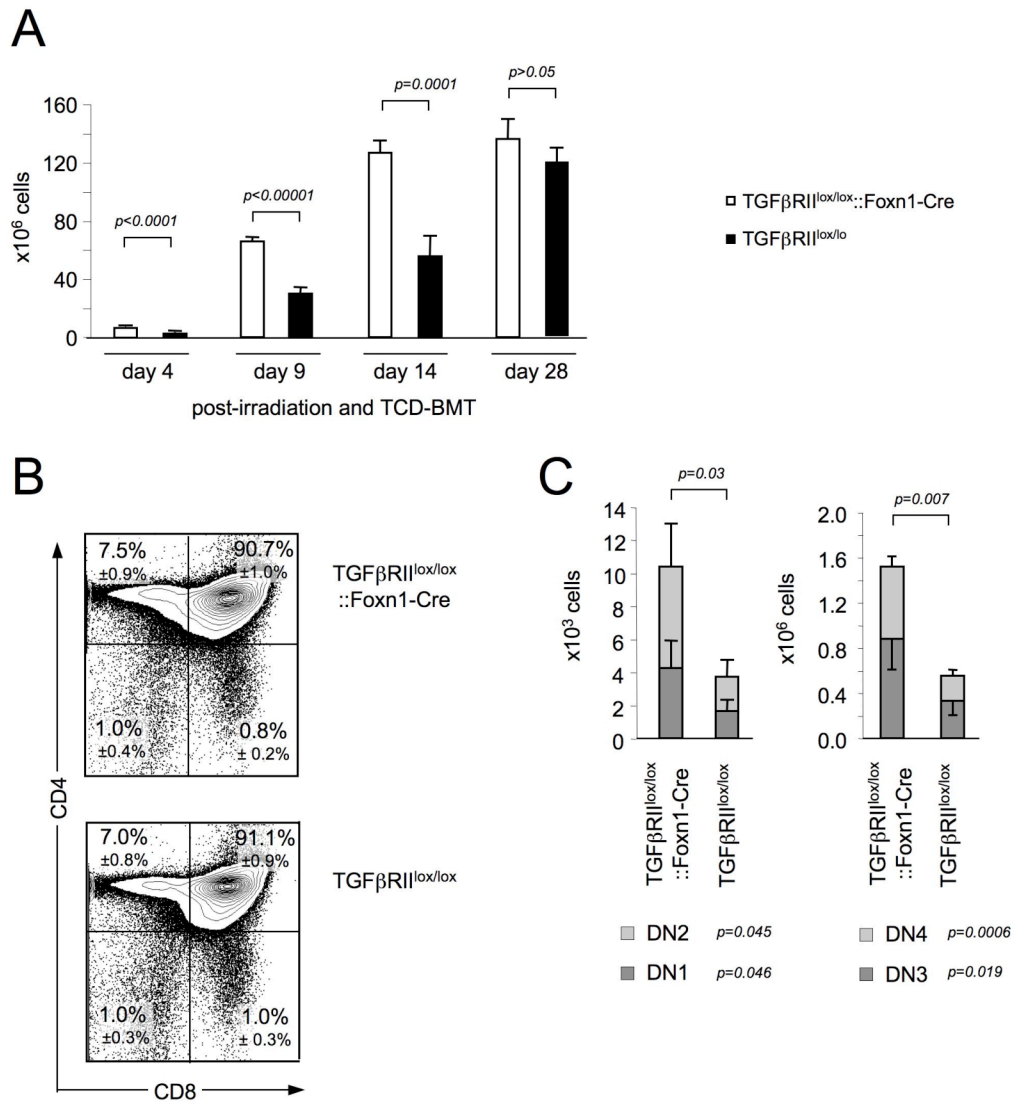
Figure 23

Figure 24

Figure 24. Enhanced thymic reconstitution in TGFβRII^{lox/lox}::Foxn1-Cre mice
(A) Thymic cellularity at different time points after lethal irradiation (950rad)
(B) Distribution of thymocyte populations on day 14 post-irradiation/BMT
(C) Absolute numbers of DN populations 14 days post irradiation
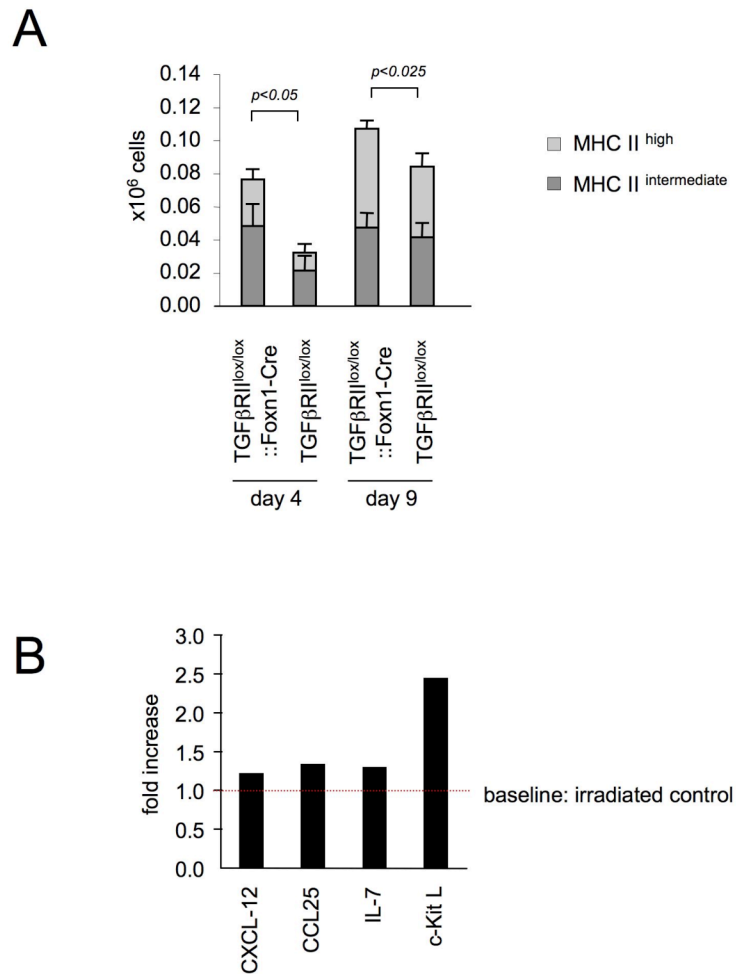
Figure 25

A

B

Figure 25. Increased TEC cellularity following lethal irradiation/BMT in the absence of TGFβ-signaling

(A) Absolute TEC numbers with MHCII[high] and MHC[intermediate] subpopulations at the indicated time points after irradiation/BMT. (B) Expression of indicated genes in hymi derived from irradiated TGFβRII[lox/lox]::Foxn1-Cre mice in comparison to their expression in thymi from irradiated control mice 48 hours after irradiation, displayed as fold increase
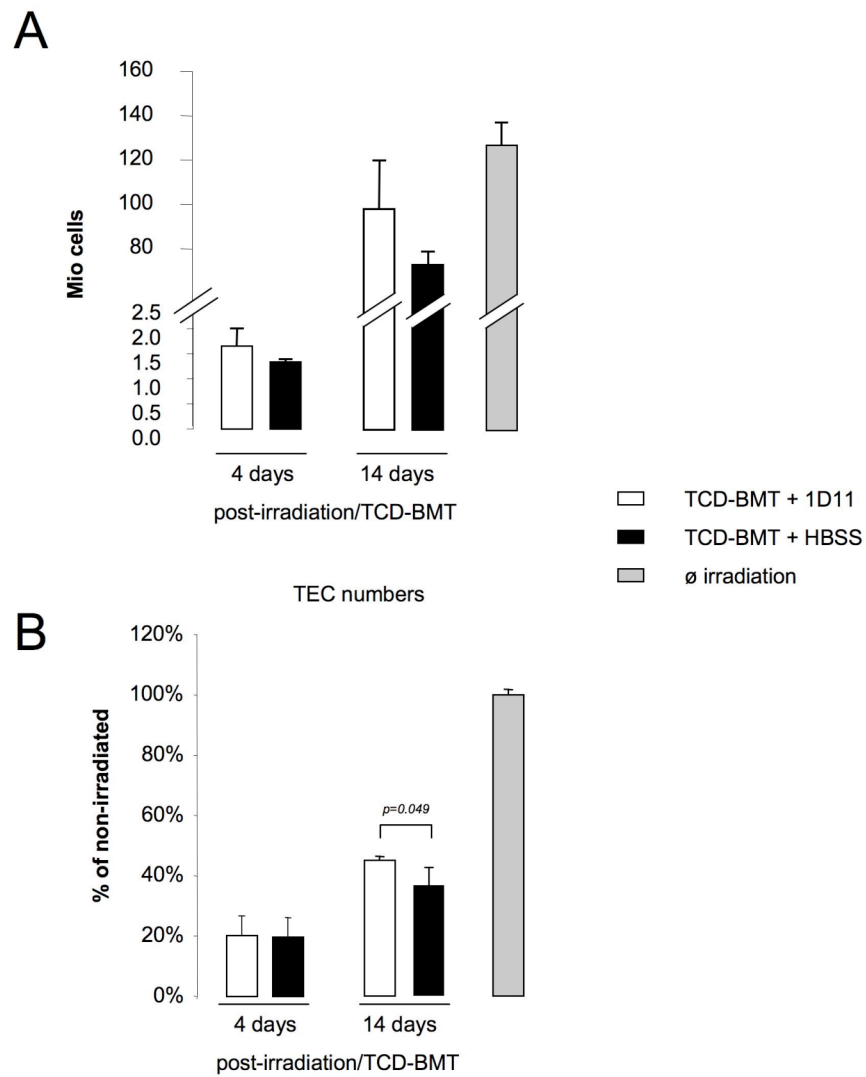
Figure 26

Figure 26. **Increased thymocyte and TEC cellularity upon treatment of wildtype mice with α-TGFβ-Ab prior to lethal irradiation/BMT**

(A) Absolute thymocyte numbers 4 and 14 days after irradiation/BMT, groups (white bar) received 2x 400μg α-TGFβ1-3 (clone 1D11) or control antibody (black bar) 3 and 1 hours before 950rad total body irradiation

(B) Absolute TEC numbers 4 and 14 days after irradiation/BMT, conditions as in (A)
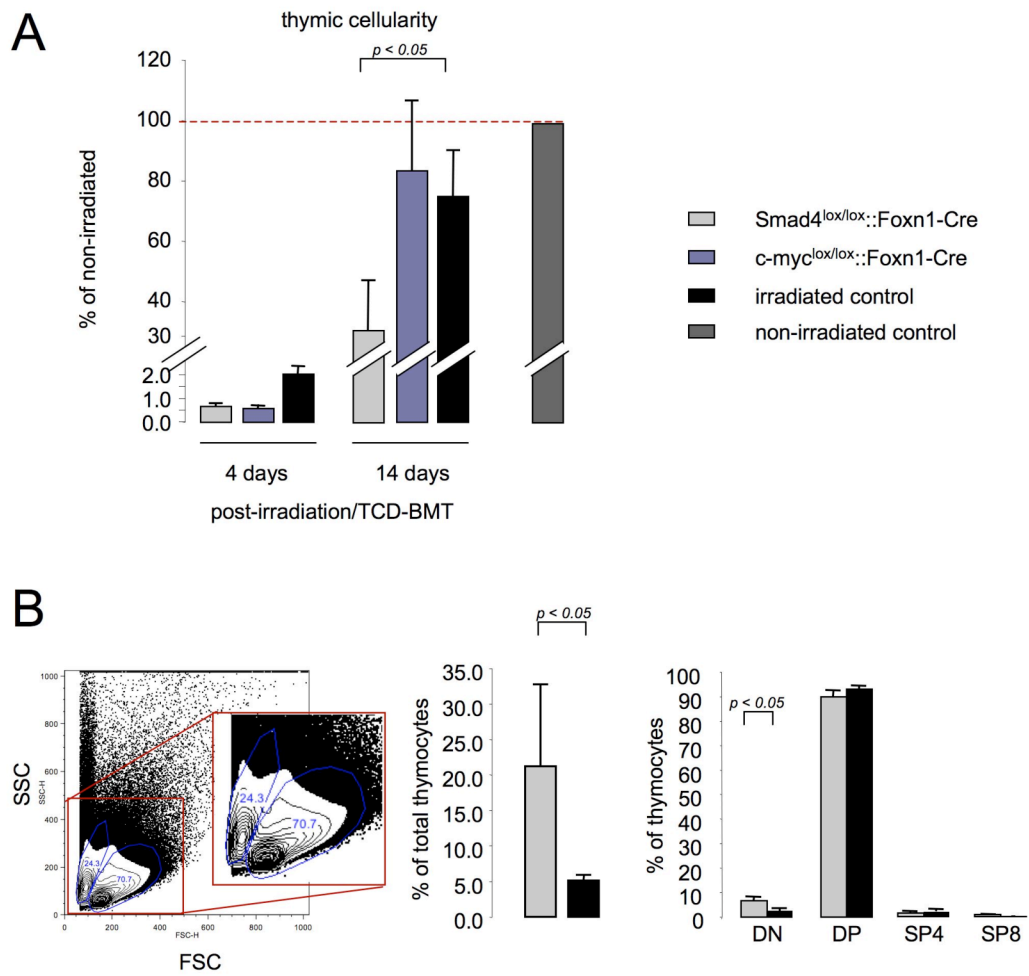
Figure 27

Figure 27. Efficient thymocyte reconstitution depends on Smad4 but is independent of c-myc expression in TEC
(A) Absolute thymocyte numbers 4 and 14 days after irradiation/BMT
(B) increased frequency of thymocytes with $FSC^{low}SSC^{high}$ pattern (left and middle panel) and DN thymocytes (right panel) in Smad4$^{lox/lox}$::Foxn1-Cre mice 14 days after irradiation
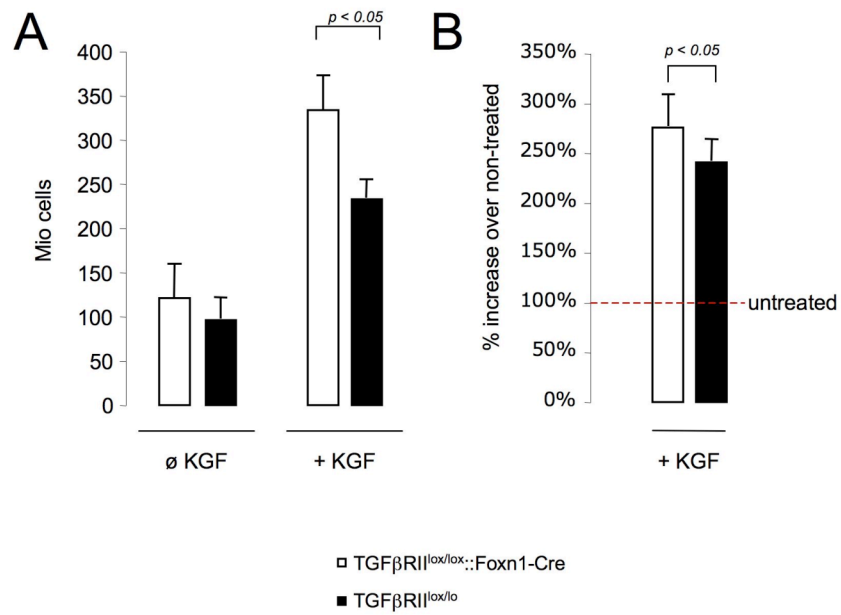
Figure 28

Figure 28. Enhanced action of KGFon thymocyte cellularity in the absence of TGFβ-signaling in TEC

(A) Absolute thymocyte cellularity in TGFβRII[lox/lox]::Foxn1-Cre and TGFβRII[lox/lox] mice without or two weeks after exogenous addition of KGF

(B) Same data as in (A) but plotted as increase over untreated Cre+ or Cre- controls

Figure 29
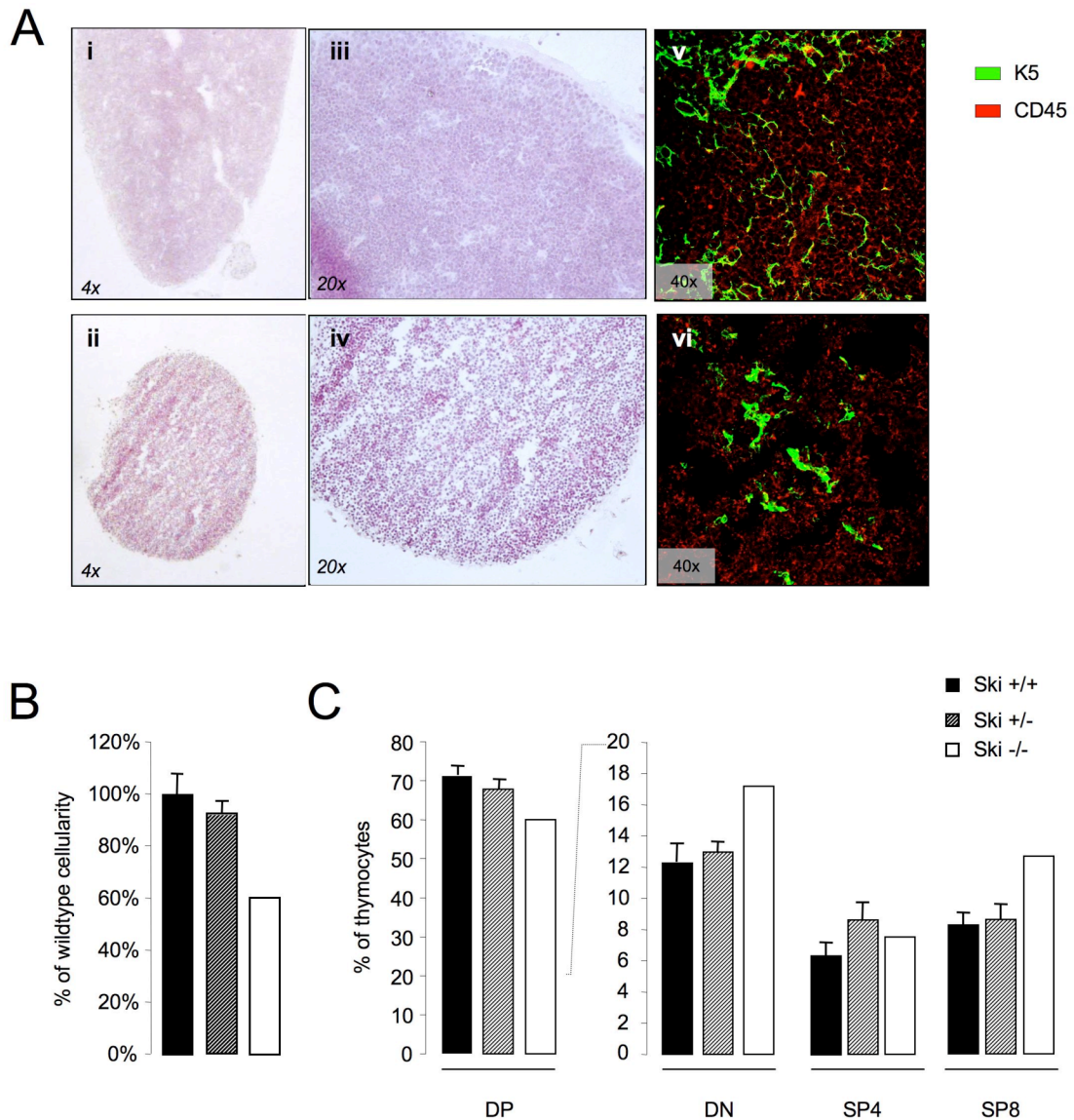
Figure 29. Ski-deficiency results in thymic hypoplasia and perturbed thymic architecture

(A) E18 thymic lobes derived from wildtype (i, iii, v) and Ski-/- (ii, iv, vi) were sectioned and stained with H&E (i-iv) or for cytokeratin-5 and CD45 (v, vi)

(B) Total cellularity of lobes derived from wildtype, Ski+/- and Ski-/- E14 embryos, cultured for 7 days. (C) Thymocyte subpopulations of the lobes in (B) displayed according their CD4-CD8-staining pattern by FACS.

Figure 30

Figure 30. Ski-deficient TEC develop into a normal thymus displaying normal T cell output when transplanted into *nu/nu* hosts
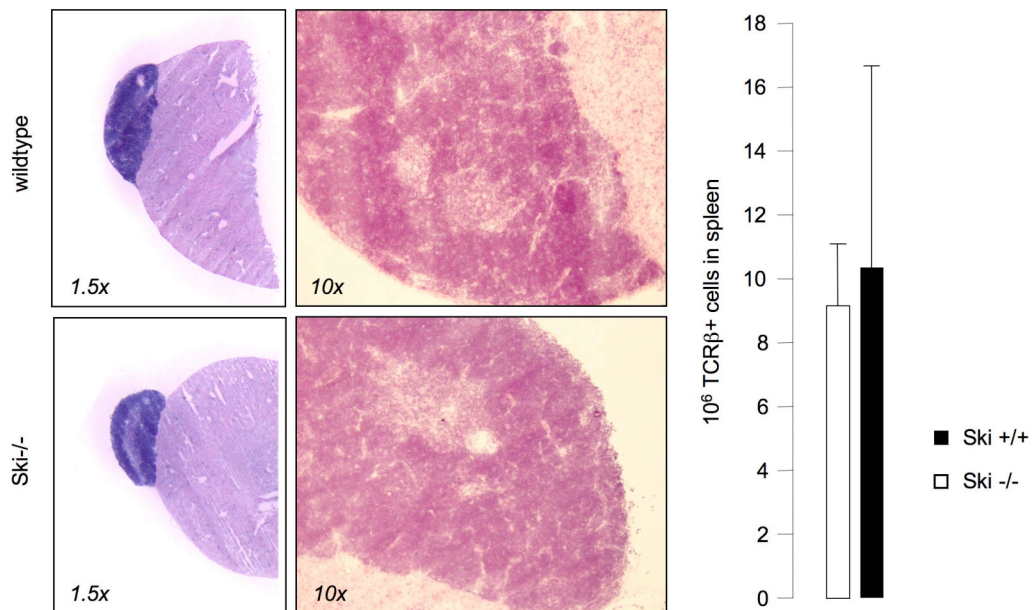
E14.5 thymic lobes derived from Ski-/- and wildtype embryos were depleted of endogenous thymocytes using d-Guo for 5 days, thereafter the tymi were transferred under the kidney capsule of syngeneic nu/nu hosts. Histological analysis of grafts was performed 10 weeks after transplantation (left and middle panels).

Peripheral T cells were quantified in spleens of the same mice (right panel).

Figure 31. Ski-deficient hematopoietic precursors show mildly aberrant T cell development

(A) Absolute numbers of thymocytes in lethally irradiated recipients of E14.5 fetal liver from Ski-/- heterozygote or wildtype embryos (left panel) and relative distribution of these thymocytes (middle and right panels)

(B) Absolute numbers of CD4+ and CD8+ SP thymocytes, same mice as in (A)

(C) Absolute numbers of splenocytes of mice described in (A) with frequency of CD8a+ and CD4+ T cells.

(D) Western blot analysis of lysates derived from sorted DN, DP, SP4 SP8 thymocytes, total thymus and total spleen. Equal amounts of protein were loaded and loading was controlled with coomassie -staining of the membrane. Membranes were probed for Ski protein (left panels, note different exposition times) and for phosphorylated Smad2 (left panel).
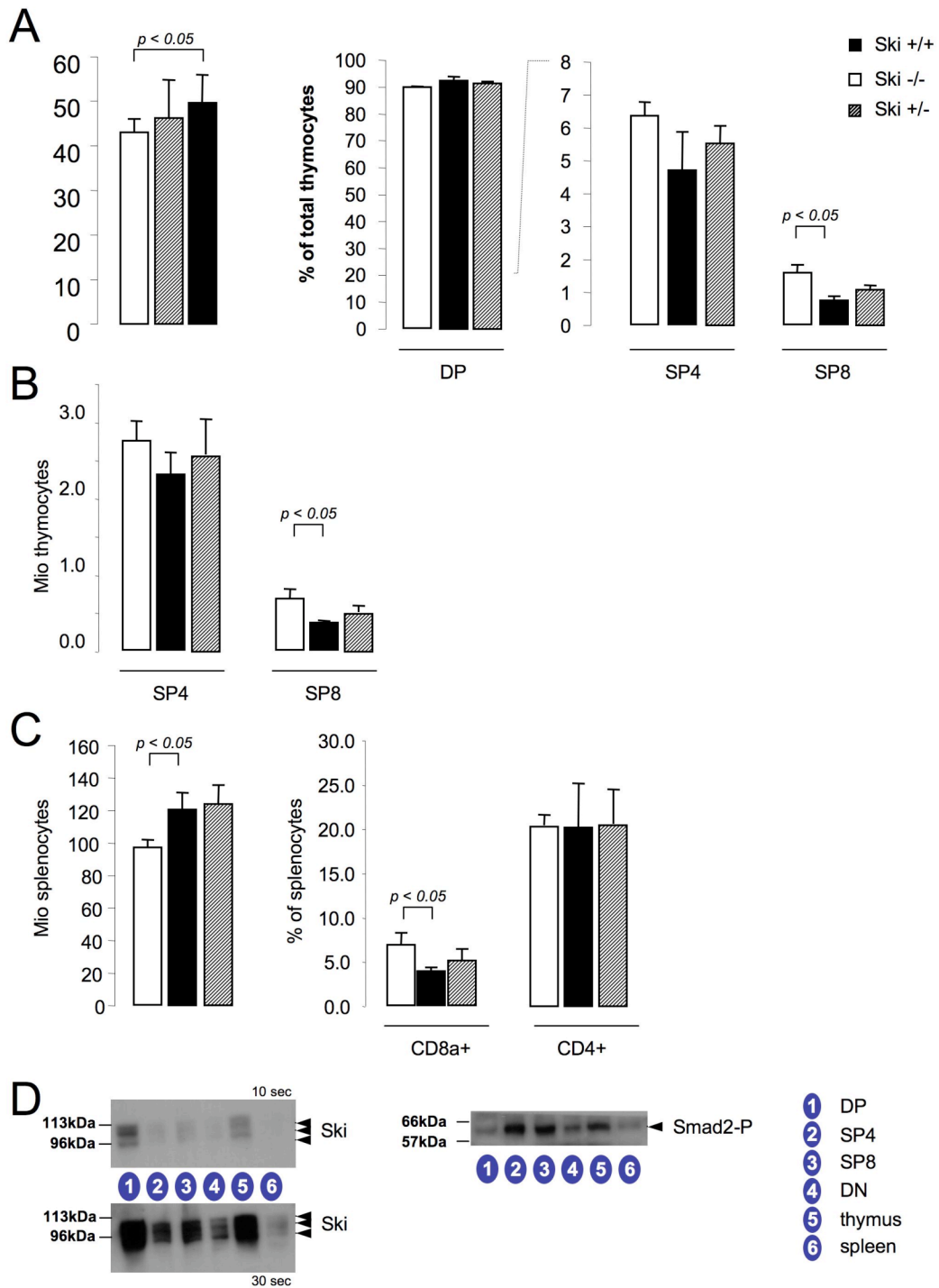
Figure 31

Table 1

	E10.5 dorsal	E10.5 ventral	E15 MTS24-	E15 MTS24+	adult MTS24-	adult MTS24+	CD45- MHCII+	TEC1.2	TEC1.4	TEMC6	TECC9	TEM3.10
LIGANDS												
TGFβ₁	-	-	(+)	(+)	(+)	(+)						
TGFβ₂	-	+	-	-	+	+						
TGFβ₃	-	-	(+)	(+)	+	+						
RECEPTORS												
TGFβRI	+	+						+	+	+	+	+
TGFβRII	+	+	++	++	+	+	+	+	+	+	+	+
TGFβRIII	-	-										
REGULATORS												
Ski	+	+										
Sno	-	-										

+ = expressed
- = no expression

Table 1. Expression of ligands, receptors and regulators involved in TGFβ-signaling at different developmental stages in primary TEC and TEC lines

Table 2

			day 5 TGFβRII$^{lox/lox}$	day 5 TGFβRII$^{lox/lox}$::Foxn1-Cre	week 5 TGFβRII$^{lox/lox}$	week 5 TGFβRII$^{lox/lox}$::Foxn1-Cre	week 28 TGFβRII$^{lox/lox}$	week 28 TGFβRII$^{lox/lox}$::Foxn1-Cre
SP4	total	(% of total)	3.5 ± 0.3	5.5 ± 1.1	7.3 ± 1.0	10.3 ± 1.5	7.6 ± 5.2	10.7 ± 5.2
				$p = 0.012$		$p = 0.003$		$p = 0.2$
		x10⁶	1.5 ± 0.1	2.1 ± 0.7	17.4 ± 3.7	25.6 ± 3.7	3.4 ± 2.3	7.1 ± 4.1
				$p = 0.086$		$p = 0.004$		$p = 0.04$
	CD24^{low}	(% of total)	1.4 ± 0.2	2.4 ± 0.7	3.4 ± 1.1	6.6 ± 1.3	2.7 ± 2	5.3 ± 2.8
				$p = 0.038$		$p = 0.001$		$p = 0.03$
		x10⁶	0.6 ± 0.1	0.9 ± 0.4	8.9 ± 3.5	17.5 ± 3.8	1.2 ± 0.9	3.4 ± 2.0
				$p = 0.11$		$p = 0.002$		$p = 0.017$
SP8	total	(% of total)	0.9 ± 0.2	1.1 ± 0.3	2.6 ± 0.8	3.9 ± 1.0	1.3 ± 0.9	2.2 ± 1.4
				$p = 0.39$		$p = 0.027$		$p = 0.13$
		x10⁶	0.4 ± 0.1	0.4 ± 0.1	6.2 ± 2.2	9.9 ± 3.0	0.6 ± 0.4	1.5 ± 1.1
				$p = 0.81$		$p = 0.032$		$p = 0.068$
	CD24^{low}	(% of total)	0.47 ± 0.07	0.64 ± 0.19	1.5 ± 0.7	2.7 ± 0.9	0.59 ± 0.55	1.41 ± 1.1
				$p = 0.139$		$p = 0.023$		$p = 0.047$
		x10⁶	0.2 ± 0.1	0.3 ± 0.1	4.1 ± 2.2	7.9 ± 3.0	0.26 ± 0.24	0.92 ± 0.81
				$p = 0.36$		$p = 0.028$		$p = 0.057$

Table 2. Frequency and absolute numbers of mature (TCR^{high}CD24^{low}) SP thymocytes in TGFβRII$^{lox/lox}$::Foxn1-Cre and TGFβRII$^{lox/lox}$ mice at different ages (5 days, 5 weeks and 28 weeks old)